Coordination Chemistry of a Phosphadiazonium Lewis Acceptor

by

Heather Anne Spinney

Submitted in partial fulfillment of the requirements
for the degree of Doctor of Philosophy

at

Dalhousie University
Halifax, Nova Scotia
March, 2005

Your file Votre référence
ISBN: 0-494-00968-3
Our file Notre référence
ISBN: 0-494-00968-3

DALHOUSIE UNIVERSITY

To comply with the Canadian Privacy Act the National Library of Canada has requested that the following pages be removed from this copy of the thesis:

Preliminary Pages
- Examiners Signature Page (pii)
- Dalhousie Library Copyright Agreement (piii)

Appendices
- Copyright Releases (if applicable)

Table of Contents

List of Figures

List of Tables

Abstract

The two most common oxidation states for phosphorus are phosphorus(III) and phosphorus(V). Although the ability of phosphorus(V) centres to behave as electron pair acceptors (Lewis acids) is well established, the exploitation of the Lewis acidity of phosphorus(III) represents a more recent and developing area. Phosphorus(III) centres (or phosphines) have a lone pair of electrons, are formally electron rich, and are generally recognized as effective electron donors (Lewis bases). Nevertheless, it has been demonstrated that coordinatively unsaturated phosphorus(III) centres have the potential to exhibit electron acceptor behaviour even with the presence of a non-bonding pair of electrons at the acceptor site.

The synthesis and comprehensive characterization (NMR, FT-IR, FT-Raman, X-ray) of a series of coordination complexes in which an electron-rich (lone pair bearing) phosphorus(III) centre acts as a Lewis acceptor is presented. Previous work has shown that iminophosphines of the type Mes*NPX (Mes* = 2,4,6-tri-*t*-butylphenyl, X = Cl, OSO_2CF_3) react with a variety of ligands (e.g., imidazol-2-ylidene, amine, phosphine), which effect nucleophilic displacement of X as an anion. The resulting cations are best described as 1:1 adducts of a neutral ligand on a phosphadiazonium Lewis acceptor ($Mes*NP^+$). This chemistry has now been extended to include complexes of the phosphadiazonium cation with both bidentate- and tridentate-chelating ligands, as well as donor-rich adducts where more than one monodentate ligand coordinates to the acceptor. In a similar fashion, dicationic, acceptor-rich phosphadiazonium complexes have been synthesized through the use of bridging ligands. The isolation and characterization of these coordination complexes has resulted in the observation of a number of novel bonding environments for phosphorus, including hypervalent phosphorus(III) species. The coordination of neutral donors to the phosphadiazonium cation represents a new synthetic methodology in phosphorus chemistry, where phosphorus-element (element = C, N, O, S, Se, P) bonds are formed through donor-acceptor interactions.

List of Abbreviations and Symbols Used

Å	angstrom
An	generalized anion
2,2'-BIPY	2,2'-bipyridine
4,4'-BIPY	4,4'-bipyridine
br	broad
χ	mole fraction
CCD	charge coupled device
Ch	chalcogen
CP	cross polarization
Cp*	pentamethylcyclopenta-dienyl
δ(A)	chemical shift of nucleus A (NMR)
δ_{iso}(A)	isotropic chemical shift of nucleus A (NMR)
d	doublet
DABCO	1,4-diazabicyclo[2.2.2]-octane
DBN	1,5-diazabicyclo[4.3.0]-non-5-ene
DEPE	1,2-bis(diethylphos-phino)ethane
DIPHOS	1,2-bis(diphenylphos-phino)ethane
DMAP	4-dimethylaminopyridine
DMPE	1,2-bis(dimethylphos-phino)ethane
d.p.	decomposition point
ε	extinction coefficient
E	Main group element from Group 13, 14, 15, or 16
E.A.	elemental analysis
Et	ethyl
FT	fourier transform
GOF	goodness of fit
HOMO	highest occupied molecular orbital
Im	1,3-diisopropyl-4,5-dimethylimidazol-2-ylidene
^{i}Pr	isopropyl
IR	infrared spectroscopy
iso	isotropic
λ	wavelength
L	generalized ligand
LB	Lewis base
LUMO	lowest unoccupied molecular orbital
K	kelvin

m	multiplet
MAS	magic angle spinning
Me	methyl
Mes	2,4,6-trimethylphenyl
Mes*	2,4,6-tri-*t*-butylphenyl
MO	molecular orbital
m.p.	melting point
$^{n}J_{AB}$	coupling constant between nuclei A and B, connected through n bonds
N-	substituted at nitrogen
NHC	N-heterocyclic carbene
NMR	nuclear magnetic resonance
o.d.	outer diameter
OIm	1,3-diisopropyl-4,5-dimethylimidazole-2(3*H*)-one
OTf	trifluoromethylsulfonyl-oxy
OU	1,3-dimethyldiphenylurea
P-	substituted at phosphorus
Ph	phenyl
pK_a	acidity constant
PMDETA	N,N,N',N'',N''-pentamethyldiethylene-triamine
Pn	pnictogen
ppm	parts per million
Pr	propyl
q	quartet
R	substituent
R	residual factor
RT	room temperature
s	singlet
SIm	1,3-diisopropyl-4,5-dimethylimidazole-2(3*H*)-thione
SeIm	1,3-diisopropyl-4,5-dimethylimidazole-2(3*H*)-selenone
t	triplet
^{t}Bu	tertiary butyl
TeIm	1,3-diisopropyl-4,5-dimethylimidazole-2(3*H*)-tellurone
TMEDA	N,N,N',N'-tetramethylethylene-diamine
TRIPHOS	bis(2-diphenylphos-phinoethyl)phenyl-phosphine
UV-Visible	ultra violet-visible
V	volume
wR_2	weighted residual factor

X	halogen	Z	number of molecules in the unit cell

Conventions and Nomenclature

For the Lewis drawings in this thesis, lone pairs are placed on the principal atom or atoms of interest, and for clarity, omitted from peripheral substituents. Bonds drawn as arrows represent a coordinate or dative interaction. Lewis drawings do not necessarily depict the geometry observed in the solid state structures of the compounds. Only atoms of interest are labelled in solid state structures.

Nomenclature follows that found in the published literature, which does not always follow the guidelines recommended by IUPAC (International Union of Pure and Applied Chemists).

Compound numbering is chapter specific. Each time a new compound is introduced (either one previously reported in the literature or a new compound presented in this thesis) it is assigned a number identifying the chapter in which it is discussed followed by a sequential indicator. For example, the first compound noted in Chapter 1 is given the identifier **1.1**.

Acknowledgements

I would like to take a moment to thank everyone who has made my time at Dalhousie a positive experience. I have indeed enjoyed the last four and a half years.

First of all, I would like to thank my supervisor, Dr. Neil Burford, for his guidance, encouragement, enthusiasm, and most of all, his patience. I never seem to be able to go straight from point A to point B, and Neil has always let me find my own path. I appreciate the opportunity I was given to teach some undergraduate classes at Dalhousie, and the fact that Neil trusted me with this added responsibility.

"Team Burford" is a great group of people, and if nothing else, my coworkers are a constant source of amusement. I would like to thank Robyn Ovans, Heather Phillips, Katie Groom, Adam Dyker, Jeff Landry, and Ken Sharp for their support, friendship, and exquisite proofreading skills. I also need to acknowledge the members of the Stradiotto Research Group (Dr. Mark Stradiotto, Brad Wile, Matt Rankin, Dominik Wechsler, and Judy Cipot) and the Thompson Research Group (Dr. Alison Thompson, Tabitha Wood, Cory Beshara, and Nathan Dalgleish) for answering my constant stream of questions, letting me borrow things, and for being generally helpful people.

Meaghan Grundy worked with me as an undergraduate project student in the summer of 2003, and did the preliminary work with the 1,2-bis(diphosphino)ethane ligands. Laura Whyte also worked in our group as an undergraduate student and often made starting materials for me. Thanks to both Meaghan and Laura for all of their help, and for making the summers more enjoyable.

The members of my supervisory committee, Dr. Russell Boyd, Dr. Jim Pincock, and Dr. Kevin Grundy, need to be acknowledged for their continued support over the

years. They have always made themselves available whenever I needed their input. I would especially like to thank Dr. Pincock for showing me the ropes in first year chemistry, and for teaching me a lot about teaching others. I would also like to thank Dr. Martin Cowie of the University of Alberta for acting as my external examiner and for all his helpful comments in the editing process.

I am deeply indebted to Drs. Bob McDonald and Mike Ferguson at the University of Alberta for their excellent X-ray crystallography work. One couldn't ask for better people with which to collaborate. Dr. Kathy Robertson has also been very helpful in answering any crystallography-related questions here at Dalhousie. I need to thank ARMRC for use of instrumentation and Drs. Mike Lunsden, Bob Berno, and Ulli Werner-Zwanziger for all of their help with NMR-related issues. Mike and Ulli have contributed a lot to this thesis with their collection of solid state ^{31}P NMR data.

There are a number of other people in the Department of Chemistry who I would like to acknowledge. The ladies in the main office have been extremely helpful with all manner of things, especially Giselle Andrews and Deanna Wentzell who have taken very good care of me. I have enjoyed working in the undergraduate laboratories with Donna Silvert, and I appreciate her support over the years. The machine shop staff, Rick Conrad, Mike Boutilier, and the late Ross Shortt, have helped to keep lab equipment running smoothly, and Jurgen Muller's excellent glass blowing has proved to be essential to research progress. The technical support of Gino Ranieri and Brian Millier has bailed me out of all manner of computer-related disasters.

I would especially like to thank my friends Brad Wile, Tabitha Wood, Nathan and Chrissy Dalgleish, Cory Beshara, Robyn Ovans, Heather Phillips, Katie Groom, and Amy

Kierstead for keeping me sane; my Mum and Dad for listening to my frantic phone calls; the old Mt. A. crew for constantly cheering me on; and Molly for her insightful philosophical discussions and general editorial comments.

My graduate program was funded by NSERC, the Killam Foundation, the Eliza Ritchie Foundation, the Walter C. Sumner Foundation, and Dalhousie University.

Chapter 1: Introduction

1.1 General Introduction to Phosphorus Chemistry

Phosphorus has fascinated chemists since its initial discovery in the late seventeenth century. Just imagine the sheer delight of Robert Boyle and others as they gazed at the ghostly glow of white phosphorus, little cognizant of the dangerous power they had unleashed. For here is an element whose compounds have the ability to sustain life (phosphate fertilizers), yet also to destroy it (incendiary bombs, nerve gases, poisons). An intriguing enigma, the chemistry of phosphorus has had a tumultuous history.[1]

Phosphorus continues to fascinate the modern-day chemist by the wealth of structural arrangements it can adopt in its numerous compounds. Phosphorus is often compared to carbon in its ability to catenate and to form multiply-bonded systems, and is quite often touted as a "carbon copy."[2] Indeed, the chemistry of carbon is much more similar to phosphorus than to its heavier Group 14 analogue silicon; however, there are also some important differences. Phosphorus is a Group 15 element and has five valence electrons, compared to carbon's four. As well, phosphorus is a third-row element, and thus has the ability to expand its valence shell beyond the standard octet, allowing it to access many bonding environments that are unattainable for carbon. The ability of phosphorus to "mimic" the chemistry of carbon, while still possessing its own unique electronic properties, makes it ideal for incorporation in functional materials.[3]

In order to appreciate the diversity in structure and bonding for phosphorus, Lewis representations of potential phosphorus bonding environments, with coordination numbers of one to six, are presented in Figure 1.1.[4] The majority of these structural arrangements have been observed in stable compounds, **C, E, F**, and **G** being notable

exceptions. Each possible bonding environment imparts a unique pattern of reactivity to the phosphorus atom, making phosphorus one of the most versatile elements in the periodic table.

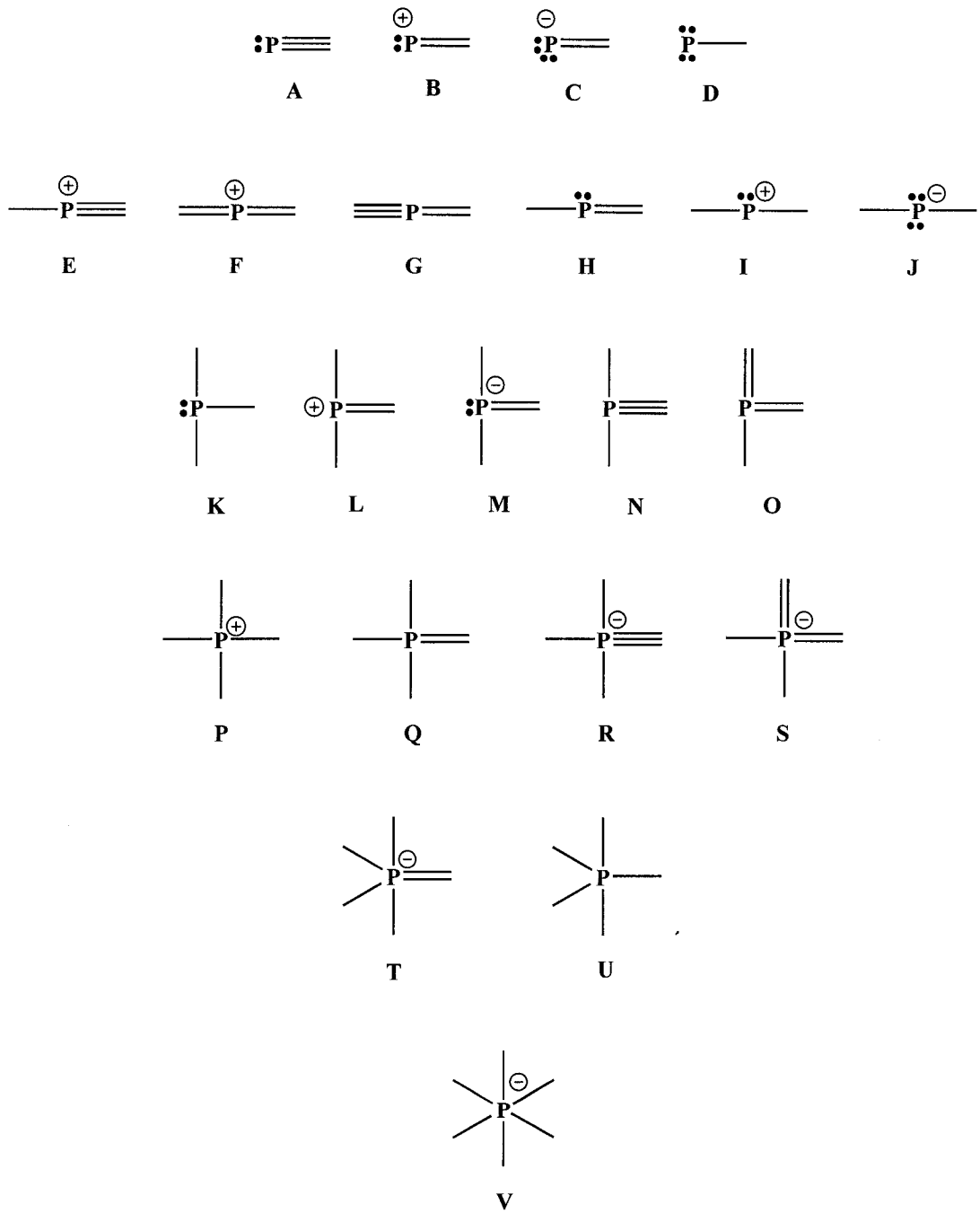

Figure 1.1 Potential bonding environments for phosphorus with coordination numbers of one to six (modified from reference 4).

The most commonly encountered bonding environments for phosphorus are the tricoordinate phosphine, **K**, the tetracoordinate phosphonium cation, **P**, the tetracoordinate phosphorus ylide (or Wittig reagent), **Q**, the pentacoordinate phosphorane, **U**, and the hexacoordinate phosphate anion, **V**. Representative molecules or ions (**1.1 – 1.5**) containing these bonding environments are depicted below. With the exception of the phosphine, **K**, all of these bonding environments contain phosphorus in a +5 oxidation state, where all of the valence electrons on phosphorus are used to form bonds. In the phosphine, a lone pair of electrons is retained on the phosphorus atom, giving it an oxidation state of +3.

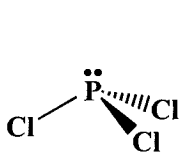

1.1

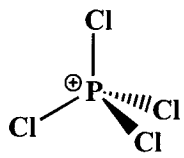

1.2

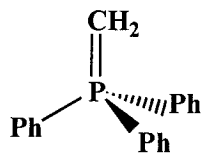

1.3

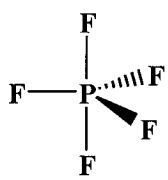

1.4

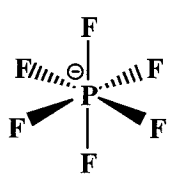

1.5

Examples of compounds containing the other, less familiar three-, four-, and five-coordinate bonding environments pictured in Figure 1.1 are known. Although environment **Q** is generally used to depict the bonding in phosphine oxides (R_3PO), molecular orbital theory predicts the existence of a 3dπ-3pπ triple bond in these compounds, making bonding environment **R** (**1.6**) another valid description.[5] Environment **S** is a possible resonance contributor to the structures of phosphate salts and oxoacids of phosphorus, while environment **T** is thought to be the most accurate structural depiction of the anions POF_4^- (**1.7**) and $POCl_4^-$. These ions have been detected in the gas phase, but no solid state characterization is currently available.[6] Compounds

containing trigonal planar phosphorus(V) centres (**O**) also appear in the literature; the first examples, bis(imino)phosphoranes (**1.8**), were reported by the groups of Niecke[7] and Scherer[8] in 1974. In addition to bis(imino)phosphoranes,[9] analogous compounds with P-C, P-P, P-O, P-S, and P-Se multiple bonds are known, and have been comprehensively reviewed.[10-12]

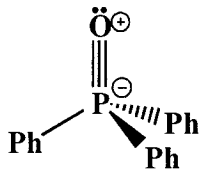

1.6

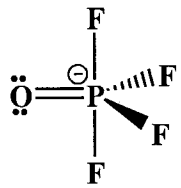

1.7

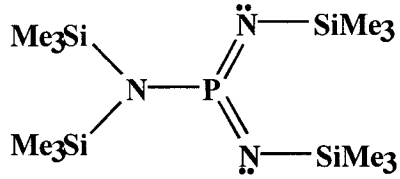

1.8

Few examples exist of the tricoordinate phosphorus bonding environments, **L**, **M**, and **N**, and the chemistry of these species is still being actively developed.[4] In 1988, Bertrand and coworkers isolated an alkylidynephosphorane (**1.9**), the first and, up to now, only stable compound featuring a tricoordinate, pentavalent, triple-bonded phosphorus atom (**N**).[13] Despite their relative instability, alkylidynephosphoranes and the corresponding nitrilophosphoranes (**1.10**), have been proposed as reactive intermediates in a variety of reactions.[14;15] A year later, Bertrand's group also isolated the first example of **L**, a methylenephosphonium ion (**1.11**), which is isovalent with an alkene.[16] In all of the structurally characterized methylenephosphonium ions, both the phosphorus and the carbon atoms adopt a trigonal planar geometry, and the P-C bond lengths are short; however, the double bond is dramatically twisted (up to 60° depending on the substituents).[17] The first example of bonding environment **M**, referred to as an

iminophosphide (**1.12**), was isolated by Burford and coworkers in 2000, and will be discussed in detail in Section 1.4.[18]

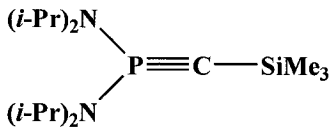

1.9

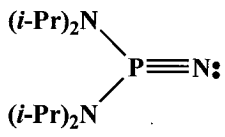

1.10

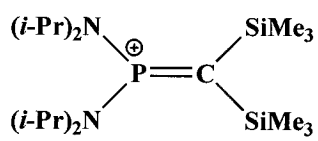

1.11

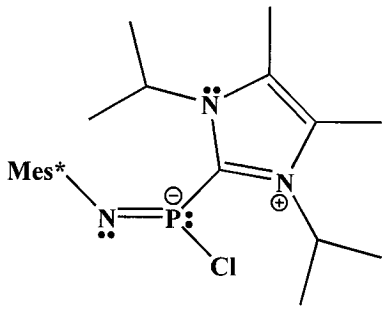

1.12

Until the 1960s, the chemistry of phosphorus was restricted to three-, four-, five-, and six-coordinate species. It was thought that bonding environments **A-J**, which contain coordinatively unsaturated phosphorus centres (phosphorus centres with less than a full complement of ligands or substituents), and pπ-pπ multiple bonds, were simply not isolable. In the 1950s, many prominent chemists were proponents of a "double bond rule", which stated that elements beyond the second row of the main group do not form stable pπ-pπ bonds.[19;20] The first evidence to the contrary was obtained by Gier in 1961; he was able to isolate phosphaacetylene (**1.13,** bonding environment **A**) as a gas, stable only at low temperatures, by passing PH_3 through an electric arc between graphite electrodes.[21] Nevertheless, the scientific establishment remained unconvinced, and

phosphorus compounds containing pπ-pπ bonds were included in a monograph of "nonexistent compounds" in 1965.[22]

1.13

In 1964, Dimroth and Hoffmann isolated the first room temperature stable species containing a dicoordinate phosphorus centre, the phosphamethine cyanine cation (**1.14**).[23] The existence of a delocalized C-P 2pπ-3pπ bond in the cation was later supported by X-ray analysis.[24] Further support for the existence of phosphorus-containing pπ-pπ multiple bonds, came in the form of Ashe's elegant 1971 synthesis of the unsubstituted phosphabenzene (**1.15**), in which the pπ-pπ bonds are also stabilized by resonance.[25] In 1973, Niecke isolated the first example of bonding environment **H** in a neutral acyclic compound, an iminophosphine (**1.16**), containing a P-N 3pπ-2pπ multiple bond.[26] Niecke made use of a relatively new synthetic strategy, where compounds containing pπ-pπ multiple bonds between heavier main group elements are kinetically stabilized through the use of sterically demanding (bulky) substituents. Although there are also thermodynamic consequences of steric hindrance,[27] the bulky substituents act as a shield, preventing the molecular collisions necessary for oligomerization.[28]

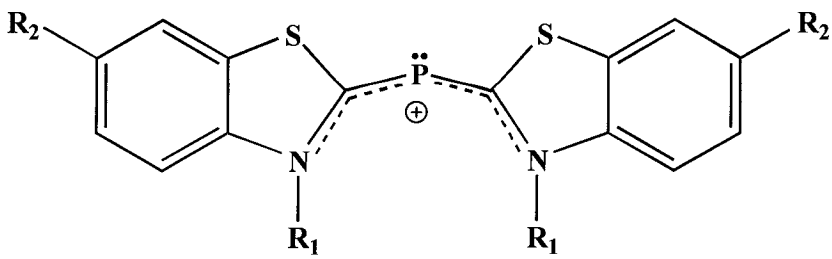

1.14

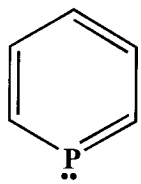

1.15

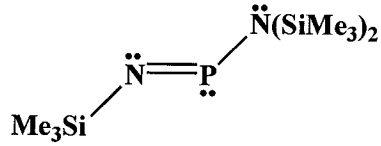

1.16

Sterically demanding substituents have since been used to assist in the isolation of a variety of stable phosphorus-containing alkyne analogues (**A**) and alkene analogues (**H**). For instance, Becker used a combination of tertiarybutyl and trimethylsilyloxy substituents to isolate the first stable examples of a phosphaalkene (**1.17**) in 1976,[29] and a phosphaalkyne (**1.18**) in 1981.[30] Around the same time, Yoshifuji isolated the first example of a diphosphene (**1.19**) using the bulky organic group 2,4,6-tri-*tert*-butylphenyl (Mes*).[31] Since this pioneering work, a number of other compounds containing P-E (E = main group element) multiple bonds have been isolated, including double bonds to arsenic, antimony, and bismuth.[32-35]

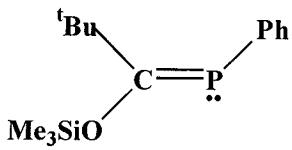

1.17

1.18

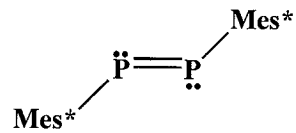

1.19

Examples of cationic (**I**) and anionic (**J**) dicoordinate phosphorus bonding environments have also been isolated. Since the early work of Dimroth and Hoffmann, a plethora of dicoordinate phosphorus cations (phosphenium cations, **I**) have been synthesized.[36;37] The distinction with bonding environment **H** here is subtle in that

spectroscopic and structural data indicate π-delocalization onto phosphorus. All bonding models for phosphenium cations involve the phosphorus centre on an allylic manifold, which is mediated by the electronic structure of the substituents.[4] Two of these models are pictured in Scheme 1.1, although others are possible. In type (1) cations, the phosphorus centre exhibits a positive π-charge (**I**) and may be classified as an ambiphilic centre that exhibits both electrophilic and nucleophilic (lone pair) character. In contrast, the positive charge in type (2) cations is localized exclusively on the substituents. The phosphorus centre is neutral or even has a negative π-charge (**J**), and is therefore expected to be a mainly nucleophilic centre.[37] Typical representatives of type (1) cations are diaminophosphenium ions,[38] while type (2) cations are exemplified by triphosphenium ions[39] and phosphamethine cyanine ions.[23]

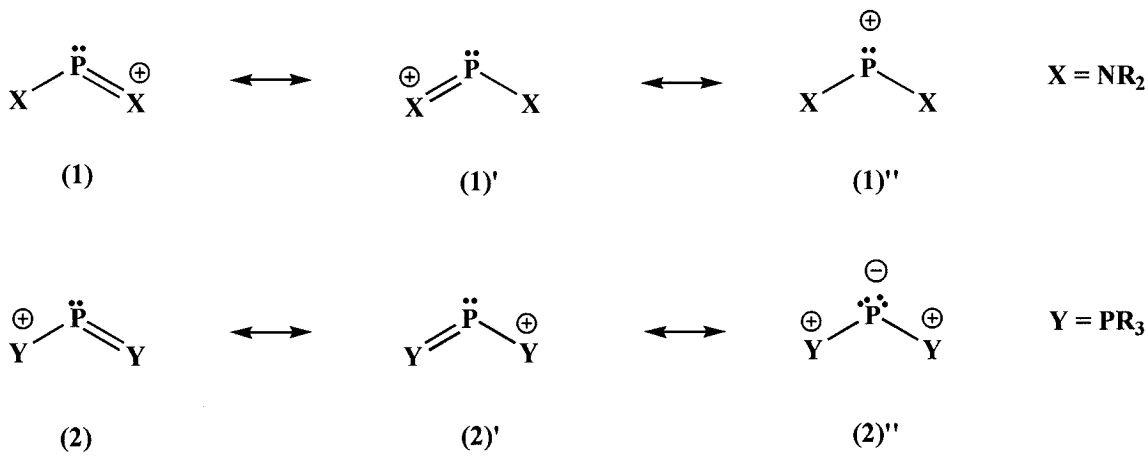

Scheme 1.1[37]

Apart from phosphaalkynes, few compounds containing mono-coordinate phosphorus centres have been isolated. In 1988, Niecke and coworkers isolated a phosphadiazonium salt [Mes*NP]$AlCl_4$ (**1.21**) via halide abstraction from the

chloro(imino)phosphine Mes*NPCl (**1.20**, Scheme 1.2).[40] The phosphadiazonium cation is isovalent with the all-nitrogen diazonium analogue ($R\text{-}N{\equiv}N^{+}$)[41] and is a cationic example of bonding environment **A**. Sometimes referred to as iminophosphenium ions, phosphadiazonium ions can also be described by a resonance contributor containing a cationic P-N double bond (**B**); however, the length of the P-N bond is very short (1.475(8) Å), and the solid state structure indicates sp-hybridization at nitrogen.[40]

1.20 **1.21**

Scheme 1.2

The mono-coordinate phosphinidenes, bonding environment **D**, are very reactive and no stable "free" phosphinidenes have been structurally characterized, although they have been invoked as reactive intermediates in a number of processes.[42] Nevertheless, phosphinidenes can be stabilized through bonding to transition metal or main group donors.[43] For instance, Arduengo and coworkers isolated a ligand-stabilized phosphinidene, using an imidazol-2-ylidene donor (**1.22**).[44] The existence of two lone pairs on the phosphorus centre was confirmed by coordination of **1.22** to two BH_3 units (**1.23**).[45]

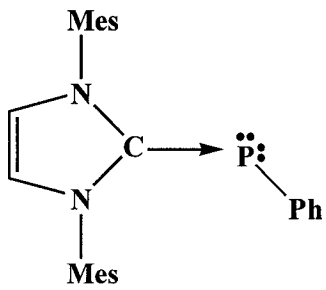

1.22

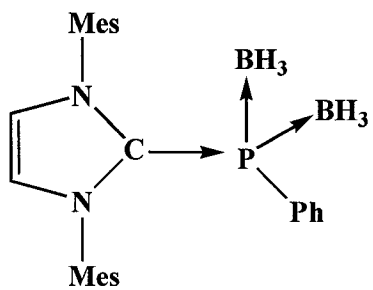

1.23

Figure 1.1 can still be expanded to include other bonding possibilities for phosphorus as, with the exception of **M**, it does not contain any hypervalent phosphorus(III) bonding environments. These interesting structural arrangements are characterized by phosphorus centres with more than eight valence electrons, which still possess a non-bonded or lone pair of electrons. Currently, the only way to generate such an environment is through the Lewis acid chemistry of phosphorus(III).

1.2 Phosphorus(III) as a Lewis Acid

Tricoordinate phosphine centres (bonding environment **K**, **1.1**) are traditionally considered Lewis bases by virtue of their non-bonding pair of electrons, and indeed, phosphines have been used extensively as ligands in main group and transition metal coordination chemistry. Nevertheless, phosphines have the ability to act as Lewis acids in the presence of suitable Lewis bases.[4] The simplest example of this is the PBr_4^- anion (**1.23a**, **1.23b**), formed from the reaction of phosphorus tribromide with the tetraalkylammonium halide salt, $[NPr_4]Br$.[46] The solid state structure of the PBr_4^- anion shows the four bromine substituents arranged about the central phosphorus atom in a

distorted disphenoidal geometry, indicating the presence of a stereochemically active lone pair.[47] The PBr_4^- anion can be depicted as a phosphoranide[48] (**1.23a**) with a formal negative charge at phosphorus, or as the Lewis acid-base adduct formed between a Br^- anion and PBr_3 (**1.23b**). An arrow is used to designate the presence of a coordinate bond in representation **1.23b**, and this convention will be used throughout the entire text of the thesis. Both representations **1.23a** and **1.23b** indicate the presence of 10 valence electrons situated about a tetracoordinate phosphorus centre, invoking the hypervalent phosphorus(III) bonding environment **W**.

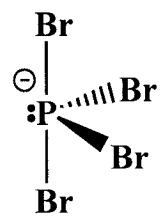

1.23a

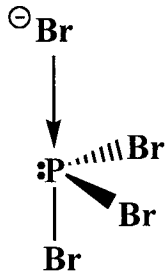

1.23b

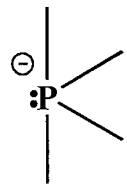

W

Phosphines can also act as Lewis acceptors in the presence of neutral donor ligands, as demonstrated by the amine and phosphine complexes of PBr_3, **1.24** and **1.25**.[49;50] An interesting example of homoatomic coordination (P→P) is seen in **1.25**, where a phosphine donor forms an adduct with a phosphine acceptor. Coordination of the neutral ligands to PBr_3 causes partial dissociation of the P-Br bonds trans to the incoming donor ligands, yet the P-Br interactions remain within the sum of the van der Waals radii for phosphorus and bromine (3.7 Å),[51] and **W** is a good representation for the phosphorus bonding environment in the complexes.

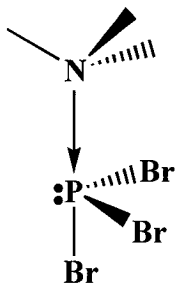

1.24

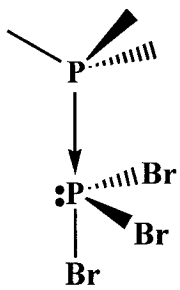

1.25

For phosphines bearing a sufficiently good leaving group (X), Lewis bases can effect nucleophilic displacement of an anion (X^-) with consequential formation of a cationic species involving a tricoordinate phosphorus(III) environment, **K** (Scheme 1.3). The resulting donor-acceptor interactions are viewed as complexes of a neutral ligand on a phosphenium cation (**1.26**),[52] and there are representative examples of arsenium[53;54] and stibenium[55] analogues. Bertrand and coworkers reported the first example of a solid state structure of a ligand-stabilized phosphenium cation in 1993 (**1.27**).[56] The complex was synthesized *via* the reaction of one equivalent of 1,5-diazabicyclo[4.3.0]non-5-ene (DBN) with a (diamino)chlorophosphine, followed by an anion exchange reaction with potassium hexafluorophosphate.

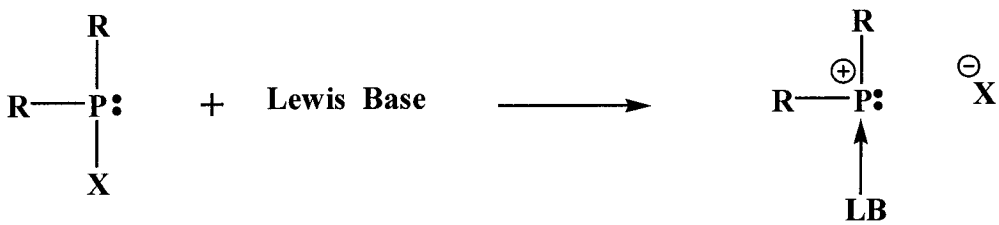

1.26

Scheme 1.3

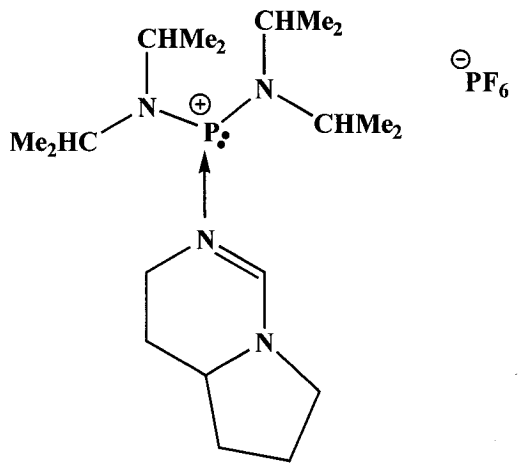

1.27

Ligand-stabilized phosphenium cations can also be generated under halide abstraction conditions. Burford and coworkers have isolated a series of complexes of dialkylphosphenium and diarylphosphenium cations from reactions of (dialkyl/diaryl)chlorophosphines with gallium trichloride.[52] As shown in Scheme 1.4, two equivalents of diphenylchlorophosphine react with one equivalent of gallium trichloride to form the phosphine-phosphenium complex **1.28**. The presence of a coordinate bond in **1.28** is confirmed by the compound's ligand exchange behaviour; addition of a more basic phosphine (e.g. PPh_3, PMe_3) to **1.28** results in quantitative release of Ph_2PCl and formation of a new phosphine-phosphenium complex **1.29**. The Lewis amphoteric nature of phosphenium cations is demonstrated in a related complex **1.30**, where the dimethylphosphenium cation is behaving as both a Lewis acid and a Lewis base simultaneously, an example of "in-series" coordination.[57]

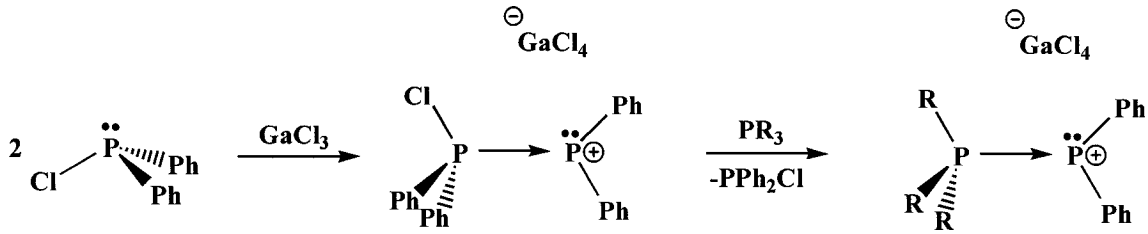

1.28 **1.29**

Scheme 1.4

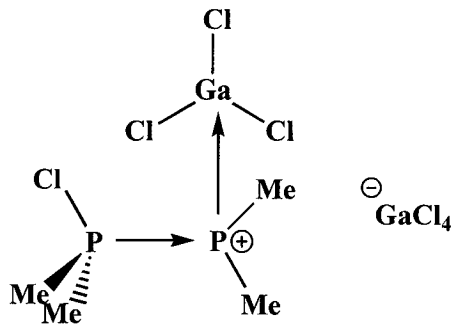

1.30

Coordinatively unsaturated phosphines (bonding environment **H**) can also behave as Lewis acids, and if they bear a sufficiently good leaving group, Lewis bases can effect nucleophilic displacement of an anion with consequential formation of a cationic species involving a dicoordinate phosphorus(III) environment. In 1994, Niecke and coworkers demonstrated that reaction of phosphaalkene **1.31** with triphenylphosphine generated the ligand-stabilized methylenediylphosphenium ion, **1.32** (Scheme 1.5).[58] This was followed by the work of Burford and coworkers in 1996, who showed that the same reaction between triphenylphosphine and iminophosphine **1.33** yielded the ligand-stabilized phosphadiazonium cation, **1.34** (Scheme 1.6).[59]

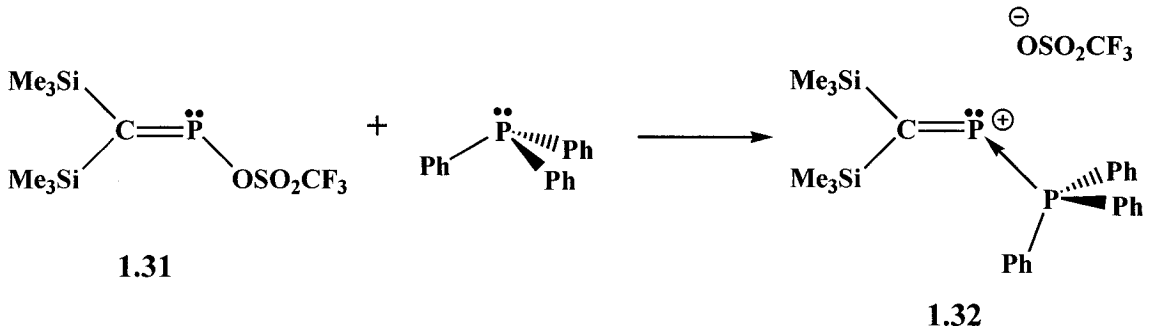

1.31 **1.32**

Scheme 1.5

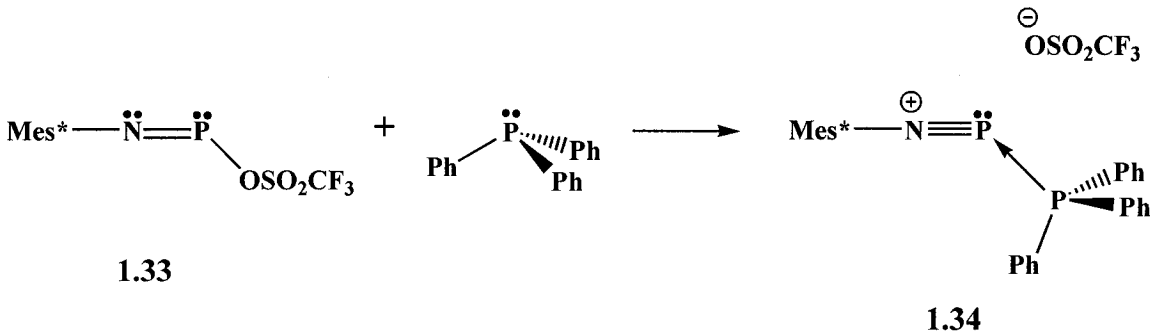

1.33 **1.34**

Scheme 1.6

As revealed in their solid state structures, complexes **1.32** and **1.34** contain distinctly different phosphorus bonding environments. The C-P bond in **1.32** (1.635(6) Å) is typical of those observed in phosphaalkenes,[32] and the sum of the angles about carbon indicates sp^2-hybridization at this centre.[58] Complex **1.32** contains a cationic example of bonding environment **H**, a dicoordinate phosphorus atom with eight valence electrons. In contrast, the P-N bond in **1.34** is very short (1.486(4) Å)[59] and similar in length to that of the P-N triple bond in the phosphadiazonium salt **1.21** (1.475(8) Å).[40] As well, the (Mes*)C-N-P angle in **1.34** is wide (169.5(4)°),[59] indicating an sp-hybridized nitrogen centre. The structural features of complex **1.34** are best described by the

hypervalent phosphorus(III) bonding environment **X**, involving a dicoordinate phosphorus atom with 10 valence electrons. Interestingly, a triphenylphosphine complex of the diphosphadiazonium cation, Mes^*PP^+ (**1.35**), isolated by Romanenko and coworkers, has structural features more akin to **1.32** than **1.34**.[60] A (Mes*)P-P double bond (2.025(1) Å) and an acute (Mes*)C-P-P angle (98.8(2)°) are observed in the complex,[60] making it another cationic example of bonding environment **H**.

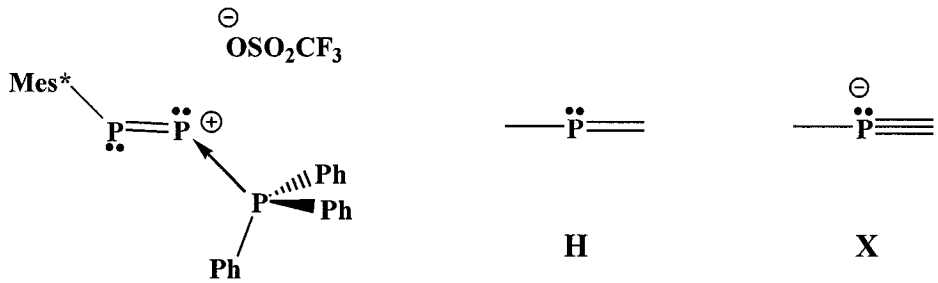

1.35

The phosphadiazonium cation is relatively stable compared to the methylenediylphosphenium and diphosphadiazonium cations. It can be isolated as a "free" salt without ligand stabilization,[40] and is less likely to isomerize or oligomerize in solution than these other low coordinate phosphorus species.[58;60] This, along with the potential to generate hypervalent phosphorus(III) bonding environments, make the phosphadiazonium cation attractive for use in coordination chemistry. The monocoordinate phosphorus centre in the cation has the potential to interact with multiple donor molecules, leading to the observation of hypervalent bonding environments **M** or **Y**.

M **Y**

The iminophosphines used to generate the phosphadiazonium cation are relatively easy to synthesize, and are ideal phosphine Lewis acids for a number of other reasons. For one, a great number of iminophosphines have been comprehensively characterized, and as a result, there is a wealth of structural and spectroscopic data already available.[61;62] In addition, iminophosphines have been the focus of several theoretical studies, and much is already known about the electronic structures of these compounds.[63;64] Finally, and perhaps most importantly, the electronic environment about the phosphorus centre in iminophosphines can be readily adjusted through varying the substituents at phosphorus and nitrogen.[65;66]

1.3 Iminophosphines and the Phosphadiazonium Cation

1.3.1 Synthesis of Iminophosphines

The first stable iminophosphine compound, **1.16**, was isolated by Niecke in 1973 through the reaction of [bis(trimethylsilyl)amino]difluorophosphine with lithium bis(trimethylsilyl)amide (Scheme 1.7).[26] The structure assigned to **1.16** was confirmed by elemental analysis, mass spectrometry, IR, and ^{1}H, ^{29}Si, and ^{31}P NMR spectroscopy. Compound **1.16** is relatively stable under mild conditions (note the use of the bulky trimethylsilyl substituents), but was found to be extremely sensitive to hydrolysis. This

reactivity with acidic protons is a feature of all iminophosphine compounds, and thus they must be handled under moisture-free conditions.

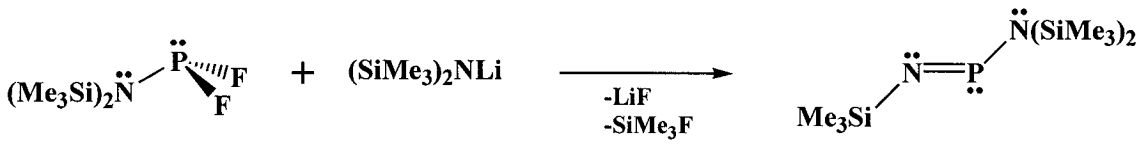

1.16

Scheme 1.7

The thermal elimination of halosilanes from (amino)halophosphines has since been used to prepare iminophosphine compounds with a variety of different substituents.[61;62] Another similar preparation method involves the thermal elimination of a lithium halide salt from an (amino)halophosphine. The *N*-lithiated (amino)halophosphine precursor is produced via H/Li-exchange starting from an appropriately substituted (monoalkylamino)halophosphine (Scheme 1.8). The metallation reaction requires the use of a strong base, B^-, which must possess a certain steric bulk (e.g., tertiarybutyl anion) in order to prevent nucleophilic addition to the phosphorus centre or, following salt elimination, addition of BH to the P-N double bond. Typically, the *N*-lithiated (amino)halophosphines are less stable than their *N*-silylated derivatives, and consequently lower temperatures can be used to promote the necessary 1,2-elimination reaction to generate the iminophosphine (< 20 °C, compared to > 150 ° C).[67]

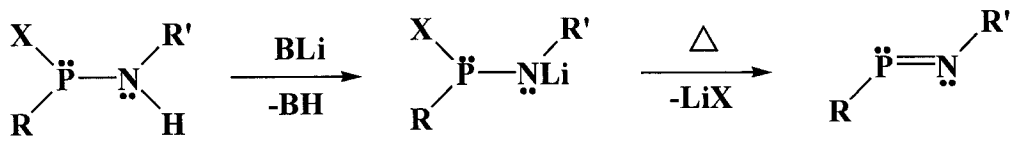

Scheme 1.8

Base-induced dehydrohalogenation reactions of (amino)halophosphines can also be used to prepare iminophosphines; however, this method is restricted to only a small number of systems where the amine nitrogen is coordinated to an extremely large, bulky substituent (i.e., Mes*).[68] If the steric bulk of the amine substituent is not sufficient (i.e, Dipp = 2,6-diisopropylphenyl), the reaction favours the formation of a phosphetidine ring (Scheme 1.9). The phosphetidine ring can be considered a cyclo-dimer of two iminophosphine monomers, and with appropriate selection of substituents, both the dimer and the monomer species can be isolated.[69]

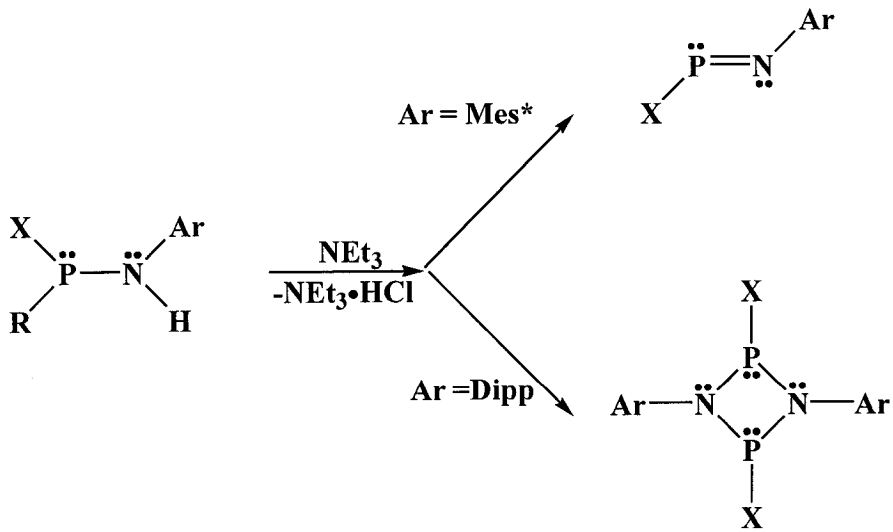

Scheme 1.9

1.3.2 Frontier Orbitals in Iminophosphines

The identity of the frontier orbitals (HOMO and LUMO) for iminophosphines are highly dependent on substituent effects.[65;66] The energetically high lying orbitals in iminophosphines are the π- and π*-orbitals of the P-N π-bond, and the σ_n-orbital from the lone pair at the phosphorus atom. Depending upon the substituents present at phosphorus and nitrogen, there are two possible frontier orbital arrangements (Figure 1.2):

1. The HOMO is a π-orbital and the LUMO is a π*-orbital, giving the iminophosphine the same frontier orbitals as an alkene.

2. The HOMO is a σ-orbital and the LUMO is a π*-orbital, giving the iminophosphine the same frontier orbitals as a singlet carbene.

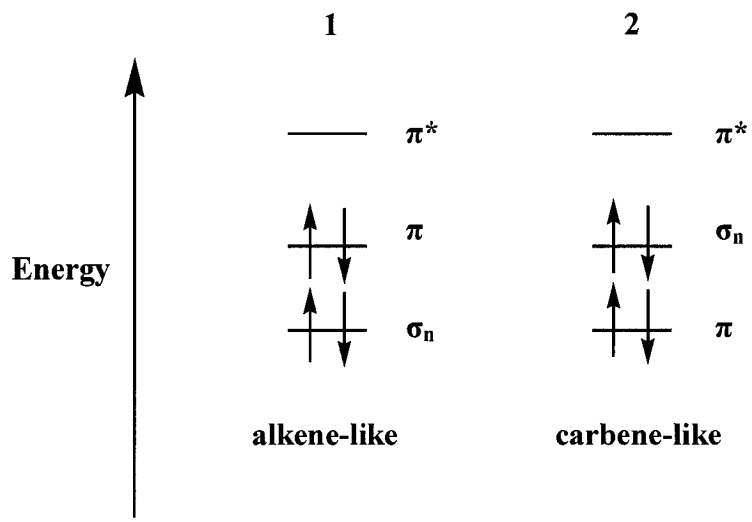

Figure 1.2 Possible frontier orbital energy sequences for iminophosphines.

Generally speaking, *P*-alkyl-substituted iminophosphines demonstrate carbene-like reactivity, while *P*-amino-substituted iminophosphines demonstrate olefin-like reactivity. It is postulated that the attachment of π-donating substituents (i.e., amino) at phosphorus produces an inversion of the energetic sequence of the σ- and π-orbitals in iminophosphines. The formation of a delocalized π-bonding system in the molecule is accompanied by a strong destabilization of the π-orbital that raises it in energy above the σ-orbital, creating a different set of frontier orbitals for these species.[65]

Regardless of the identity of the HOMO, and the reactivity derived therefrom, the LUMO in iminophosphine compounds is a N-P π*-orbital that is predominantly phosphorus in character.[63] The P-N bond in iminophosphines is polarized such that the phosphorus centre carries a partial positive charge (N = -0.81, P = +0.49),[63] and this charge distribution, along with the identity of the LUMO, causes the phosphorus atom to act as the Lewis acidic site in an iminophosphine molecule. Cowley and coworkers demonstrated that the phosphorus centre was the preferred site of attack in the reduction of *P*-(amino)iminophosphines with $LiAlH_4$/water (Scheme 1.10).[70;71] Deuterium labelling experiments were used to demonstrate that the hydride adds first to phosphorus, forming the *P*-hydrophosphinoamide salt **1.36**, which was then hydrolyzed to the diaminophosphine **1.37**.

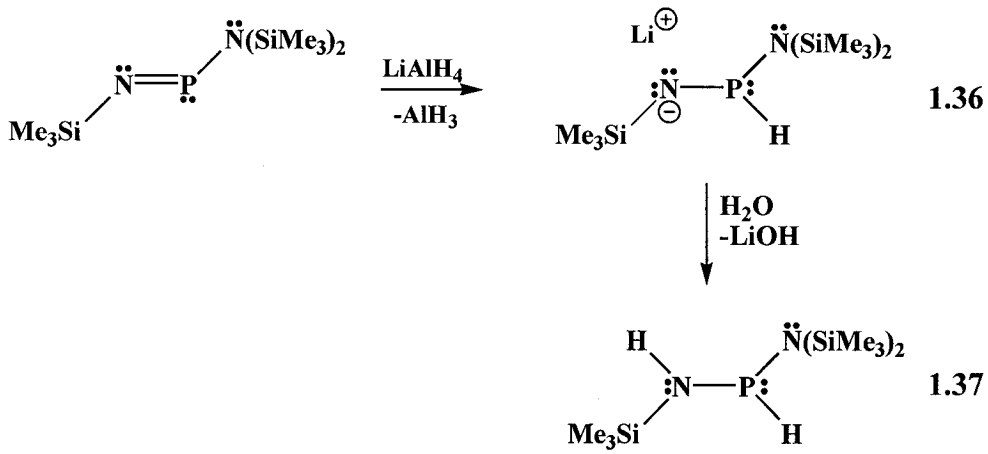

Scheme 1.10

1.3.3 Structural Features of Iminophosphines

Substituents not only affect the identity of the frontier orbitals in iminophosphines, but also the structural features of the compounds themselves. For example, the length of the P-N multiple bonds observed in iminophosphines vary significantly from 1.467(4) Å to 1.619(2) Å.[72;73] The large amount of structural data for iminophosphines prompted Schoeller and coworkers to categorize the effects of various substituents on the P-N double bond.[74;75] Their observations are as follows:

1. At phosphorus, a σ-accepting substituent (e.g., F) strengthens while a σ-donating substituent (e.g., SiH_3) weakens the P-N bond.

2. At nitrogen, the reverse is true, that is, the substituents exert the opposite effects to those described in 1.

3. At phosphorus and /or nitrogen, π-donor substituents weaken the P-N bond.

4. Overall, σ- and π-effects superimpose each other, being either additive or counteractive.

According to these observations, the P-N bond is maximally strengthened by a suitable combination of a σ-acceptor at phosphorus and a σ-donor at nitrogen. This substitution pattern is often referred to as "σ-push-pull substitution", where the σ-acceptor at phosphorus provides the pull and the σ-donor at nitrogen provides the push.[74]

The effects of σ-push-pull substitution on the P-N double bond can be rationalized using a simple molecular orbital model. Consider the MO energy diagrams for the π-systems of HPNH (**1.38**) and $FPNSiMe_3$ (**1.39**) in Figure 1.3. The π-bond in an iminophosphine is formed from the parallel overlap of a 3p orbital on phosphorus and a 2p orbital on nitrogen. The replacement of the hydrogen substituent at phosphorus by a stronger σ-acceptor, fluorine, causes the phosphorus atom to become more electron deficient, resulting in a lowering of energy of its 3p atomic orbital. The replacement of the hydrogen substituent at nitrogen by a stronger σ-donor, $SiMe_3$, causes the nitrogen atom to become more electron rich, resulting in a raising of energy of its 2p atomic orbital. As a result of σ-push-pull substitution, the energy separation between the phosphorus and nitrogen atomic orbitals is decreased. This leads to more effective orbital overlap, which stabilizes the energy of the π-bonding molecular orbital, leading to a stronger and shorter bond.

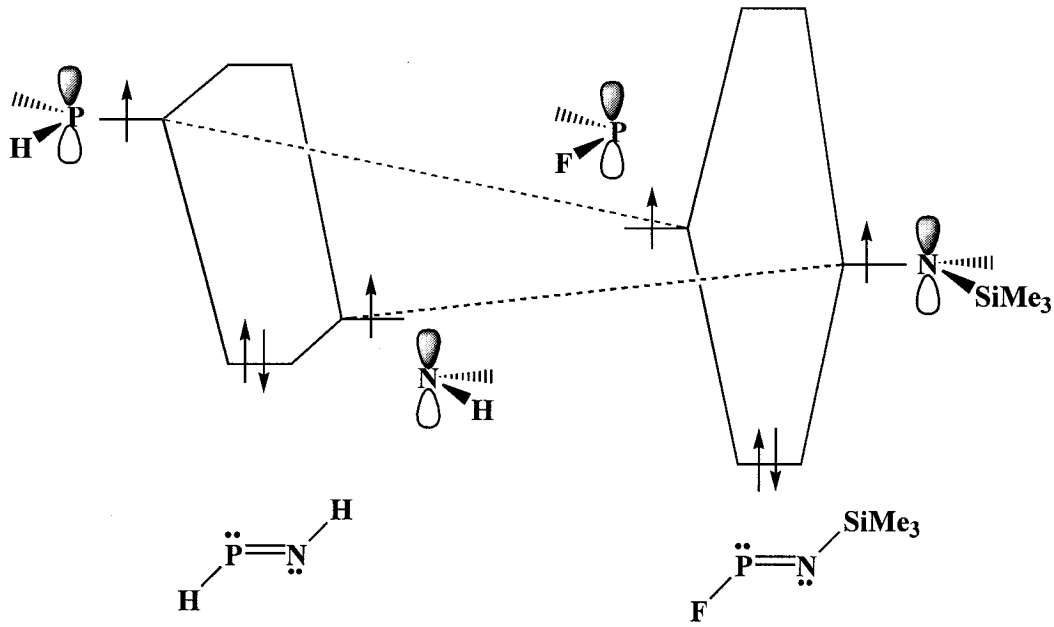

1.38 **1.39**

Figure 1.3 Molecular orbital energy diagrams for the π-systems in HPNH (**1.38**) and $FPNSiMe_3$ (**1.39**).

As would be predicted by the σ-push-pull substitution model, *P*-halo-, *P*-oxy, and *P*-sulfonyloxy-substituted iminophosphines contain the shortest P-N multiple bonds (Table 1.1). These compounds are more reactive than their *P*-amino-substituted analogues, and require the presence of a large, bulky Mes* (2,4,6-tri-*t*-butylphenyl) group at nitrogen for kinetic stabilization. Although amino groups are also σ-withdrawing substituents, their superior π-donor capability stabilizes the electron deficient phosphorus centres in *P*-aminoiminophosphines, and as a result, these compounds are less susceptible to oligomerization reactions than their *P*-halo, *P*-oxy, and *P*-sulfonyloxy-substituted analogues.

Table 1.1 Selected bond lengths (Å) and angles (°) for iminophosphines Mes*NPX.

X	P-N	(Mes*)C-N-P	P-X	Reference
Cl	1.495(4)	154.8(4)	2.127(1)	40;76
Br	1.499(6)	161.0(6)	2.337(2)	40;76
I	1.480(9)	172.5(3)	2.895(1)	62
$OSiMe_3$	1.529(3)	144.4(2)	1.585(3)	72
OSO_2-p-Me-C_6H_4	1.492(4)	150.1(3)	1.728(3)	72
OC^tBu_3	1.487(5)	175.3(4)	1.615(4)	72
OSO_2CF_3	1.467(4)	176.4(3)	1.923(3)	72

In considering some of the other structural features of iminophosphines Mes*NPX (X = halogen, oxy, or sufonyloxy) presented in Table 1.1, an interesting trend emerges. As the P-N bond length becomes shorter, the (Mes*)C-N-P angle becomes wider, and the P-X bond length increases in ionic character. The most extreme example of this is seen in the iminophosphine, Mes*NPOTf (**1.33**, OTf = trifluoromethyl-sulfonyloxy or triflate), where the P-N bond length is only 1.467(4) Å and the bond angle at nitrogen is nearly linear (176.4(3)°).[72] The P-O bond length in Mes*NPOTf is significantly longer (1.923(3) Å) than a typical phosphorus-oxygen single bond (1.63 Å)[77] and thus implicates a high degree of ionic character in Mes*NPOTf.

This trend in bond lengths and angles can be explained if the iminophosphines Mes*NPX are thought of as resonance hybrids of the covalently bound species **1.40** and the phosphadiazonium salt **1.41** (Scheme 1.11). As the ionic character of the P-X bond increases, the phosphadiazonium resonance contributor **1.41** becomes more important, and thus shorter P-N bonds and wider (Mes*)C-N-P angles are observed. The partial dissociation of the P-X bond in iminophosphines Mes*NPX enhances the Lewis acidity of the phosphorus centres in these compounds. Interaction of a neutral donor ligand with

Mes*NPX results in nucleophilic displacement of X^- from phosphorus to yield a ligand-stabilized phosphadiazonium cation.

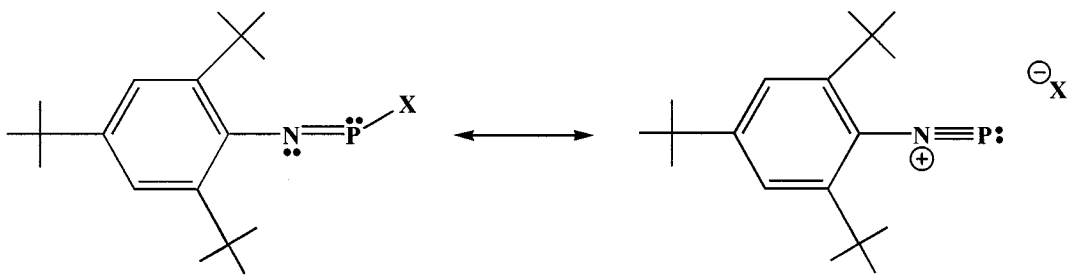

1.40 **1.41**

Scheme 1.11

1.4 Coordination Complexes of the Phosphadiazonium Cation

As discussed in Section 1.1, the phosphadiazonium salt [Mes*NP]$AlCl_4$ (**1.21**) represents the first example of a structurally characterized P-N triple bond; however, close inspection of the solid state structure reveals that there is a toluene solvent molecule in close proximity to the phosphorus centre of the phosphadiazonium cation.[40] As well, long contacts (greater than 3.0 Å) exist between the phosphorus centre of the cation and the chlorine atoms of the anion. It would appear that the coordinatively unsaturated and electron deficient phosphorus centre in the phosphadiazonium cation requires some stabilization from nearby π- and σ-electron donors.

This hypothesis is supported by the work of Burford and coworkers, who comprehensively characterized a series of gallate ($GaCl_4^-$) and digallate ($Ga_2Cl_7^-$) salts of arene complexes of the phosphadiazonium cation.[78;79] The salts were crystallized from

three different arene solvents (benzene, toluene, and mesitylene), and in all cases the phosphorus centre in the $Mes*NP^+$ cation is hexahapto-bound (η^6) to an arene ring. The phosphorus centre represents an orthogonal projection from the centroid of the arene, and the P-arene(centroid) distances (benzene > toluene > mesitylene) are in accord with the π-donor capabilities of the arene.[79] The salts [Mes*NP·arene][An] (**1.42**, An = $GaCl_4^-$ or $Ga_2Cl_7^-$) can therefore be viewed as Lewis acid-base adducts between an arene π-donor and a phosphadiazonium Lewis acceptor.

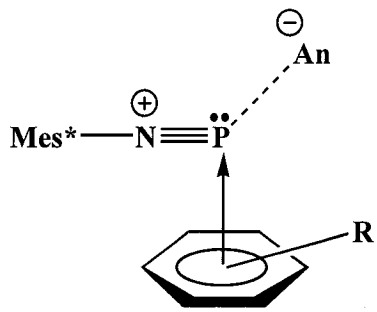

1.42

Since the initial isolation of the π-donor complexes of the phosphadiazonium cation, Burford and coworkers have isolated several σ-donor complexes, illustrating the versatility of this phosphine Lewis acceptor.[4] The synthesis of the triphenylphosphine-phosphadiazonium complex, [Mes*NP·PPh_3]OTf (**1.34**),[59] from the iminophosphine Mes*NPOTf (**1.33**)[72] was described in Section 1.2. This iminophosphine has since been shown to react with a number of neutral donor ligands, which effect nucleophilic displacement of the trifluoromethylsulfonyloxy group (OTf) as an anion.[18;80-82] The resulting cations are best described as 1:1 adducts of a neutral ligand on a phosphadiazonium Lewis acceptor ($Mes*NP^+$), and represent interesting examples of

dicoordinate (bonding environment **X**) and tricoordinate (bonding environment **Y**) phosphorus(III) centres. In most cases, ligand interactions exert only minor influence on the structural features of the acceptor Mes*NP$^+$ unit. The (Mes*)N-P bond lengths are slightly longer in the adducts than in the Lewis acid Mes*NPOTf, and the (Mes*)C-N-P angles are slightly more acute (Table 1.2), implicating retention of P-N multiple-bonding in the phosphadiazonium unit.[83]

Table 1.2 Selected bond lengths (Å) and angles (°) in coordination complexes of the phosphadiazonium cation, [Mes*NP·ligand]OTf.

Ligand	Label	P-N	P-OTf	(Mes*)C-N-P	Reference
none	**1.33**	1.467(4)	1.923(3)	176.4(3)	72
PPh_3	**1.34**	1.486(4)	2.298(4)	169.5(4)	59
pyridine	**1.43**	1.472(8)	2.712(7)	161.7(7)	80;81
quinuclidine	**1.44**	1.519(2)	2.697(3)	143.9(2)	80;81
2,2'-bipyridine	**1.45**	1.497(4)	*a*	169.4(4)	80
imidazol-2-ylidene (Im)	**1.46**	1.574(4)	2.952(5)	116.2(3)	18

[a] P-OTf distance greater than the sum of the van der Waals radii (P-O = 3.3 Å).

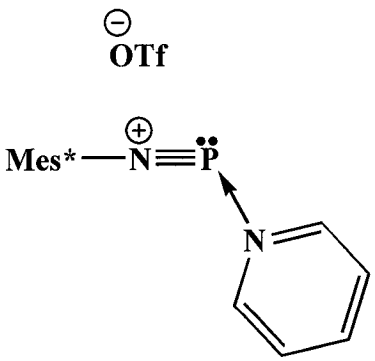

1.43

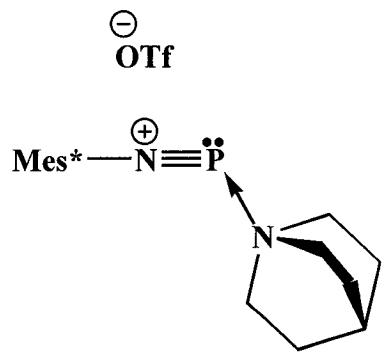

1.44

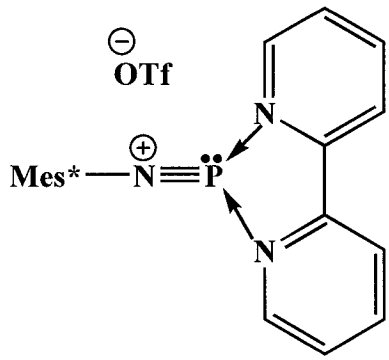

1.45

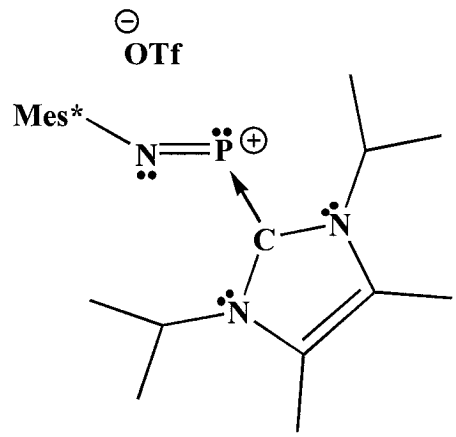

1.46

Complexes of the phosphadiazonium cation with pyridine (**1.43**),[81] quinuclidine (**1.44**),[81] and 2,2'-bipyridine (**1.45**)[80] ligands are pictured above. Single crystal X-ray diffraction studies indicate that the closest contact of the donor occurs at phosphorus in all cases, representing compounds that contain examples of N→P coordinate bonds. The coordination complex [Mes*NP·(2,2'-BIPY)]OTf (**1.45**) represents the first example of an adduct formed between the phosphadiazonium cation and a chelating bidentate ligand.[80] The coordination of both nitrogen donors to the phosphadiazonium cation does not cause significant structural perturbations in the $Mes*NP^{+}$ unit.

The strongly basic 1,3-diisopropyl-4,5-dimethyl-2-ylidene (Im) ligand also reacts with Mes*NPOTf to form a coordination complex (**1.46**).[82] Although the phosphadiazonium cation can still formally be viewed as the acceptor species, the structural features of this complex are distinct from those involving amine, pyridine, or phosphine ligands. The P-N bond length (1.574(4) Å) and the acute (Mes*)C-N-P angle (116.2(3)°) suggest the existence of a P-N double bond, rather than a P-N triple bond in [Mes*NP·Im]OTf (**1.46**).[82]

The ligand Im also forms a coordination complex with the iminophosphine Mes*NPCl (**1.20**), but in this instance coordination of the ligand does not cause anionic displacement of the chlorine bound to phosphorus. The P-Cl bond in the complex Mes*NP(Im)Cl (**1.12**, P-Cl = 2.417(2) Å)[82] is only slightly longer than in the free Lewis acceptor (Mes*NPCl, P-Cl = 2.127(1) Å),[40] and is well within the sum of the van der Waals radii for phosphorus and chlorine (3.6 Å).[51] The P-N bond in Mes*NP(Cl)Im (1.585(5) Å) is in the range typical of P-N double bonds and the sum of the angles about phosphorus (301.2°) indicates the presence of a stereochemically active lone pair.[82] As such, Mes*NP(Im)Cl represents the first example of a neutral compound containing an iminophosphide bonding environment **M**, involving a pyramidal tricoordinate phosphorus centre with a lone pair and a distinctive P-N double bond. This hypervalent phosphorus(III) bonding environment is only accessible *via* the coordination chemistry of phosphine Lewis acceptors.

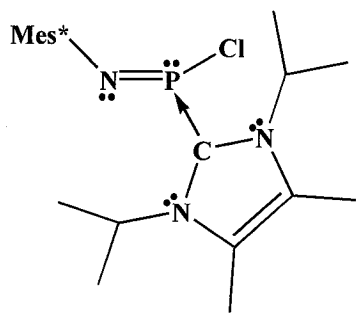

1.12

The utility of the coordination chemistry of the phosphadiazonium cation is twofold. Not only does it allow access to interesting hypervalent phosphorus(III) bonding environments, but the coordination of neutral donors to the phosphadiazonium

cation also represents a new synthetic methodology in phosphorus chemistry, where phosphorus-element (element = C, N, P) bonds are formed through donor-acceptor interactions. This chemistry can be readily extended to other main group donor atoms, and should have wide reaching synthetic applications.

1.5 Overview of Chapters in the Thesis

In the chapters to follow, several aspects of the coordination chemistry of the phosphadiazonium cation will be discussed. In Chapter 2, a new synthetic methodology for the formation of phosphorus-chalcogen (chalcogen = O, S, Se) bonds through donor-acceptor chemistry is presented. The structural features of a series of chalcogeno-urea complexes of the phosphadiazonium cation are also examined. The third chapter describes the coordination of bidentate and tridentate ligands to the phosphadiazonium cation, and the unique hypervalent phosphorus(III) bonding environments that arise in the resulting complexes. In Chapter 4, the Lewis acid chemistry of the phosphadiazonium cation is further diversified through the synthesis and characterization of the first ligand-rich complexes of a phosphorus(III) Lewis acceptor. The first examples of acceptor-rich complexes, where two phosphadiazonium cations are tethered by a bridging ligand, are also presented.

In order to develop a better appreciation of the fundamental chemistry of iminophosphines and the phosphadiazonium cation, Chapter 5 explores the role of the leaving group at phosphorus in donor-acceptor chemistry through a series of reactions of (halo)iminophosphines with an imidazol-2-ylidene donor. Chapter 6 then moves on to describe the results of spectroscopic studies (NMR, UV-Vis) on all known complexes of

the phosphadiazonium cation. The dissertation concludes by offering some general conclusions and ideas for future work in Chapter 7. Details of experimental procedures, and spectroscopic and X-ray crystallographic data are presented in Chapter 8.

Chapter 2: Chalcogeno-urea Ligands on a Phosphadiazonium Lewis Acceptor

2.1 Introduction

Many low oxidation state non-metal centres exhibit substantial Lewis acidity despite the presence of non-bonding electrons (lone pairs). Phosphines, as "classic" ligands, are perhaps the most interesting Lewis acids, and their acceptor ability offers a versatile new synthetic approach in phosphorus chemistry, demonstrated here by the isolation and characterization of the first intermolecular chalcogeno-urea complexes of the phosphadiazonium cation.

Prior to this work, complexes involving Lewis acceptor phosphorus(III) centres with arene,[79] amine,[81;84] imine,[80;81;85;86] phosphine,[39;52;57-60;87-93] gallane,[94] and carbene[18] ligands were known. With the isolation of E→P(III) coordinate bonds (E = C, N, P, Ga) already accomplished, it seemed logical to extend this donor-acceptor chemistry to the electron rich elements of Group 16, the chalcogens (Ch = O, S, Se, Te). Although some examples of Ch→P(III) (Ch = O, S) coordination have been reported in the literature, in most cases, these can be classified as weak intramolecular interactions. For instance, Holmes and coworkers have comprehensively characterized a series of electron-deficient phosphites involving intramolecular coordination of carbonyl (**2.1**),[95] sulfonyl (**2.2**),[96] and sulfide (**2.3**)[97] groups to the P(III) centre. The Ch→P(III) contacts in these compounds are quite long (**2.1**, O→P 2.788(6) Å; **2.2** O→P 2.652(5) Å; **2.3**, S→P 2.816(2) Å), yet are sufficient to enforce a distorted trigonal bipyramidal geometry on the phosphorus centre.

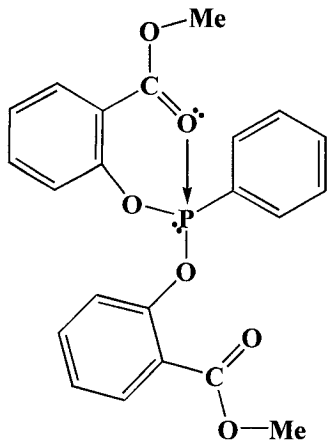

2.1

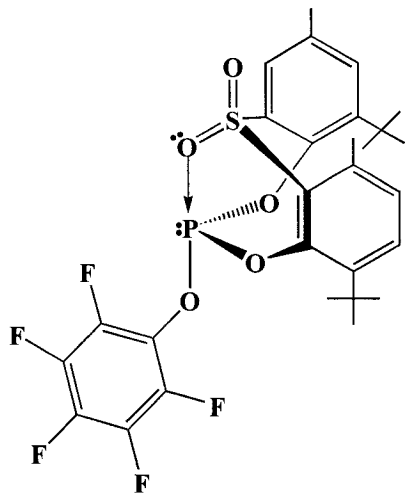

2.2

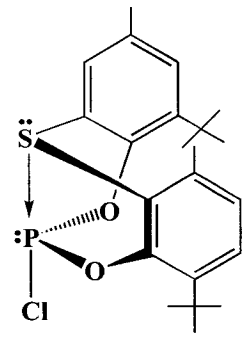

2.3

Typically, *P*-chalcogenoiminophosphines are prepared *via* the halide salt elimination reaction depicted in Scheme 2.1.[72] The use of the synthetic methodology presented here eliminates the need for metallated reagents, which can be difficult to prepare. In addition, the lack of salt formation allows for a more expedient isolation of the desired product in higher purity. The successful formation of Ch-P bonds *via* donor-acceptor chemistry illustrates the general applicability of this method to all main group element donors.

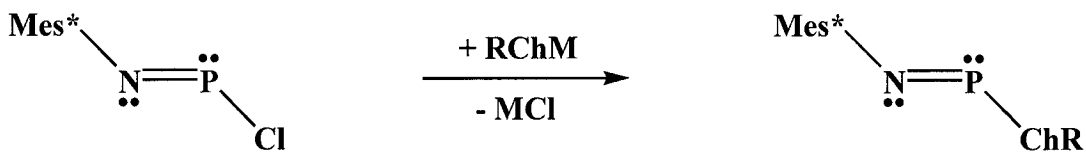

M = Li, Na, Ag
Ch = O, S

Scheme 2.1

The chalcogen donor ligands used in this study are the chalcogenoimidazolines (ChIm, **2.4**, Ch = O, S, Se, Te)[98-100] and 1,3-dimethyldiphenylurea (OU, **2.5**). The thioimidazoline SIm is a precursor compound in the synthesis of the 1,3-diisopropyl-4,5-dimethylimidazol-2-ylidene ligand (Im, **2.6**),[98] which has been used extensively as a strong base by the Burford research group.[18;82] The seleno- and telluroimidazolines are available by reaction of Im with elemental selenium and tellurium.[99;100] The chalcogenoimidazolines were initially chosen because of their ease of preparation, and their increased basicity over other chalcogen donors (the resonance contributor **2.4b** places a negative charge on the chalcogen atom). The commercially available 1,3-dimethyldiphenylurea (OU, **2.5**) was included in the study to see if acyclic urea ligands would coordinate to phosphorus in the same manner as the chalcogenoimidazolines.

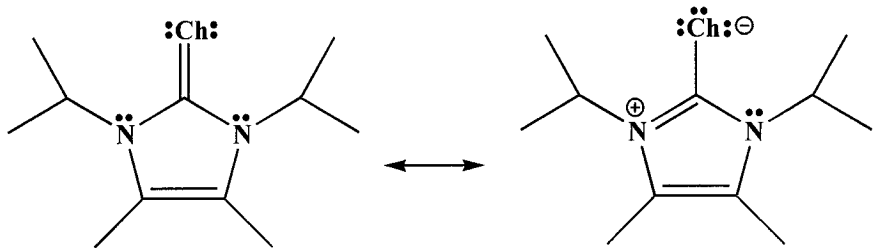

2.4, Ch = O, S, Se, Te **2.4b**

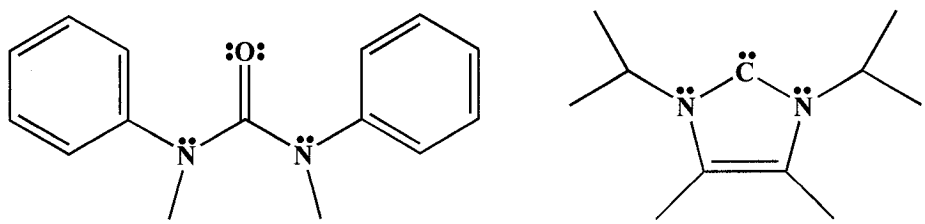

2.5 **2.6**

Andrew Phillips, a former graduate student in the Burford research group, initiated this study. He obtained the crystal structures of the adducts [Mes*NP·ChIm]OTf (**2.7**, Ch = O, S, Se), and the initial IR and NMR data; however, at the time of his departure from Dalhousie, the characterization of the compounds remained incomplete. The author of this thesis completed the characterization of [Mes*NP·SIm]OTf and [Mes*NP·SeIm]OTf, obtaining the compounds in reliable yields, and confirming that the crystals grown for X-ray diffraction studies were spectroscopically identically to the powders initially isolated. In addition to obtaining elemental analysis data, and solid state ^{31}P NMR and FT-Raman spectra for [Mes*NP·SIm]OTf and [Mes*NP·SeIm]OTf, the author also carried out the synthesis and complete characterization of the adduct [Mes*NP·OU]OTf (**2.8**). The results of the study, described in the following section, were published as a full paper in *Inorganic Chemistry* in 2003.[83]

2.2 Results and Discussion

Trifluoromethylsulfonyloxy(2,4,6-tri-*tert*-butylphenylimino)phosphine (Mes*NPOTf, **1.33**) reacts rapidly at room temperature with chalcogenoimidazolines (ChIm **2.4**, Ch = O, S, Se) and 1,3-dimethylphenylurea (OU, **2.5**). Solution ^{31}P NMR spectra of the reaction mixtures show primary components (> 90%) that correspond to the isolated products characterized as [Mes*NP·ChIm]OTf (**2.7,** Ch = O, S, Se) and [Mes*NP·OU]OTf (**2.8**), respectively. Attempts by Phillips to synthesize [Mes*NP·TeIm]OTf (**2.7**, Ch = Te) using similar procedures resulted in precipitation of a black solid that is speculated to be elemental tellurium,[101] and a signal in the ^{31}P NMR

spectrum of the reaction mixture is assigned to the previously reported imidazol-2-ylidene complex, [Mes*NP·Im]OTf (**1.46**).[82]

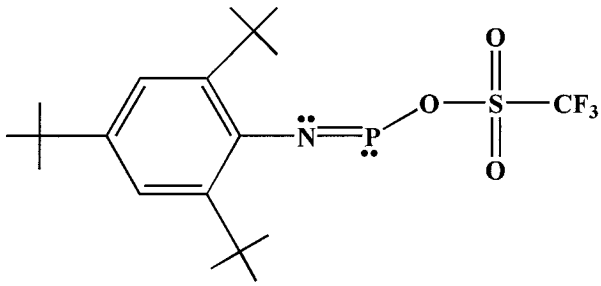

1.33

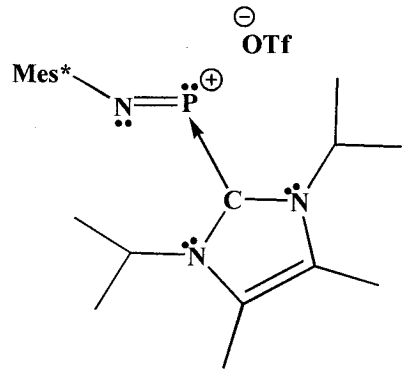

1.46

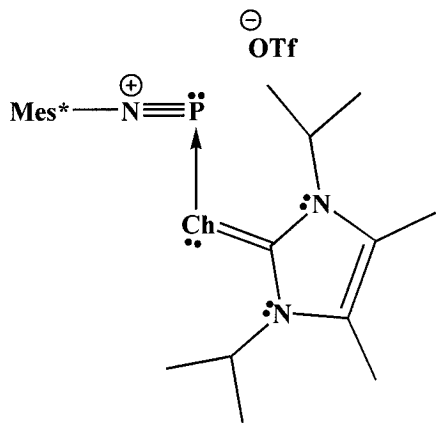

2.7, Ch = O, S, Se

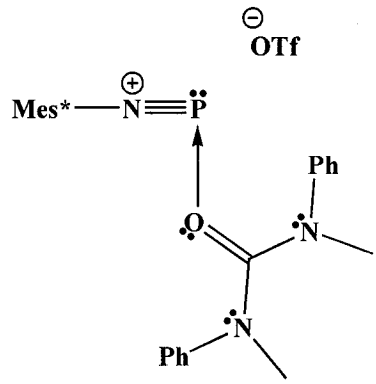

2.8

The solid state structures of [Mes*NP·ChIm]OTf (Ch = O, S, Se) and [Mes*NP·OU]OTf confirm their formulations as adducts of Mes*NPOTf. As shown in Figures 2.1 and 2.2, and quantified in Table 2.1, the closest contact of the donor occurs at phosphorus in all cases, so that the structures represent compounds that contain examples of O→P, S→P, and Se→P coordinate bonds. Solution ^{31}P NMR studies have shown that

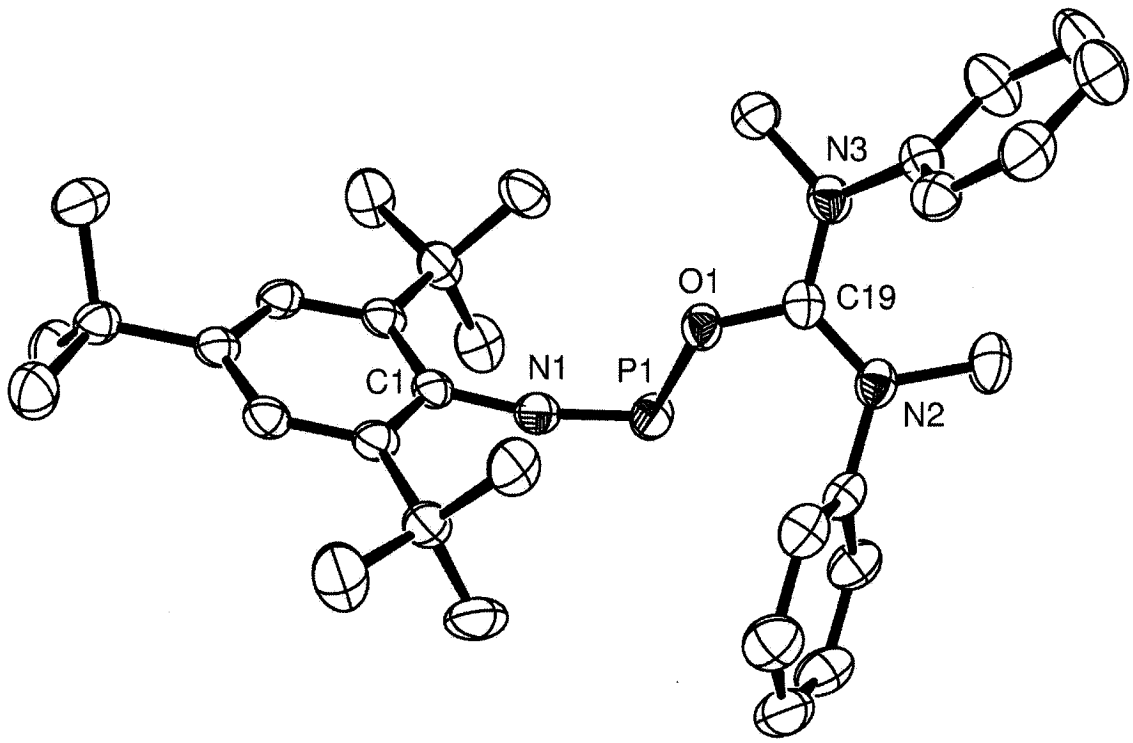

Figure 2.1 Solid state structure of the cation in [Mes*NP·OU]OTf (**2.8**) drawn with 50% probability displacement ellipsoids. Hydrogen atoms have been omitted for clarity.

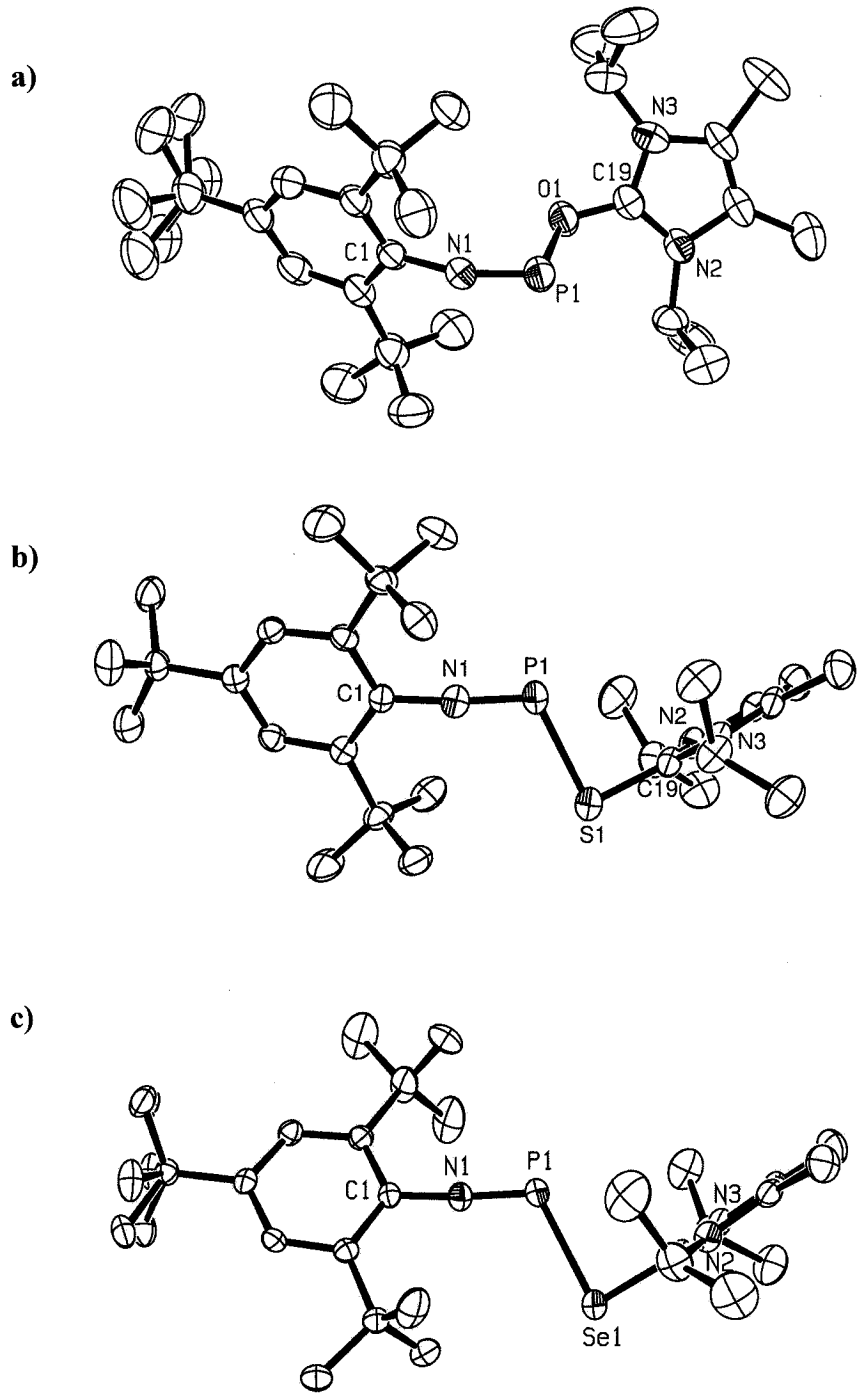

Figure 2.2 Solid state structure of the cations in (a) [Mes*NP·OIm]OTf (**2.7**, Ch = O), (b) [Mes*NP·SIm]OTf (**2.7**, Ch = S), and (c) [Mes*NP·SeIm]OTf (**2.7**, Ch = Se) drawn with 50% probability displacement ellipsoids. Hydrogen atoms have been omitted for clarity. The *p-tert*-butyl group of the Mes* substituent is disordered between two positions in [Mes*NP·OIm]OTf and [Mes*NP·SeIm]OTf. Data obtained from reference 101.

Table 2.1 Selected bond lengths (Å), angles (°), and torsion angles (deg) for [Mes*NP·OIm]OTf (**2.7**, Ch = O),[101] [Mes*NP·OU]OTf (**2.8**), [Mes*NP·SIm]OTf (**2.7**, Ch = S),[101] SIm (**2.4**, Ch = S),[101] [Mes*NP·SeIm]OTf (**2.7**, Ch = Se),[101] and SeIm (**2.4**, Ch = Se)[99].

[Mes*NP·OIm]OTf[101]	[Mes*NP·OU]OTf	[Mes*NP·SIm]OTf[101]	SIm[101]	[Mes*NP·SeIm]OTf[101]	SeIm[99]
P(1)-N(1) 1.494(3)	P(1)-N(1) 1.486(2)	P(1)-N(1) 1.498(2)		P(1)-N(1) 1.500(2)	
P(1)-O(1) 1.773(3)	P(1)-O(1) 1.790(2)	P(1)-S(1) 2.266(1)		P(1)-Se(1) 2.407(9)	
P(1)-O(4) 2.774(4)	P(1)-O(4) 2.942(3)				
N(2)-C(19) 1.330(5)	N(2)-C(19) 1.331(3)	N(2)-C(19) 1.346(3)	N(1)-C(1) 1.357(4)	N(2)-C(19) 1.345(3)	N(1)-C(1) 1.357(3)
N(3)-C(19) 1.336(5)	N(3)-C(19) 1.334(3)	N(3)-C(19) 1.358(3)	N(1A)-C(1) 1.357(4)	N(3)-C(19) 1.355(3)	N(1A)-C(1) 1.357(3)
N(1)-C(1) 1.404(5)	N(1)-C(1) 1.405(3)	N(1)-C(1) 1.382(3)		N(1)-C(1) 1.381(3)	
O(1)-C(19) 1.342(5)	O(1)-C(19) 1.317(3)	S(1)-C(19) 1.736(3)	S(1)-C(1) 1.690(5)	Se(1)-C(19) 1.889(3)	Se(1)-C(1) 1.853(4)
C(1)-N(1)-P(1) 159.7(3)	C(1)-N(1)-P(1) 166.2(2)	C(1)-N(1)-P(1) 174.4(2)		C(1)-N(1)-P(1) 175.5(2)	
N(1)-P(1)-O(1) 107.5(2)	N(1)-P(1)-O(1) 105.72(9)	N(1)-P(1)-S(1) 114.11(9)		N(1)-P(1)-Se(1) 115.35(9)	
N(2)-C(19)-N(3) 110.9(4)	N(2)-C(19)-N(3) 122.9(2)	N(2)-C(19)-N(3) 107.5(2)	N(1)-C(1)-N(1A) 106.3(4)	N(2)-C(19)-N(3) 108.1(2)	N(1)-C(1)-N(1A) 106.4(3)
C(19)-O(1)-P(1) 120.5(3)	C(19)-O(1)-P(1) 124.8(13)	C(19)-S(1)-P(1) 91.78(9)		C(19)-Se(1)-P(1) 88.29(8)	
N(2)-C(19)-O(1) 126.0(4)	N(2)-C(19)-O(1) 120.5(2)	N(2)-C(19)-S(1) 125.6(2)	N(1)-C(1)-S(1) 126.9(2)	N(2)-C(19)-Se(1) 125.4(2)	N(1)-C(1)-Se(1) 126.8(1)
N(3)-C(19)-O(1) 123.1(4)	N(3)-C(19)-O(1) 116.6(2)	N(3)-C(19)-S(1) 126.7(2)	N(1A)-C(1)-S(1) 126.9(2)	N(3)-C(19)-Se(1) 126.4(2)	N(1A)-C(1)-Se(1) 126.8(1)
P(1)-O(1)-C(19)-N(2) 60.7(6)	P(1)-O(1)-C(19)-N(2) -44.2(3)	P(1)-S(1)-C(19)-N(2) -97.0(2)		P(1)-Se(1)-C(19)-N(2) 97.8(2)	
P(1)-O(1)-C(19)-N(3) -120.4(4)	P(1)-O(1)-C(19)-N(3) 136.2(2)	P(1)-S(1)-C(19)-N(3) 77.4(2)		P(1)-Se(1)-C(19)-N(3) -76.3(2)	
N(1)-P(1)-O(1)-C(19) 170.4(3)	N(1)-P(1)-O(1)-C(19) -178.6(2)	N(1)-P(1)-S(1)-C(19) 168.6(1)		N(1)-P(1)-Se(1)-C(19) -171.9(14)	
C(1)-N(1)-P(1)-O(1) -5.3(10)	C(1)-N(1)-P(1)-O(1) 14.4(8)	C(1)-N(1)-P(1)-S(1) -148(2)		C(1)-N(1)-P(1)-Se(1) 148(3)	

ethers and ketones do not coordinate to the phosphadiazonium cation in solution, and as such, the urea functionality is necessary for the formation of an O→P coordinate bond.

The triflate (trifluoromethylsulfonyloxy, OTf) unit is structurally similar in each complex, but is modified from that in the starting iminophosphine,[72] presumably due to the significant displacement of the anion $[OTf]^-$ from the cation $[Mes^*NP{\cdot}L]^+$ (L = ligand). In the case of [Mes*NP·SIm]OTf and [Mes*NP·SeIm]OTf, the closest P-OTf contacts are greater than the sum of the van der Waals radii (P-O = 3.3 Å),[51] and the P-OTf contacts for [Mes*NP·OIm]OTf and [Mes*NP·OU]OTf (2.774(4) Å and 2.942(3) Å, respectively) are substantially greater than in the free acid Mes*NPOTf (P-O = 1.923(3) Å).[72] Solution ^{19}F NMR data of [Mes*NP·ChIm]OTf (Ch = O, S, Se) and [Mes*NP·OU]OTf give chemical shifts very similar to that of the ionic triflate salt $[^nBu_4N][OTf]$.[86] As well, peaks in the IR spectra of the complexes (1280-1265cm^{-1}) are typical of one of the asymmetric SO_3 stretching modes of unbound triflate anions.[86] Accordingly, an ionic formulation has been assigned to all adducts, and they are considered as ligand-stabilized phosphadiazonium salts. In this context, the complexes are distinct from the phosphadiazonium dichalcogenophosphinate salts $[Mes^*NP][S_2P(^tBu)_2]$ (**2.9**, Ch = S)[61] and $[Mes^*NP][Se_2P(^tBu)_2]$ (**2.9**, Ch = Se),[102] which exhibit long P-Ch cation-anion interactions.

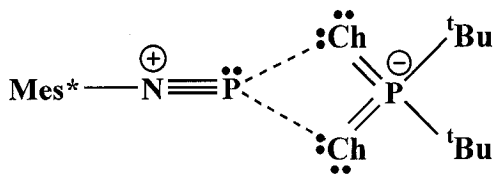

2.9, Ch = S, Se

A consistently short N(1)-P(1) bond length is observed for all complexes (OIm, N-P = 1.494(3) Å; OU, N-P = 1.486(2) Å; SIm, N-P = 1.498(2) Å; SeIm, N-P = 1.500(2) Å). It is only slightly longer than the N(1)-P(1) in the free acceptor (N-P = 1.467(4) Å),[72] and is much shorter than that observed in the carbene complex, [Mes*NP·Im]OTf (N-P = 1.574(4) Å).[82] Retention of N-P multiple bonding in the complexes is also evidenced by the intense band observed in the Raman spectra at approximately 1450 cm^{-1}. A similar band observed at 1474 cm^{-1} in the Raman spectrum of Mes*NPOTf has been assigned as a N-P stretching frequency.[103] The C(1)-N(1)-P(1) angles (OIm, C-N-P = 159.7(3)°; OU, C-N-P = 166.2(2)°; SIm, C-N-P = 174.4(2)°; SeIm, C-N-P = 175.5(2)°) are all more acute than that of the free Lewis acid Mes*NPOTf (C-N-P = 176.4(3)°).[72] However, the angular adjustments upon coordination of ChIm and OU to phosphorus are not as dramatic as that observed for coordination of the carbene in [Mes*NP·Im]OTf (C-N-P = 116.2(3)°).[82]

Table 2.2 Selected bond lengths (Å) and angles (°) in complexes [Mes*NP·L]OTf.

Ligand (L)	Label	N(1)-P(1)	P(1)-OTf	C(1)-N(1)-P(1)	Reference
none	**1.33**	1.467(4)	1.923(3)	176.4(3)	72
pyridine	**1.43**	1.472(8)	2.712(7)	161.7(7)	81
PPh_3	**1.34**	1.486(4)	2.298(4)	161.7(7)	59
OU	**2.8**	1.486(2)	2.942(3)	166.19(17)	83
OIm	**2.7**	1.494(3)	2.774(4)	159.7(3)	83;101
SIm	**2.7**	1.4982)	-[a]	174.4(2)	83;101
SeIm	**2.7**	1.500(2)	-[a]	175.5(2)	83;101
quinuclidine	**1.44**	1.519(2)	2.697(3)	143.9(2)	81
Im	**1.46**	1.574(4)	2.952(5)	116.2(3)	82

[a] P(1)-OTf distance greater than the sum of the van der Waals radii (P-O = 3.3 Å).

A summary of N(1)-P(1) bond lengths and C(1)-N(1)-P(1) bond angles for all reported complexes [Mes*NP·L]OTf is presented in Table 2.2. It is clear that in most cases the ligand causes little distortion in the Mes*NPOTf framework; the complexes retain very short N(1)-P(1) bond lengths and large C(1)-N(1)-P(1) angles. The structure of [Mes*NP·Im]OTf is anomalous with a long N-P bond and a narrow angle at nitrogen, which may be related to the relatively high basicity of the ligand (cf. pK_a ImH^+ = 23,[104] pK_a pyridineH^+ = 5.2[105]). As the basicity of the ligand increases, more electron density is donated into the acceptor N-P π*-orbital of Mes*NPOTf, which weakens the N-P π-bond in the coordination complex.

The structural features of the imidazole fragments in all [Mes*NP·ChIm]OTf compounds are identical to, or differ only slightly from, those of the corresponding free ligands. Coordination effects slight elongation of the C-Ch bonds (C-S = 1.736(3) Å, cf. 1.690(5) Å;[101] C-Se = 1.889(3) Å, cf. 1.853(4) Å[99]), which are shorter than typical C-Ch single bonds (C-S =1.819(19) Å; C-Se = 1.892(17) Å)[106] and identical (within experimental error) to those reported for ChIm-pentacarbonylchromium complexes (**2.10**, C-S = 1.737(5) Å; C-Se = 1.892(17) Å).[107]

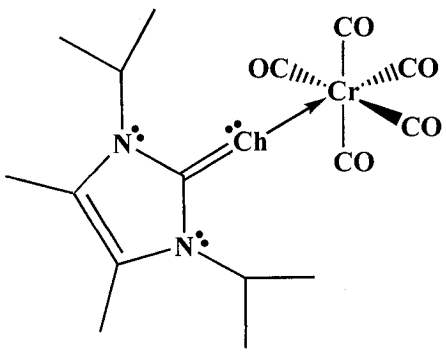

2.10, Ch = S, Se

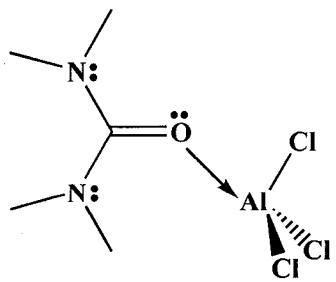

2.11

Solid state structures of OIm and OU have not been determined, but the crystal structures of tetramethylurea (C-O = 1.226(2) Å),[108] 1,3-diethyldiphenylurea (C-O = 1.217(6) Å),[109] and related cyclic saturated ureas (e.g., $OC((NH)CH_2)_2$ C-O = 1.262(4) Å)[110;111] provide a database of C-O bonds that are substantially shorter than those in [Mes*NP·OIm]OTf and [Mes*NP·OU]OTf. The C-O bond lengths in [Mes*NP·OIm]OTf (1.342(5) Å) and [Mes*NP·OU]OTf (1.317(3) Å) are still shorter than typical C-O single bonds (1.43(1) Å),[106] and are closer in length to the value observed in the tetramethylurea-$AlCl_3$ complex (**2.11**, C-O = 1.302(3) Å).[112] The OU ligand has previously been used in the coordination chemistry of the actinide elements thorium and uranium. The OU complexes $Th(OU)_3Cl_4$,[113] $U(OU)_2Cl_4$,[114] and $U(OU)_2Br_4$[114] exhibit a range of C-O bond lengths (1.24(1) – 1.31(2) Å), [113;114] that are elongated from the value expected in the free ligand, toward the value noted in [Mes*NP·OU]OTf.

The P-Ch bonds in [Mes*NP·ChIm]OTf (P-O = 1.773(3) Å; P-S = 2.266(1) Å; P-Se = 2.407(1) Å) are longer than those in typical tris(chalcogeno)phosphines (e.g., $P(OC_6H_4OMe\text{-}2)_3$, P-O = 1.624(4) Å;[115] $P(SC_6H_5)_3$, P-S = 2.122(1) Å;[116] $P(SeC_6H_5)_3$, P-Se = 2.271(2) Å[117]) and P-chalcogeno-iminophosphines (e.g., Mes*NPOR, P-O = 1.585(3) Å (R = $SiMe_3$) to 1.728(3) Å (R=$OSO_2C_6H_4(Me)$-4);[72;118-122] Mes*NPS^{t}Bu, P-S =2.098(1) Å[123]). Nevertheless, the P-Ch bonds in [Mes*NP·SIm]OTf (P-S = 2.266(1) Å) and [Mes*NP·SeIm]OTf (P-Se = 2.407(1) Å) are substantially shorter than those in the phosphadiazonium salts [Mes*NP][$S_2P(^tBu)_2$] (**2.9**, P-S = 2.442(2), 2.739(2) Å)[61] and [Mes*NP][$Se_2P(^tBu)_2$] (**2.9**, P-Se = 2.636(5), 2.788(5) Å),[102] as would be expected in comparing P-Ch coordinate bonds to P-Ch cation-anion contacts.

The complexes [Mes*NP·SIm]OTf and [Mes*NP·SeIm]OTf are isostructural, with nearly identical unit cell parameters. [Mes*NP·OIm]OTf and [Mes*NP·OU]OTf also exhibit similar structural and spectroscopic features distinct from those of the sulfur and selenium compounds. For instance, the P-Ch-C bond angles are substantially larger in [Mes*NP·OIm]OTf (120.5(3)°) and [Mes*NP·OU]OTf (124.8(1)°) than in [Mes*NP·SIm]OTf (91.8(1)°) and [Mes*NP·SeIm]OTf (88.3(1)°). Moreover, the ureas OIm and OU behave as in-plane donors, while the plane of the thio- and seleno-ureas are perpendicular to the axis of the phosphadiazonium cation (Figure 2.3). In this context, complexes of the ureas are considered to involve σ-electrons (i.e., lone pair), while the thio- and seleno-ureas ureas use π-electrons to interact with phosphorus, consistent with the established coordination chemistry of the chalcogen-based ligands.[124]

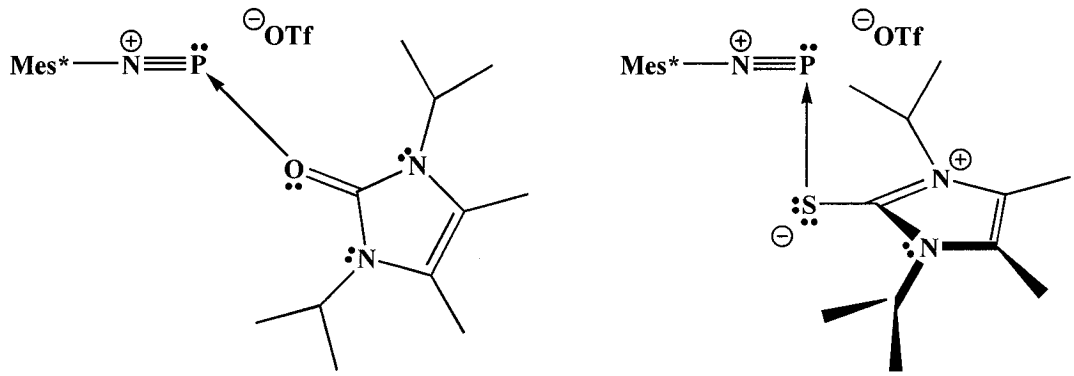

σ-electron donation **π-electron donation**

Figure 2.3 Different modes of coordination to the phosphadiazonium cation.

2.3 Conclusions

Mes*NPOTf readily forms Lewis acid-base complexes with chalcogeno-ureas to effect displacement of the OTf anion, with only minor distortion of the C-N-P iminophosphine framework. The resulting cations $[Mes^*NP{\cdot}L]^+$ are best described as complexes of a neutral ligand on a phosphadiazonium acceptor and represent a new synthetic approach to the formation of P-Ch bonds. The complexes highlight the potential for electron-rich centres to behave as Lewis acids despite the presence of a lone pair of electrons at the acceptor site.

Chapter 3: Hypervalent, Low Coordinate Phosphorus(III) Centres in Complexes of the Phosphadiazonium Cation with Chelating Ligands

3.1 Introduction

As demonstrated in the previous chapter, the iminophosphine Mes*NPOTf (**1.33**, Mes* = 2,4,6-tri-*tert*-butylphenyl, OTf = trifluoromethylsulfonyloxy, triflate)[72] is a particularly versatile reagent that engages ligands with consequential dissociation of the triflate anion. Nevertheless, with one notable exception (**1.45**),[80] coordination complexes of the phosphadiazonium cation acceptor all involve coordination of a single donor atom to phosphorus (**3.1**).[59;81-83] In an attempt to probe the limits of the acceptor capability of the phosphadiazonium cation, a series of reactions of Mes*NPOTf with both bifunctional and trifunctional chelating ligands was examined. The subsequent isolation and characterization of chelate complexes of the phosphadiazonium cation has led to the observation of new hypervalent bonding environments for phosphorus(III).

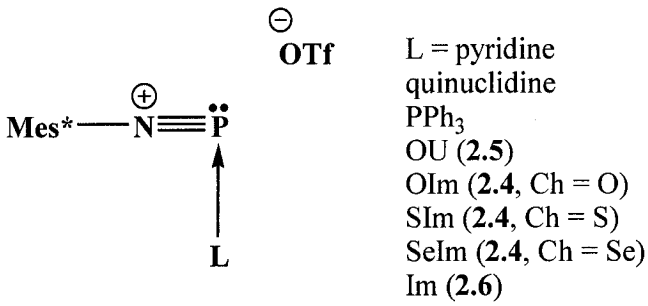

L = pyridine
quinuclidine
PPh_3
OU (**2.5**)
OIm (**2.4**, Ch = O)
SIm (**2.4**, Ch = S)
SeIm (**2.4**, Ch = Se)
Im (**2.6**)

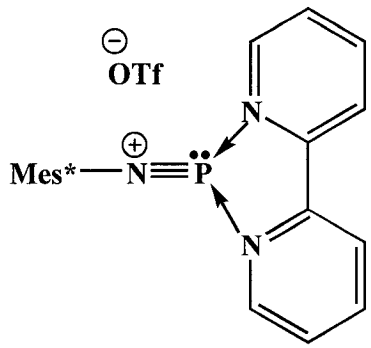

3.1 **1.45**

The first chelate complex of the phosphadiazonium cation, [Mes*NP·(2,2'-BIPY)]OTf (**1.45**) was isolated by Burford and coworkers in 2000, from the reaction of one equivalent of 2,2'-bipyridine with Mes*NPOTf.[80] The ligand binds the

phosphadiazonium acceptor *via* two indistinguishable N→P coordinate interactions, creating a five-membered PN_2C_2 ring. The planar aromatic backbone of the 2,2'-bipyridine ligand precludes other modes of coordination to the phosphadiazonium cation; however, if a bifunctional ligand with a less rigid backbone is reacted with Mes*NPOTf, such as N,N,N',N'-tetramethylethylenediamine (TMEDA, **3.2**) or 1,2-bis(dimethyl-phosphino)ethane (DMPE, **3.3**, R = Me), there are three possible outcomes: the formation of a chelate complex (**3.4**, Pn = N, P), the formation of a tethered complex involving two phosphadiazonium cations and one bifunctional ligand (**3.5,** Pn = N, P), or the formation of a pendant donor complex (**3.6,** Pn = N, P). In order to investigate these possibilities, the bifunctional ligands TMEDA, DMPE, 1,2-bis(diethylphosphino)ethane (DEPE, **3.3**, R = Et), and 1,2-bis(diphenylphosphino)ethane (DIPHOS, **3.3**, R = Ph) were reacted with Mes*NPOTf in varying stoichiometries. The results are presented in Section 3.2.

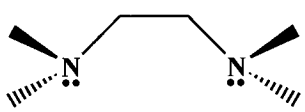

3.2

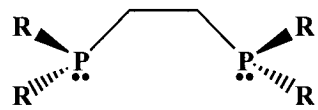

3.3, R = Me, Et, Ph

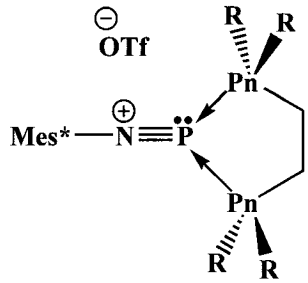

3.4, Pn = N, P

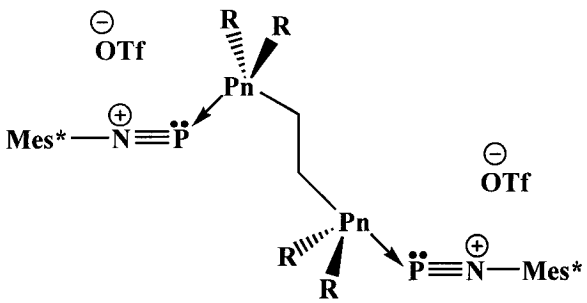

3.5, Pn = N, P

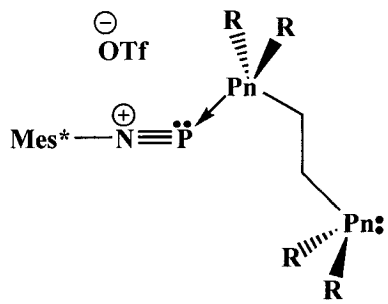

3.6, Pn = N, P

Previous to this study, Burford and coworkers observed that reaction of 1,2-bis(diphosphino)ethane ligands (**3.3**) with the diphenylphosphenium cation $[PPh_2]^+$ resulted only in the formation of tethered complexes (**3.7,** R = Me, Ph), independent of the reaction stoichiometry.[93;125] In the same year, Macdonald and coworkers discovered that reaction of DIPHOS with PI_3 yields a triphosphenium cation, which can also be depicted as a chelate complex of a phosphorus(I) cation (**3.8**).[126] Macdonald's cation is structurally similar to that previously isolated by Schmidpeter and coworkers *via* the reaction of PCl_3 and DIPHOS in the presence of a reducing agent.[89]

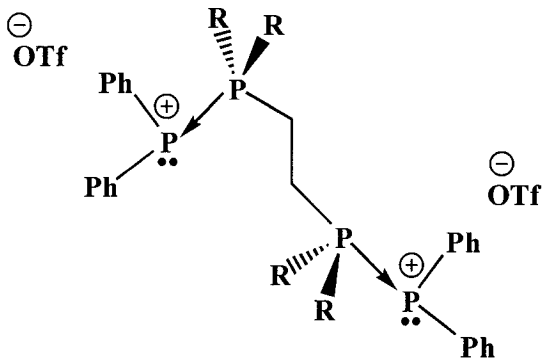

3.7, R = Me, Ph

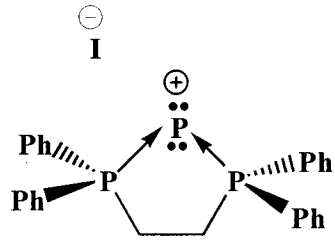

3.8

Recently, Müller and coworkers found that reaction of TMEDA with PBr_3 did not result in reduction of the phosphorus trihalide, instead a chelate complex of PBr_3 (**3.9**) was isolated, where the ligand engages in two weak N→P interactions with the phosphorus centre.[49] The phosphorus centre in the complex exhibits a distorted square pyramidal geometry, with very long P-Br bonds trans to the N→P bonds. The formation of five-membered PN_2C_2 rings, similar to that found in **3.9**, has also been observed in phosphines bearing the N,N',N'-trimethylethylenediamine substituent (**3.10**).[84;127] In these compounds, extensively characterized by Schmutzler and coworkers, ring

formation results from intramolecular N→P coordination, and consequent anionic displacement of a halide ion.[84] Gololobov and coworkers have also reported a related example of intramolecular coordination in a phosphine bearing two tethered amine ligands (**3.11**).[128;129]

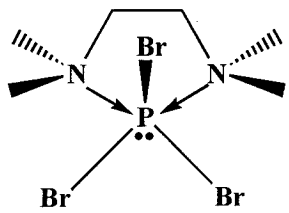

3.9

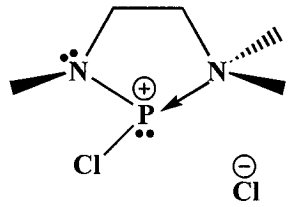

3.10

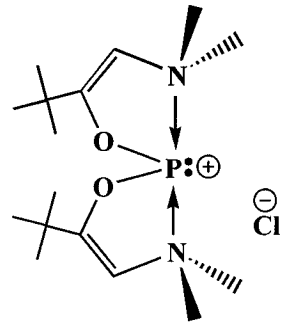

3.11

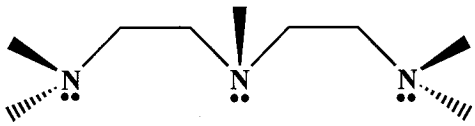

3.12

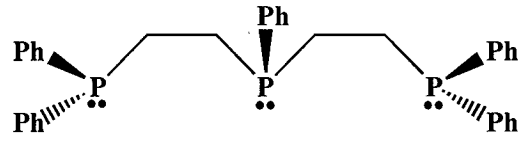

3.13

In addition to the bifunctional ligands TMEDA, DMPE, DEPE, and DIPHOS, reactions of the trifunctional ligands N,N,N,'N'',N''-pentamethyldiethylenetriamine (PMDETA, **3.12**) and bis(2-diphenylphosphinoethyl)phenylphosphine (TRIPHOS, **3.13**) with Mes*NPOTf were investigated. Like the bifunctional ligands, the trifunctional ligands have the potential to form various chelate, tethered, or pendant-donor complexes of the phosphadiazonium cation.

3.2 Results and Discussion

Mes*NPOTf reacts rapidly at room temperature with the bifunctional ligands TMEDA, DMPE, DEPE, and DIPHOS, and the trifunctional ligand PMDETA. The adducts [Mes*NP·TMEDA]OTf (**3.14**), [Mes*NP·DIPHOS]OTf (**3.15**, R = Ph), [Mes*NP·DEPE]OTf (**3.15**, R = Et), and [Mes*NP·PMDETA]OTf (**3.16**) have been isolated, independent of the imposed reaction stoichiometry, and [Mes*NP·DMPE]OTf (**3.15**, R = Me) has been identified by solution ^{31}P NMR spectroscopy. Although crystalline yields of the complexes are modest, ^{31}P NMR spectra of reaction mixtures confirm near quantitative reactions (> 90%). Structural views of each of the cations in [Mes*NP·TMEDA]OTf, [Mes*NP·DIPHOS]OTf, and [Mes*NP·PMDETA]OTf are presented in Figures 3.1 – 3.3, respectively. Selected structural parameters and ^{31}P NMR chemical shifts are presented in Table 3.1 together with corresponding parameters for Mes*NPOTf and related monodentate ligand complexes (**3.1**).

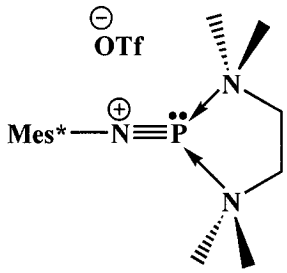

3.14

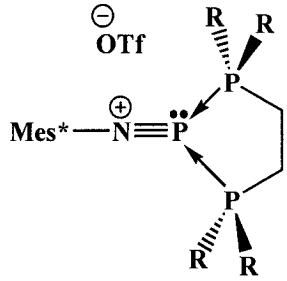

3.15, R = Me, Et, Ph

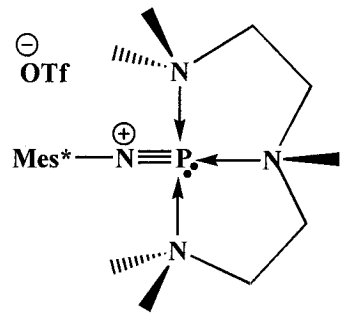

3.16

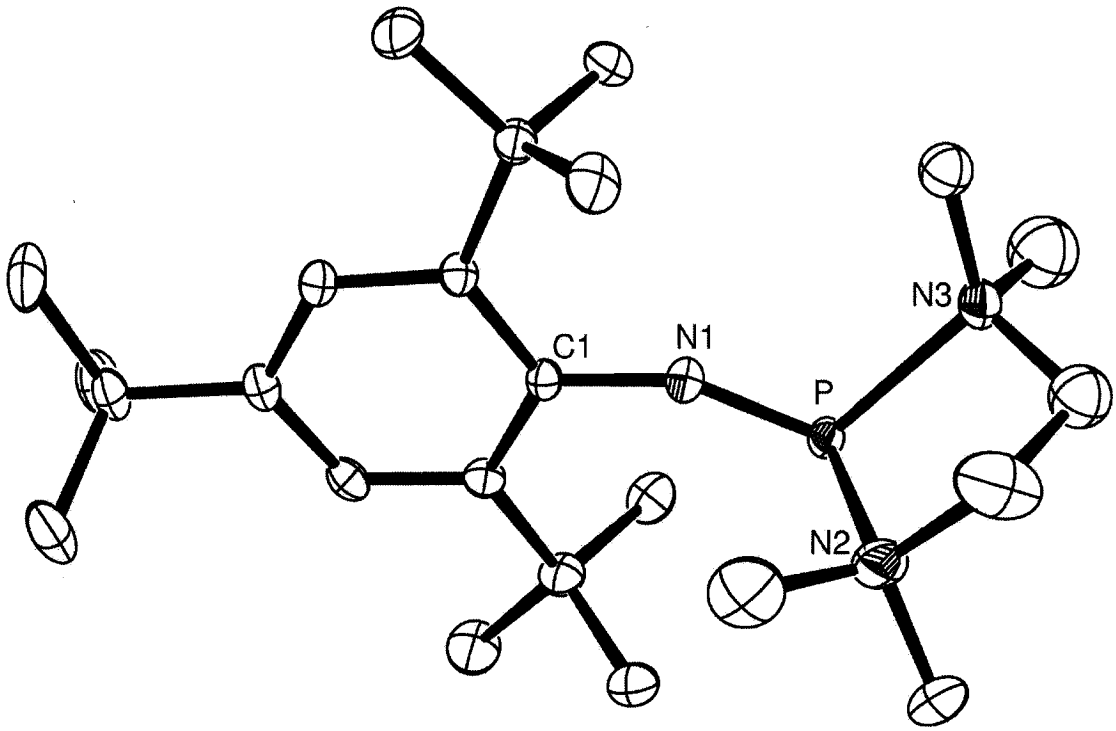

Figure 3.1 Solid state structure of the cation in [Mes*NP·TMEDA]OTf (**3.14**) drawn with 30% probability displacement ellipsoids. Hydrogen atoms and the anion have been omitted for clarity. The backbone of the TMEDA ligand is disordered over two positions (not shown).

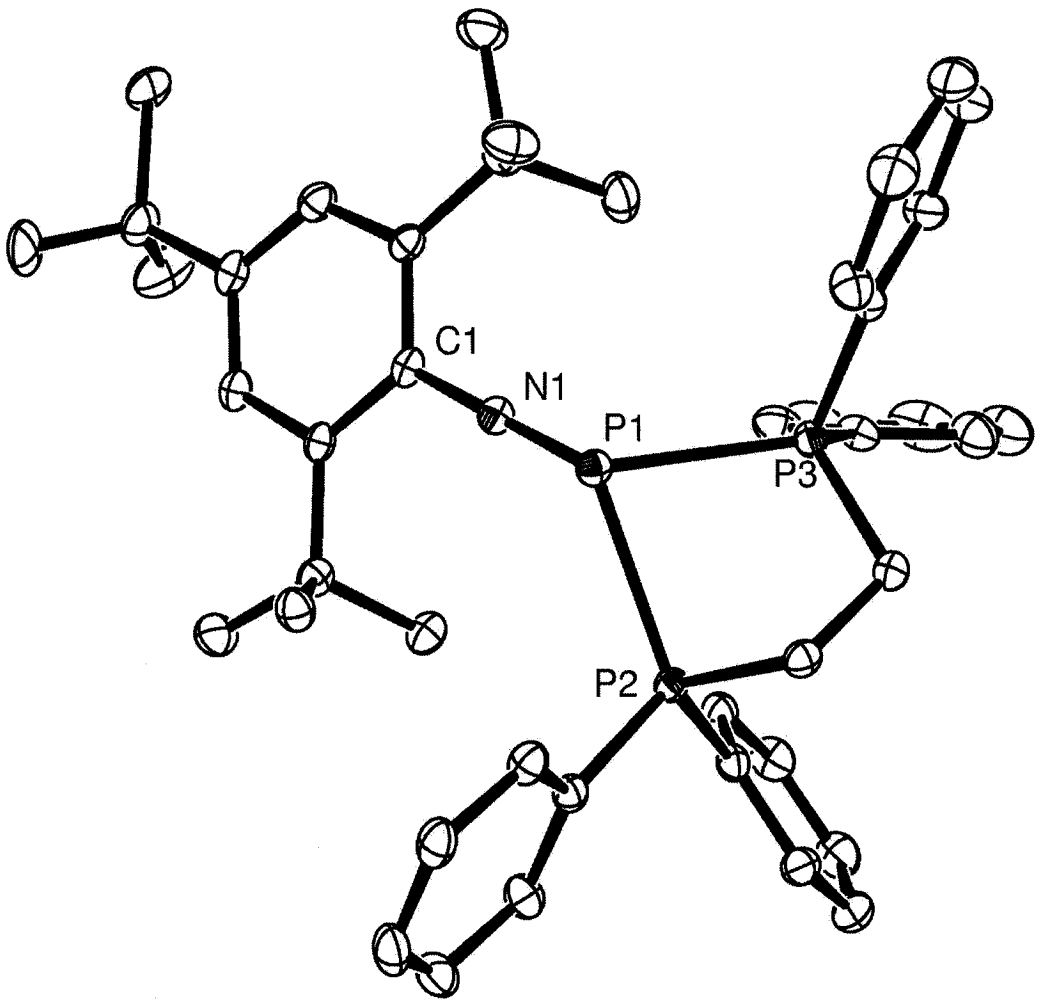

Figure 3.2 Solid state structure of the cation in [Mes*NP·DIPHOS]OTf (**3.15**, R = Ph) drawn with 30% probability displacement ellipsoids. Hydrogen atoms, the anion, and a benzene solvate molecule have been omitted for clarity. The *p-tert*-butyl group of the Mes* substituent is disordered over two positions (not shown).

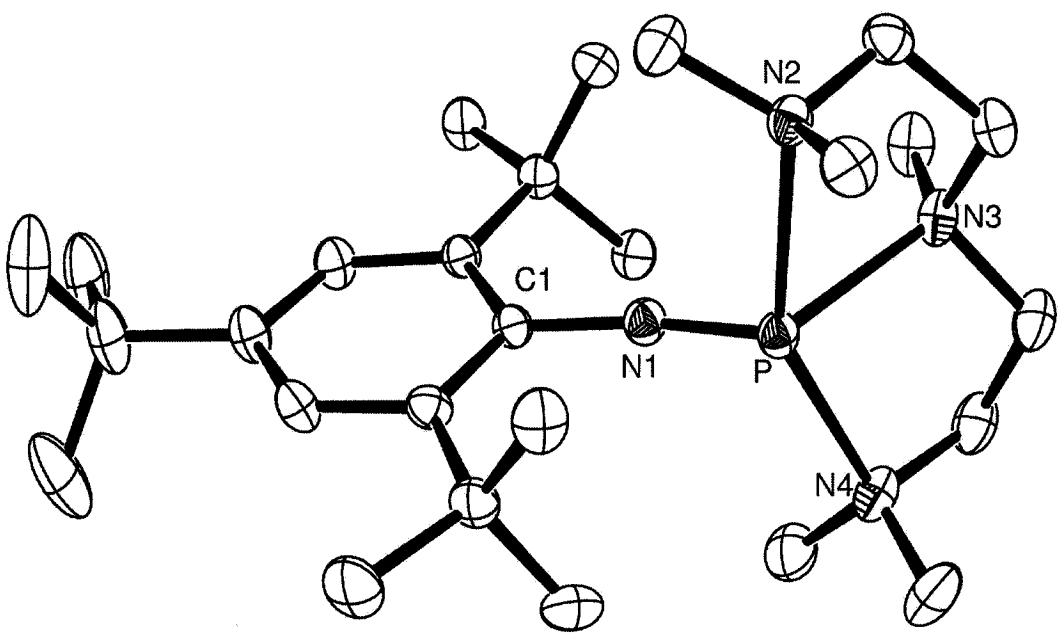

Figure 3.3 Solid state structure of the cation in [Mes*NP·PMDETA]OTf (**3.16**) drawn with 30% probability displacement ellipsoids. Hydrogen atoms, the anion, and a toluene solvate molecule have been omitted for clarity.

Table 3.1 Selected bond lengths (Å), angles (°), and ^{31}P NMR chemical shifts (ppm) for complexes [Mes*NP·L]OTf.

Ligand (L)	Label	$\delta\ ^{31}P$ (solution)	$\delta\ ^{31}P_{iso}$ (solid state)	(Mes*)N-P	(L) L→P	P-O	(Mes*)C-N-P	L-P-L	Ref.
none	**1.33**	52	49	1.467(4)	-	1.923(3)	176.4(3)	-	72
pyridine	**1.43**	71	65	1.472(8)	(N) 1.958(8)	2.712(7)	161.7(7)	-	81
quinuclidine	**1.44**	144	*a*	1.519(2)	(N) 1.933(2)	2.697(3)	143.9(2)	-	81
PPh_3	**1.34**	-5, 52[b]	-1, 71	1.486(4)	(P) 2.625(2)	2.298(4)	169.5(4)	-	59
OU	**2.8**	62	73	1.486(2)	(O) 1.790(2)	2.942(2)	166.2(2)	-	83
OIm	**2.7**	77	*a*	1.494(3)	(O) 1.773(3)	2.774(4)	159.7(3)	-	83
SIm	**2.7**	156	165	1.498(2)	(S) 2.266(1)	*e*	174.4(2)	-	83
SeIm	**2.7**	182	195	1.500(2)	(Se) 2.4068(9)	*e*	175.5(2)	-	83
Im	**1.46**	339	366	1.574(4)	(C) 1.852(5)	2.951(5)	116.2(3)	-	82
2,2'-BIPY	**1.45**	54	67	1.497(4)	(N2) 2.066(4) (N3) 2.065(4)	*e*	169.4(4)	(N) 75.10(17)	80;130
TMEDA	**3.14**	110	146	1.510(2)	(N2) 2.090(2) (N3) 2.154(3)	*e*	154.4(2)	(N) 81.99(11)	130
DIPHOS	**3.15**	10, 48[c] 10, 36[d]	-17, 12, 35	1.489(2)	(P2) 2.5392(9) (P3) 2.5708(9)	3.299(2)	179.3(2)	(N) 75.62(3)	130
DMPE	**3.15**	16, 62	*a*	*a*	*a*	*a*	*a*	*a*	130
DEPE	**3.15**	27, 53	32, 32, 49	*a*	*a*	*a*	*a*	*a*	130
PMDETA	**3.16**	89	93, 103	1.495(2)	(N2) 2.263(2) (N3) 2.436(2) (N4) 2.524(2)	*e*	164.4(2)	N2-P-N3, 77.71(8) N3-P-N4, 78.00(9) N2-P-N4, 151.82(8)	130

[a] Not determined; [b] Dissociated in solution; [c] RT, temperature dependence; [d] 193 K;
[e] P(1)-OTf distance greater than the sum of the van der Waals radii (P-O = 3.3 Å).

In each complex, the donor sites of the ligand interact primarily with the phosphorus acceptor site, effecting displacement of the triflate anion from Mes*NPOTf. The shortest P-OTf contacts in [Mes*NP·TMEDA]OTf, [Mes*NP·DIPHOS]OTf, and [Mes*NP·PMDETA]OTf are greater than or equal to the sum of the van der Waals radii for phosphorus and oxygen (P-O = 3.3 Å),[51] and are substantially greater than in the free acid Mes*NPOTf (P-O = 1.923(3) Å).[72] Consequently, the compounds represent bidentate chelate complexes (**3.14**, **3.15**) and a tridentate complex (**3.16**) of the phosphadiazonium cation.

As discussed in Section 3.1, a symmetric bidentate coordinate interaction was observed in the solid state structure of [Mes*NP·(2,2'-BIPY)]OTf (**1.45**) (N→P = 2.065(4) Å, 2.066(4) Å);[80] however, [Mes*NP·TMEDA]OTf (N→P = 2.090(2) Å, 2.154(3) Å) and [Mes*NP·DIPHOS]OTf (P→P = 2.5392(9) Å, 2.5708(9) Å) exhibit non-symmetric chelation of the phosphadiazonium cation, analogous to complexes **3.9** (N→P = 2.025(3) Å, 1.939(1) Å (isomer 1); 2.239(5) Å, 1.918(5) Å (isomer 2))[49] and **3.8** (P→P = 2.131(2) Å, 2.126(2) Å).[126] The asymmetry observed in [Mes*NP·TMEDA]OTf and [Mes*NP·DIPHOS]OTf is most likely a consequence of steric interactions occurring between the tertiarybutyl groups of the phosphadiazonium Mes* substituent and the methyl or phenyl groups on the ligands.

The inequivalence of the phosphine donor atoms in [Mes*NP·DIPHOS]OTf is apparent in the solid state ^{31}P CP-MAS NMR spectrum (Figure 3.4). The signal corresponding to the phosphadiazonium centre (P1) is a doublet of doublets due to non-equivalent coupling to the two donor phosphine centres ($^{1}J_{(P1,P2)}$ = 469 Hz and $^{1}J_{(P1,P3)}$ = 360 Hz). The donor phosphorus nuclei (P2 and P3) have different chemical shifts

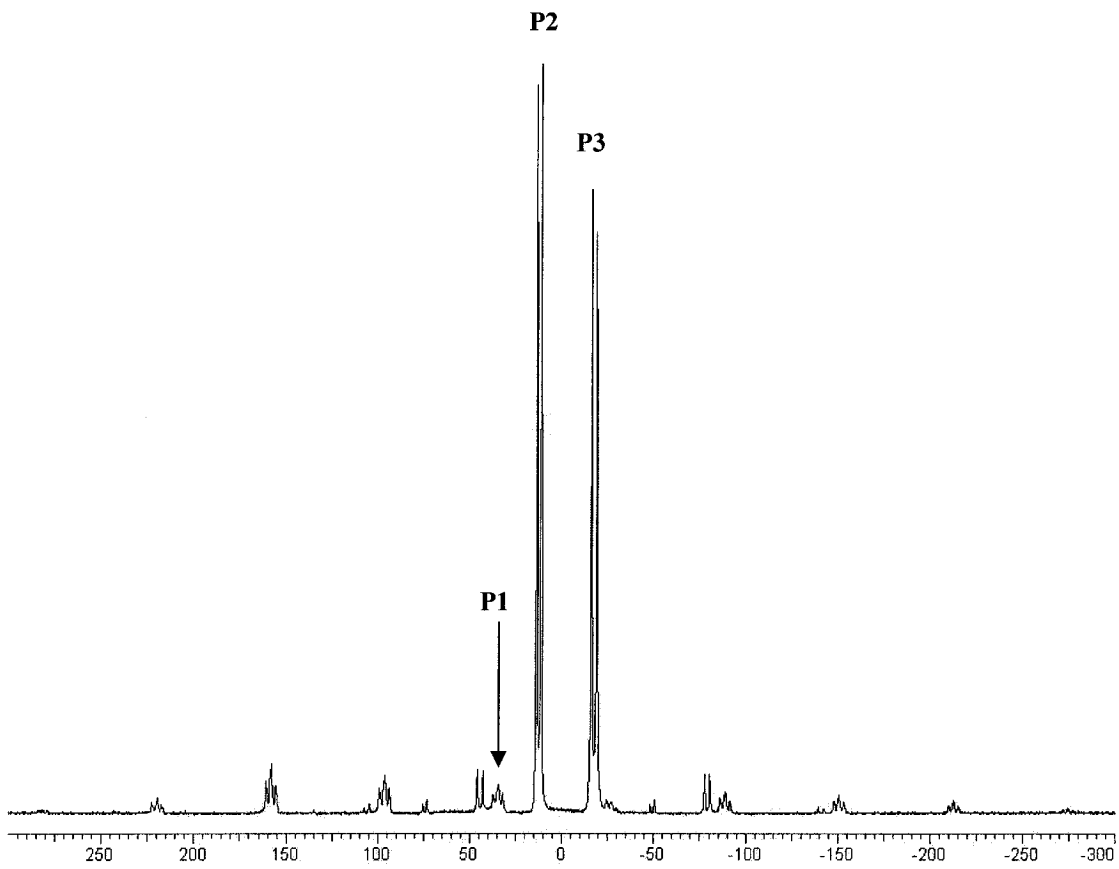

Figure 3.4 Solid state $^{31}P\{^{1}H\}$ CP-MAS NMR spectrum of [Mes*NP·DIPHOS]OTf (**3.15**, R = Ph) showing the isotropic chemical shifts of P1 (phosphadiazonium), P2 (donor) and P3 (donor).

($\Delta\delta_{(P2,P3)}$ = 30 ppm), but are not coupled to each other, so that the AMX spin system involves $J_{MX} = 0$.

The inequivalence of the phosphine donor atoms (P2 and P3) in [Mes*NP·DIPHOS]OTf is not retained in solution. Two broad peaks are observed in the solution ^{31}P NMR spectrum of [Mes*NP·DIPHOS]OTf at 298 K (Figure 3.5), which resolve into an 8-line pattern at 193 K. This pattern can be interpreted as either an AB_2 or ABB' spin system; the experimental data cannot distinguish between the two. In both spin systems, the phosphadiazonium phosphorus centre (P1) has a chemical shift of 36 ppm and the two donor phosphine centres (P2 = P3) have identical chemical shifts, appearing at 10 ppm. If it is assumed that P2 and P3 do not couple to each other, the spectrum can be interpreted as an AB_2 spin system, in which $^{1}J_{(P1,P2)} = {}^{1}J_{(P1,P3)} = 453$ Hz. Conversely, if it is assumed that P2 and P3 do couple to each other, the spectrum can be interpreted as an ABB' spin system, in which P2 and P3 couple to P1 with one-bond coupling constants of slightly different magnitudes ($^{1}J_{(P1,P2)} = 466$ Hz, $^{1}J_{(P1,P3)} = 441$ Hz, $^{2}J_{(P2,P3)} = 163$ Hz). The solution ^{31}P NMR spectra of [Mes*NP·DMPE]OTf, and [Mes*NP·DEPE]OTf exhibited the same characteristic AB_2 (or ABB') coupling pattern at 298 K.

The solution ^{31}P NMR spectra of reaction mixtures containing equimolar amounts of TRIPHOS (**3.13**) and Mes*NPOTf exhibited three broad peaks at 298 K, which were distinct from those of the starting materials. Cooling the solution to 193 K resulted in the splitting of the peaks into a complicated pattern, which could not be intepreted. It appears that the reaction of TRIPHOS with Mes*NPOTf produces more than one product containing P→P bonds. A solid state ^{31}P -MAS NMR spectrum of the yellow solid

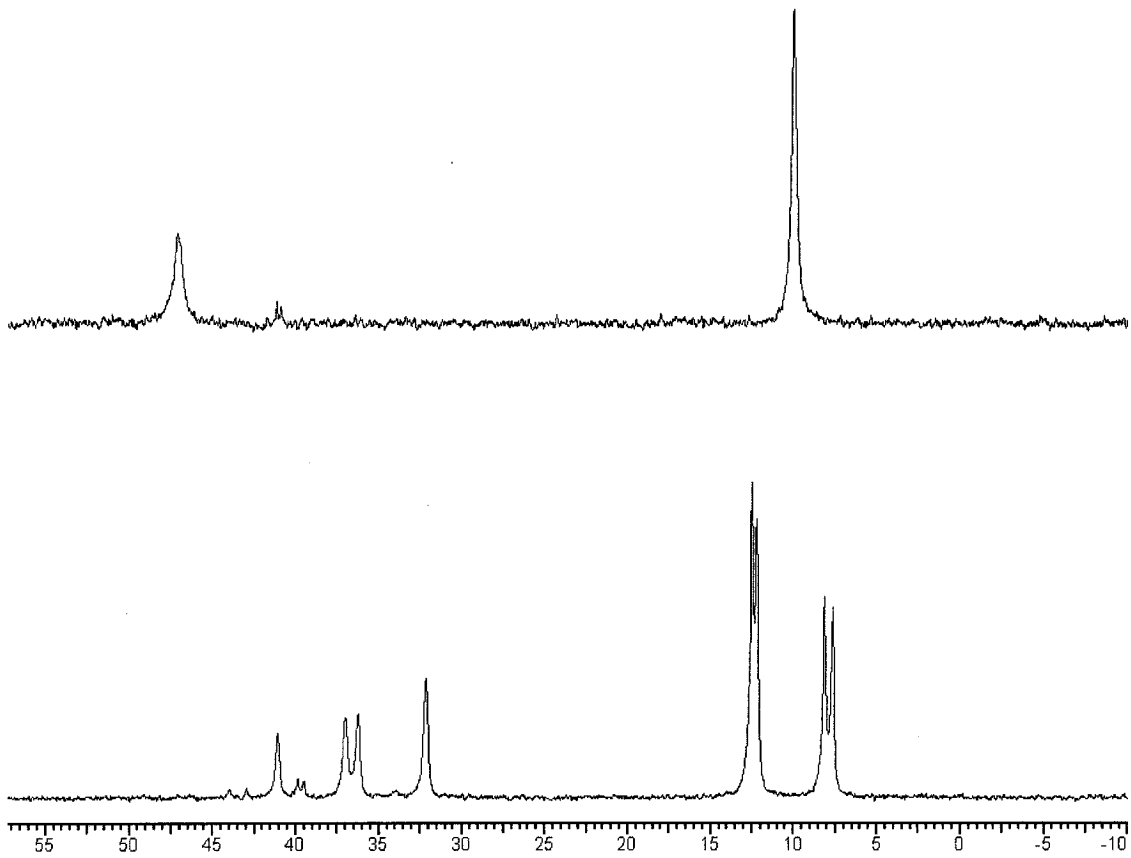

Figure 3.5 Solution $^{31}P\{^{1}H\}$ NMR spectra of [Mes*NP·DIPHOS]OTf (**3.15**, R = Ph) at 298 K (top) and at 193 K (bottom).

isolated from the reaction mixture also showed a mixture of products with one bond P-P coupling, none of which could be assigned to a tridentate complex analogous to [Mes*NP·PMDETA]OTf. The large steric bulk of the TRIPHOS ligand may prevent efficient binding to the phosphadiazonium cation.

The central N(3)→P coordinate bond (2.263(2) Å) in [Mes*NP·PMDETA]OTf is slightly shorter than those achieved by the terminal nitrogen donors of the ligand (N(2)→P = 2.436(2) Å, N(4)→P = 2.524(2) Å), and together with N(1), they impose a distorted disphenoidal geometry at phosphorus, in which N(2) and N(4) occupy axial positions. The ligand adopts a similar conformation to those in complexes of PMDETA with [AlH_2^+] (**3.17**, R = H, An = AlH_4)[131] and [$AlMe_2^+$] (**3.17**, R = Me, An = $AlMe_2Cl_2$),[132] where the aluminium centres adopt a distorted trigonal bipyramidal geometry with the terminal nitrogen atoms of the ligand occupying the axial sites. In this context, the disphenoidal geometry of the phosphorus centre in [Mes*NP·PMDETA]OTf reveals the stereochemical presence of the lone pair at the acceptor site.

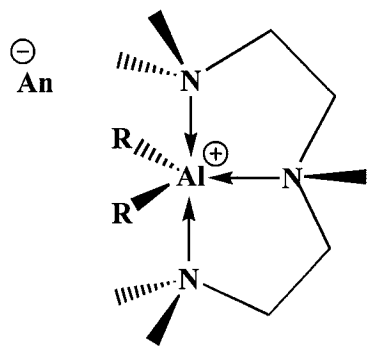

3.17, R = H, Me, An = AlH_4, $AlMe_2Cl_2$

The N→P distances in complexes **1.43**, **1.44**, **1.45**, **3.14**, and **3.16** exhibit a predictable trend corresponding to the number of nitrogen donor sites interacting with

phosphorus. The single donor ligands in [Mes*NP·pyridine]OTf (**1.43**, N→P = 1.958(8) Å)[81] and [Mes*NP·quinuclidine]OTf (**1.44**, N→P = 1.933(2) Å)[81] engage the phosphorus centre more effectively than those in the chelate complexes [Mes*NP·(2,2'-BIPY)]OTf (**1.45**, N→P = 2.065(4) Å, 2.154(3) Å)[80] and [Mes*NP·TMEDA]OTf (**3.14**, N→P = 2.090(2) Å, 2.154(3) Å, and the longest coordinate interactions are observed in [Mes*NP·PMDETA]OTf (**3.16**, N→P = 2.263(2) Å, 2.436(2) Å, 2.524(2) Å). A contrasting trend is observed for the P→P coordinate bonds, with those in [Mes*NP·DIPHOS]OTf (**3.15**, R = Ph, P→P = 2.5392(9) Å, 2.5708(9) Å) shorter than that observed in [Mes*NP·PPh_3]OTf (**1.33**, P→P = 2.625(2) Å),[59] perhaps reflecting the greater basicity of the phosphorus donors in DIPHOS. Nevertheless, all of these P→P distances are substantially longer than the narrow range (2.13-2.31 Å) observed in phosphine-phosphenium complexes (e.g., **3.7**).[52]

The N(1)-P(1) bond lengths in the chelate complexes are only slightly longer than in the free acid Mes*NPOTf, consistent with the monodentate ligand complexes (**3.1**) already characterized. Moreover, the C(1)-N(1)-P(1) angles are only slightly more acute than the almost linear geometry for nitrogen in Mes*NPOTf, indicating that interaction of the phosphorus acceptor site with one, two or three donors effects minimal disruption of the N-P π-bonding in the phosphadiazonium cation. The pyramidal geometry of phosphorus in [Mes*NP·TMEDA]OTf and [Mes*NP·DIPHOS]OTf , and the disphenoidal geometry of phosphorus in [Mes*NP·PMDETA]OTf illustrate the retention of a non-bonding pair (lone pair) of electrons at phosphorus in these complexes.

With consideration of the short N(1)-P(1) bonds and linear geometry about N(1) observed in the solid state structures of [Mes*NP·(2,2'-BIPY)]OTf,

Mes*NP·TMEDA]OTf, and [Mes*NP·DIPHOS]OTf, the bidentate chelate complexes can be designated as **12-P-3** systems, under the "N-X-L" valence electron counting model,[133] in which "N" refers to valence electrons about a central atom "X" with "L" ligands (Scheme 3.1). Retention of N-P multiple bonding in these complexes precludes the more familiar **8-P-3** environment,[134-136] and in comparison to the 12 valent environment in the hexacoordinate PF_6^- (**12-P-6**), **1.45**, **3.14**, and **3.15** represent a remarkable valence electron count (**12-P-3**) for a low coordinate centre. Most dramatic is the **14-P-4** environment for phosphorus in [Mes*NP·PMDETA]OTf representing a valence electron count at phosphorus approaching that of transition metal complexes (cf. **16-Pt-4** in $PtCl_4^{2-}$). The unusual hypervalent, low coordinate phosphorus centres in [Mes*NP·(2,2'-BIPY)]OTf, [Mes*NP·TMEDA]OTf, [Mes*NP·DIPHOS]OTf, and [Mes*NP·PMDETA]OTf diversify the fundamental chemistry and electronic structure of phosphorus beyond the extremes that were described for derivatives of 5-aza-2,8-dioxa-1-phosphabicyclo[3.3.0]octa-2,4,6-triene (**3.18**), an example of a **10-P-3** environment.[137]

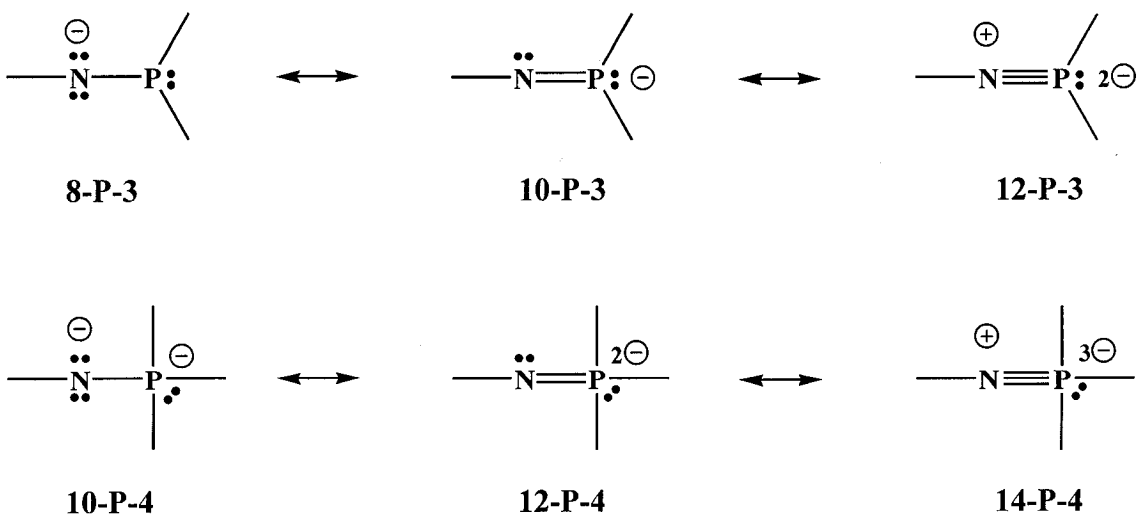

Scheme 3.1

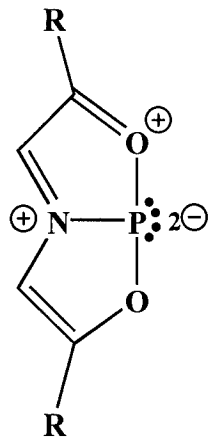

3.18

3.3 Conclusions

Mes*NPOTf reacts with bifunctional or trifunctional ligands to give chelate complexes of the phosphadiazonium cation, containing three- and four-coordinate phosphorus centres, respectively. Tethered or pendant donor complexes were not observed, regardless of the reaction stoichiometry. Solid state structures and spectroscopic data indicate retention of the (Mes*)NP π-bonding and the presence of a stereochemically active lone pair at phosphorus, highlighting new hypervalent, low coordinate phosphorus(III) bonding environments.

Chapter 4: Donor-Rich and Acceptor-Rich Phosphadiazonium Adducts: Diversifying the Lewis Acceptor Chemistry of Phosphorus(III)

4.1 Introduction

The transition metals and the heavy p-block elements (e.g., Sn, Pb, Bi) commonly adopt high coordination numbers (ML_n, n = 4-10), defining hypervalent bonding environments. In contrast, most p-block elements access relatively low coordination numbers, and complexes of Lewis acidic p-block centres usually involve a single ligand (e.g., $H_3B{\leftarrow}NR_3$).[138] Complexes of boranes are limited by the availability of only one acceptor orbital, while the presence of a lone pair at Lewis acceptor phosphine sites apparently restricts the number of ligands.[4] However, coordinative unsaturation and positive molecular charge in the phosphadiazonium cation, Mes^*NP^+ (Mes* = 2,4,6-tri-*tert*-butylphenyl),[40] impose a relatively high Lewis acidity at phosphorus, allowing it to accept donation from more than one Lewis base. This has already been observed in complexes of the phosphadiazonium cation with both bidentate and tridentate chelating ligands (Chapter 3), and is now extended here to donor-rich complexes, where two separate ligands coordinate to the phosphorus(III) acceptor. The versatile coordination chemistry of the phosphadiazonium cation is further demonstrated by the characterization of acceptor-rich complexes, where two phosphadiazonium cations are linked by a bridging ligand.

Although coordination of multiple donor ligands to one phosphorus(III) acceptor has been previously suggested on the basis of ^{31}P NMR spectroscopy,[50] no definitive structural characterization has been available until now. Two equivalents of the strong base 4-dimethylaminopyridine (DMAP, **4.1**) interact with the phosphadiazonium cation to give $[Mes^*NP{\cdot}(DMAP)_2]OTf$ (**4.2**), the first ligand-rich coordination complex of a

phosphorus(III) Lewis acceptor. The DMAP ligand has proven itself to be a useful reagent in the stabilization of highly reactive phosphorus species, the diphenylphosphenium (**4.3**)[81] and *N*-silylphosphoranimine (**4.4**)[139] cations being notable examples.

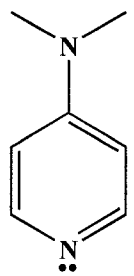

4.1

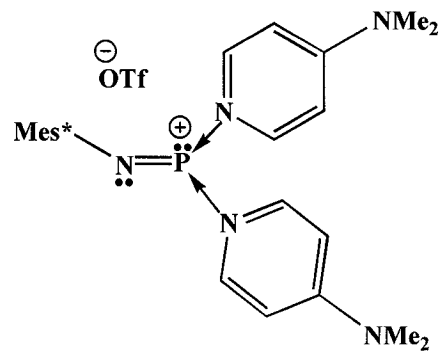

4.2

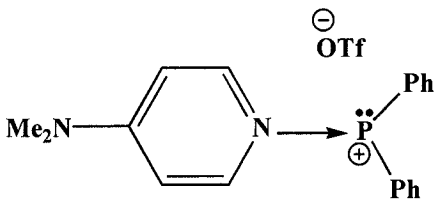

4.3

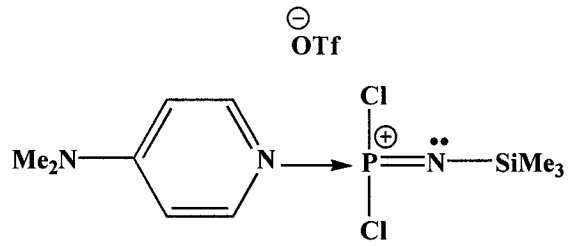

4.4

Recently, Niecke and coworkers found that treatment of the bromobis(arylimino)-phosphorane (**4.5**) with one equivalent of DMAP gave the coordination complex **4.6** in good yield (Scheme 4.1).[140] Subsequent reaction of **4.6** with a second equivalent of DMAP yielded the donor-rich adduct of the bis(imino)phosphonium cation (**4.7**). Niecke's work followed upon that of Meisel and coworkers, who used a similar synthetic

procedure to isolate a bis-pyridine adduct of the dithiophosphonium ion (**4.9**, Scheme 4.2).[141;142] The bis(imino)phosphonium cation, [Mes*NPNMes*]$^+$, can be considered a phosphorus(V) analogue of the phosphadiazonium cation, and as such, complex **4.7** is a P(V) analogue of [Mes*NP·(DMAP)$_2$]OTf.

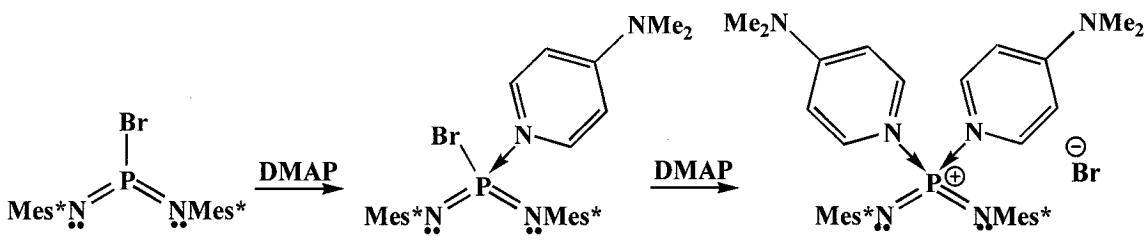

4.5 **4.6** **4.7**

Scheme 4.1

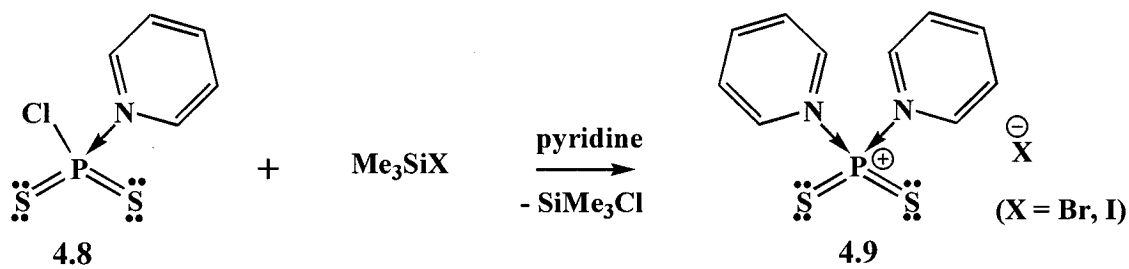

4.8 **4.9**

Scheme 4.2

Acceptor-rich complexes involve the tethering of two phosphorus(III) Lewis acceptors by a single bridging ligand. In 1996, Burford and coworkers reported the linking of two aluminatoiminophosphines by a N,N,N',N'-tetramethylethylenediamine (TMEDA) ligand (**4.10**),[81;143] and more recently, reported the synthesis of

polyphosphorus dications through the coordination of bis(diphosphino)ethane ligands to phosphenium acceptors (**3.7**, R = Me, Ph).[93;125] Müller and coworkers have also reported the tethering of two phosphorus tribromide molecules by a 1,4-dimethylpiperazine ligand (**4.11**); however, in this case, the donor acceptor interactions are extremely weak (N→P = 2.803(8) Å).[49]

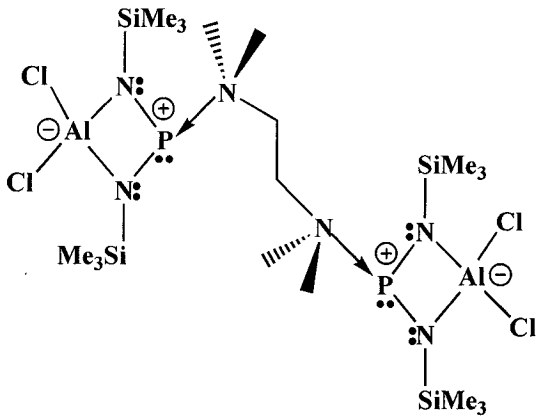

4.10

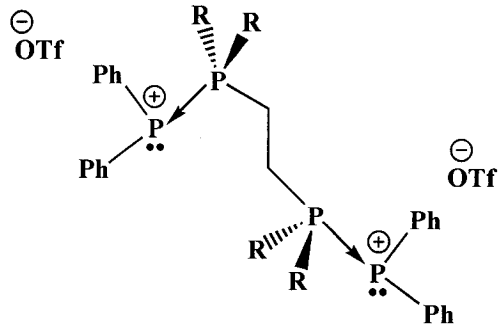

3.7, R = Me, Ph

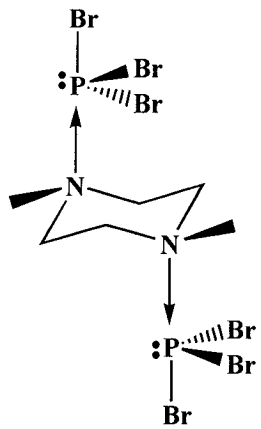

4.11

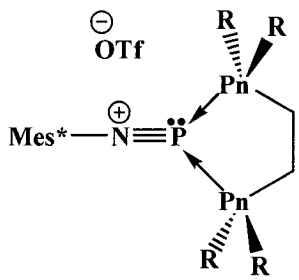

3.4, Pn = N, P

Unlike the diphenylphosphenium cation, the phosphadiazonium cation demonstrates a marked preference for the formation of chelate complexes over tethered

complexes (Chapter 3). In the presence of TMEDA or bis(diphosphino)ethane ligands chelate complexes (**3.4**, Pn = N, P) of the phosphadiazonium cation are formed exclusively, independent of the reaction stoichiometry. In order to isolate acceptor-rich phosphadiazonium adducts, rigid bifunctional ligands must be chosen, which do not have the potential to chelate the phosphorus centre. The ligands selected were 4,4'-bipyridine (4,4'-BIPY, **4.12**) and 1,4-diazabicyclo[2.2.2]octane (DABCO, **4.13**). A solid state structure of the acceptor-rich complex $[(Mes^*NP)_2 \cdot (4,4'\text{-BIPY})][OTf]_2$ (**4.14**) was obtained, representing the first example of a dication involving two phosphadiazonium moieties.

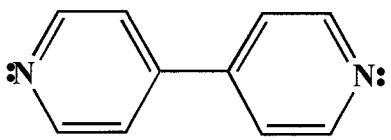

4.12

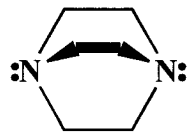

4.13

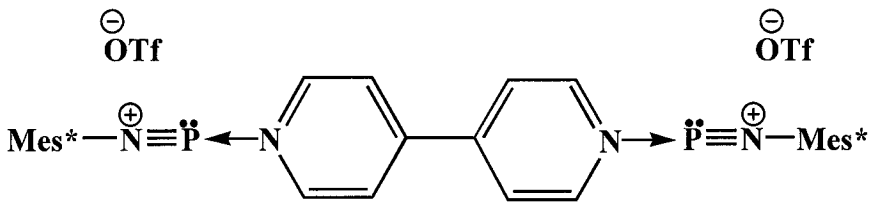

4.14

4.2 Results and Discussion

4.2.1 Donor-Rich Phosphadiazonium Adducts

Trifluoromethylsulfonyloxy-(2,4,6-tri-*tert*-butylphenylimino)phosphine (Mes*NPOTf, **1.33**)[72] reacts with a variety of ligands (L = ylidene,[82] pyridine,[80;81]

amine,[81] phosphine,[59] urea,[83] thiourea,[83] selenourea[83]), which effect nucleophilic displacement of the triflate anion (OTf$^-$ = $OSO_2CF_3^-$). The resulting cations are best described as 1:1 adducts of a neutral ligand on a phosphadiazonium Lewis acceptor (**4.15**). Solution ^{31}P NMR spectra of equimolar reaction mixtures of Mes*NPOTf and DMAP show quantitative formation of [Mes*NP·DMAP]OTf (**4.16**, pink solid, δ ^{31}P = 132 ppm), but the donor-rich complex [Mes*NP·$(DMAP)_2$]OTf (**4.2**, yellow solid, δ ^{31}P = 123 ppm) is formed quantitatively when an excess of DMAP is present. A structural view of the cation in [Mes*NP·$(DMAP)_2$]OTf is shown in Figure 4.1. Although crystals of [Mes*NP·DMAP]OTf suitable for X-ray diffraction could not be obtained, the structural features of the complex are likely very similar to those of the analogous pyridine complex [Mes*NP·pyridine]OTf (**1.43, 4.15** L = pyridine).

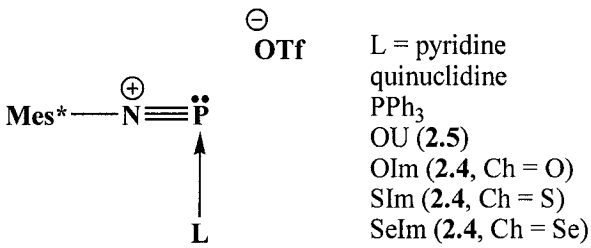

L = pyridine
quinuclidine
PPh_3
OU (**2.5**)
OIm (**2.4**, Ch = O)
SIm (**2.4**, Ch = S)
SeIm (**2.4**, Ch = Se)
Im (**2.6**)

4.15

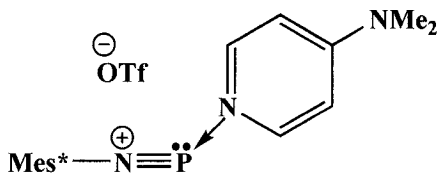

4.16

Selected structural parameters for [Mes*NP·$(DMAP)_2$]OTf and other nitrogen donor complexes of Mes*NP$^+$ are presented in Table 4.1. Comparative parameters for Mes*NPOTf and other pyridine/DMAP donor – phosphorus acceptor complexes are also included in the table. In all phosphadiazonium complexes, the nitrogen donor sites are closer to the phosphorus centre than the oxygen centres of the triflate anion, and in general, nitrogen donors effect a substantial displacement (> 0.8 Å) of the triflate anion

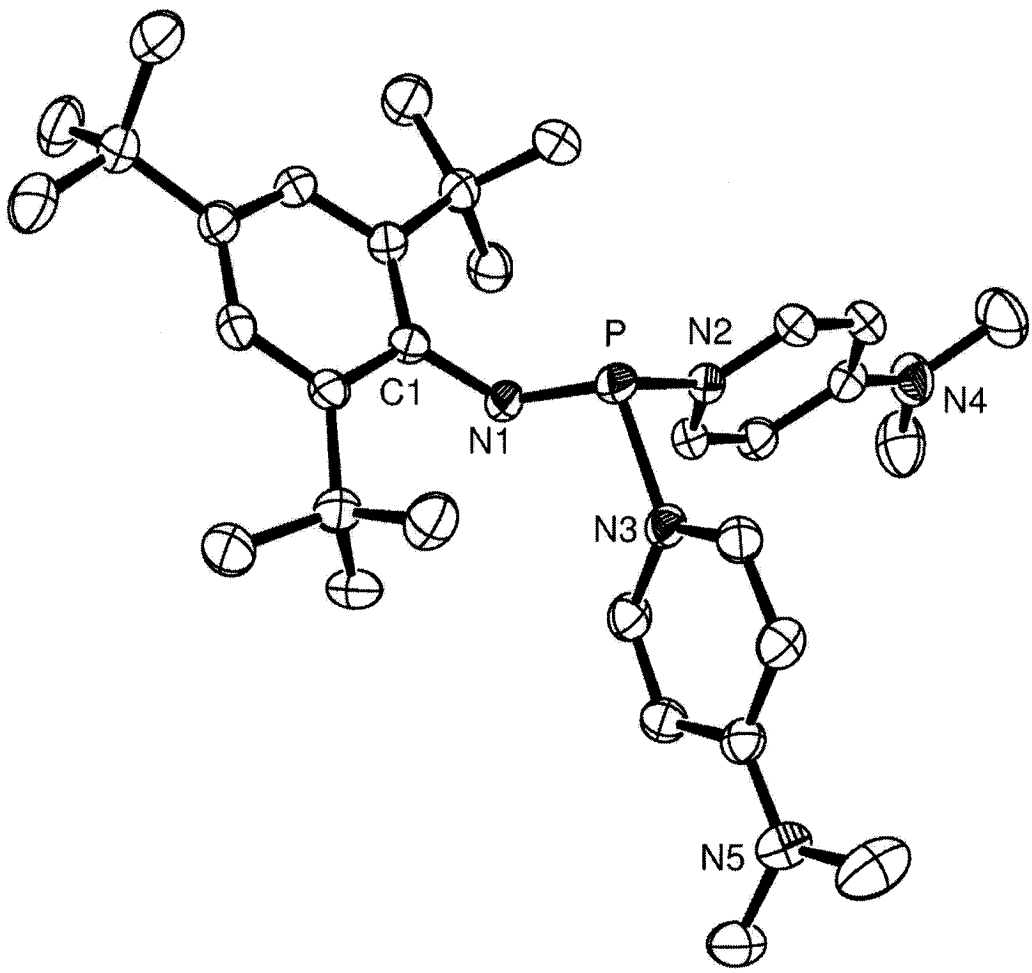

Figure 4.1 Solid state structure of the cation in [Mes*NP·(DMAP)$_2$]OTf (**4.2**) drawn with 50% probability displacement ellipsoids. Hydrogen atoms and the anion have been omitted for clarity.

Table 4.1 Selected bond lengths (Å), angles (°), and solution ^{31}P NMR (CD_2Cl_2) chemical shifts (ppm) for Mes*NPOTf and its complexes with nitrogen donor ligands, along with corresponding data for other pyridine/DMAP donor – phosphorus acceptor complexes.

Compound	Label	δ ^{31}P	P-O	N→P	(R)N-P	R-N-P	Reference
Mes*NPOTf	**1.33**	52	1.923(3)	No ligand	1.467(4)	176.4(3)	144
[Mes*NP·pyridine]OTf	**1.43**	71	2.712(7)	1.958(8)	1.472(8)	161.7(7)	81
[Mes*NP·quinuclidine]OTf	**1.44**	144	2.697(3)	1.933(2)	1.519(2)	143.9(2)	81
[Mes*NP·$(DMAP)_2$]OTf	**4.2**	123	[d]	1.873(2); 1.879(2)	1.559(2)	125.2(2)	145
[$(Mes*NP)_2$·(4,4'-BIPY)][OTf]$_2$	**4.14**	61	2.776(2) (P1) 2.879(2) (P2)	1.984(2) (P1) 2.025(2) (P2)	1.488(2) (P1) 1.489(2) (P2)	165.6(2) (P1) 164.4(2) (P2)	145
[Mes*NP·(2,2'-BIPY)]OTf	**1.45**	54	[d]	2.065(4); 2.066(4)	1.497(4)	169.4(4)	80;130
[Mes*NP·TMEDA]OTf	**3.14**	110	[d]	2.090(2); 2.154(3)	1.510(2)	154.4(2)	130
[Mes*NP·PMDETA]OTf	**3.16**	89	[d]	2.263(2); 2.436(2); 2.524(2)	1.495(2)	164.4(2)	130
[Ph_2P·DMAP]OTf	**4.3**	88	[d]	1.789(1)	-	-	81
[$Me_3SiNP(Cl)_2$·DMAP]OTf	**4.4**	-54	[d]	1.713(2)	1.490(3)	144.1(2)	139
$(Mes*N)_2P$·(DMAP)Br	**4.6**	-93[b]	-	1.815(5)	1.528(4) 1.486(5)	-[e]	140
[$(Mes*N)_2P$·$(DMAP)_2$]Br	**4.7**	-57	-	1.830(4); 1.812(4)	1.528(4) 1.526(4)	-[e]	140
S_2P·(pyridine)Br[a]	**4.8**	66[c]	-	1.849(2)	-	-	141
[S_2P·$(pyridine)_2$]Br	**4.9**	105[c]	-	1.768(14); 1.813(3)	-	-	142
PF_5·(pyridine)	**4.17**	-144	-	1.885(4)	-	-	146

[a] Bromine analogue of **4.8**; [b] C_6D_6; [c] CH_3CN; [d] P(1)-OTf distance greater than the sum of the van der Waals radii (P-O = 3.3 Å); [e] Not reported.

from phosphorus. Predictably, the two DMAP ligands in [Mes*NP·(DMAP)$_2$]OTf impose a greater P-OTf dissociation than a single ligand in derivatives of **4.15**, consistent with the chelate complexes **1.45**, **3.14**, and **3.16**.

The N→P(III) coordinate bonds in amine complexes of the phosphadiazonium cation adopt a broad range (1.93 - 2.54 Å), yet the distribution of N→P(III) bond lengths in pyridine (or DMAP) complexes of Mes*NP$^+$ is more uniform (1.87 - 2.07 Å, Table 4.1). Nevertheless, all N→P(III) bonds in phosphadiazonium complexes are longer than the benchmark N-P single bond (1.800(4) Å) in $[H_3NPO_3]^-$.[147] The N→P(III) bond in the DMAP complex of the diphenylphosphenium cation (**4.3**, N→P = 1.789(1) Å)[81] is substantially shorter than those observed in the phosphadiazonium complexes, which agrees with the trend observed for P→P bond lengths in phosphine complexes of the two cations.[52;130] Pyridine or DMAP complexes of P(V) acceptors exhibit shorter N→P coordinate bonds than their P(III) congeners with a distance range of 1.71 - 1.88 Å; the longest bond occurring in the pyridine adduct of PF_5 (**4.17**).[146]

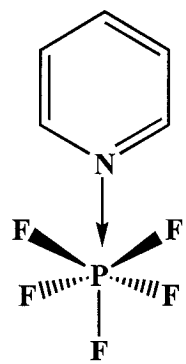

4.17

In most cases, ligand interactions have minor influence on the structural features of the acceptor $Mes*NP^+$ unit. The N(1)-P(1) bond lengths are only slightly longer in the adducts than in the Lewis acid Mes*NPOTf, and the C(1)-N(1)-P(1) bond angles are only slightly more acute, implicating retention of N-P multiple bonding in the complexes. Predictably, the imposition of two donors in the ligand-rich complex [Mes*NP·$(DMAP)_2$]OTf has the largest influence on the N(1)-P(1) distance and C(1)-N(1)-P(1) angle of the acceptor (N-P = 1.559(2) Å; C-N-P = 125.2(2)°). In contrast, the two donors in the chelate ligand 2,2'-bipyridine effect minimal structural change on the acceptor in [Mes*NP·(2,2'-BIPY]OTf (N-P = 1.497(4) Å; C-N-P = 169.4(4)°).[18] This indicates that the basicity of the donor is more influential than the number of donors present. Consistently, one quinuclidine ligand has a larger impact on the structural features of the acceptor (N-P = 1.519(2) Å; C-N-P = 143.9(2)°) than the two donor sites of the less basic chelate ligand 2,2'-bipyridine (Table 4.1). These trends are also evident in the N→P(III) coordinate bond lengths in the complexes: DMAP (1.873(2), 1.879(2) Å) < quinuclidine (1.933(2) Å) < 2,2'-bipyridine (2.065(4), 2.066(4) Å). The shortest N→P(III) coordinate bonds are observed in [Mes*NP·$(DMAP)_2$]OTf despite the possibility for competition between the two ligands.

The phosphorus centre in [Mes*NP·$(DMAP)_2$]OTf adopts a pyramidal geometry (sum of N-P-N angles = 295.8°) consistent with the presence of a stereochemically active lone pair at the acceptor site. This, along with retention of a N-P multiple bond order, implicates hypervalency in the complex. Although the geometry about the phosphorus centre in [Mes*NP·$(DMAP)_2$]OTf is similar to that in the chelate complexes [Mes*NP·TMEDA]OTf (**3.14**) and [Mes*NP·DIPHOS]OTf (**3.15**), the N(1)-P(1) bond in

the ligand-rich complex is significantly longer (1.559(2) Å) than those in the chelate complexes (TMEDA, 1.510(2) Å; DIPHOS, 1.489(2) Å).[130] The (Mes*)N-P bond length and the near-ideal sp^2 hybridization at N(1) suggest the existence of a N-P double bond, rather than a N-P triple bond in [Mes*NP·(DMAP)$_2$]OTf. As a result, the **10-P-3** bonding environment (Scheme 4.3) is a more suitable descriptor for the ligand-rich complex than the **12-P-3** environment assigned to the chelate complexes.

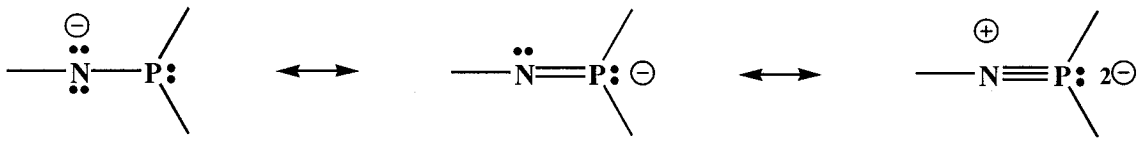

8-P-3 **10-P-3** **12-P-3**

Scheme 4.3

Attempts to isolate other ligand-rich complexes of the phosphadiazonium cation resulted in the observation of interesting ligand-acceptor solution equilibria. A series of reactions between Mes*NPOTf and n equivalents (n = 1, 1.5, 2, 3, 4) of 1,3-diisopropyl-4,5-dimethylimidazole-2(3*H*)-thione (SIm, **2.4**, Ch = S) were studied by variable temperature solution ^{31}P NMR spectroscopy, and the data are presented in Table 4.2. At room temperature, the ^{31}P chemical shift of the reaction mixture shifted to higher field with increasing values of n (increasing concentrations of ligand). Most interesting, addition of 1.5 equivalents of SIm to Mes*NPOTf resulted in the observation of only one broad peak at room temperature, which split into two peaks (152 ppm and 71 ppm) at 203 K (Figure 4.2). Consequently, the peak at 71 ppm was assigned to the ligand-rich adduct [Mes*NP·(SIm)$_2$]OTf (**4.18**), while the peak at 152 ppm was assigned to the previously

isolated complex [Mes*NP·SIm]OTf (**2.7**, Ch = S). For n > 2, only the peak at 71 ppm was observed at low temperatures, indicating that two is the maximum number of SIm molecules that can coordinate to the phosphadiazonium cation.

Table 4.2 Variable temperature ^{31}P NMR data (ppm) for reaction mixtures Mes*NPOTf + n SIm (CH_2Cl_2). The mole fractions of **2.7** (χ_{mono}) and **4.18** (χ_{bis}) present in each mixture at room temperature and the equilibrium constant K are also included.

Equivalents SIm (n)	δ ^{31}P (298 K)	δ ^{31}P (203 K)	χ_{mono}	χ_{bis}	K
1	155	152, 151[a]	1	0	0
1.5	124	152, 71	0.65	0.35	3.6
2	99	71	0.35	0.65	5.3
3	86	73	0.19	0.81	3.6
4	83	72	0.15	0.85	2.6

[a] cis-trans isomerization about P-N multiple bond

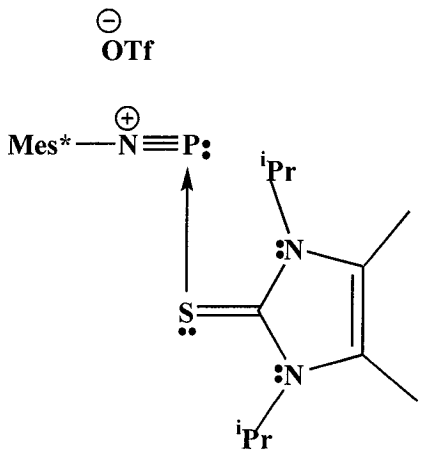

2.7

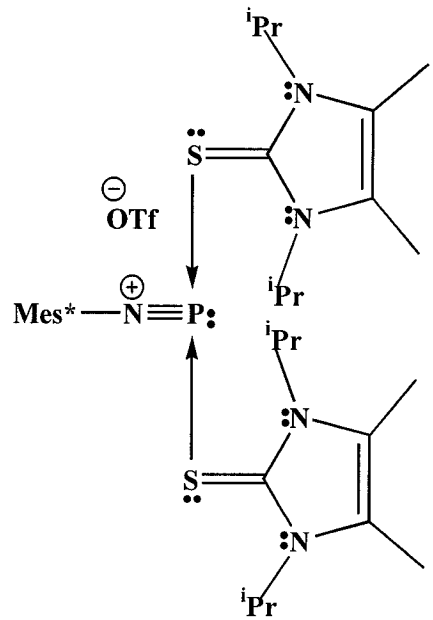

4.18

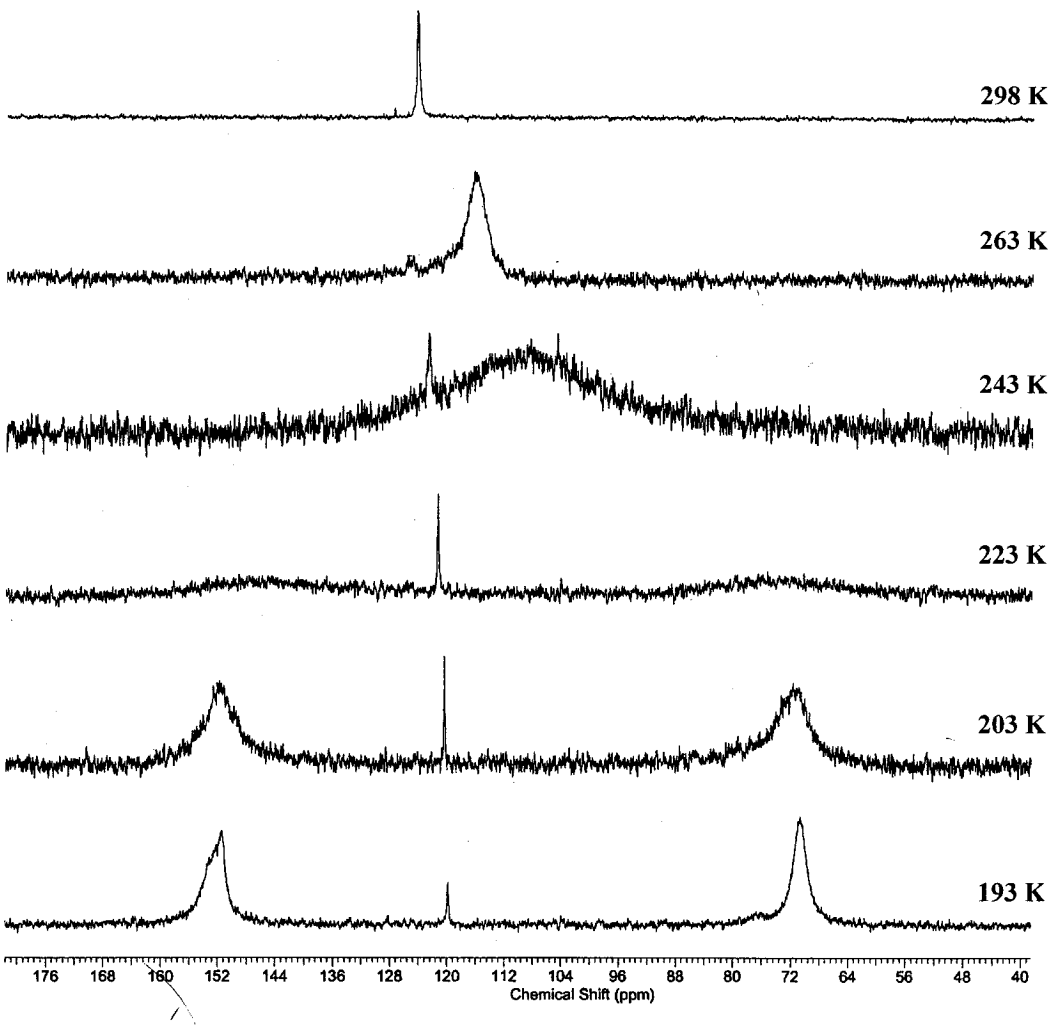

Figure 4.2 Stacked plot showing $^{31}P\{^{1}H\}$ NMR spectra of Mes*NPOTf + 1.5 SIm in CH_2Cl_2 at various temperatures. There is an impurity peak at 120 ppm in all the low temperature spectra that is coincident with the major peak in the spectrum run at 298 K.

The variable temperature ^{31}P NMR data in Table 4.2 can be explained by rapid ligand exchange at room temperature *via* the equilibrium shown in Scheme 4.4. Increasing the concentration of ligand (value of n) pushes the equilibrium to the right, increasing the concentration of the ligand-rich adduct [Mes*NP·$(SIm)_2$]OTf. The ^{31}P chemical shift of the reaction mixture at room temperature represents an average of the ligand-rich adduct **4.18** (δ ^{31}P = 71 ppm) and the mono-ligand adduct **2.7** (δ ^{31}P = 152 ppm), weighted according to their respective mole fractions in solution. This may be represented as in Equation (1):

$$\delta_s = 152(\chi_{mono}) + 71(\chi_{bis}) \qquad (1)$$

where δ_s is the chemical shift of the system, χ_{mono} is the mole fraction of **2.7**, and χ_{bis} is the mole fraction of **4.18**. Assuming $\chi_{mono} + \chi_{bis} = 1$, the relative concentrations of the species in Scheme 4.4 can be calculated, along with the equilibrium constant, K, of the reaction. The value of K has been calculated using this method for all values of n (Table 4.2), and although there is some variation in the calculated values (K = 3 - 5), they are all of similar magnitude. The variation in the calculated values of K may indicate that the solution equilibrium process is more complex than presented here.

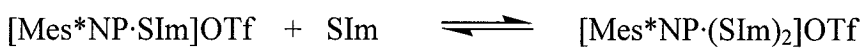

Scheme 4.4

A similar variable temperature solution ^{31}P NMR study was undertaken with reaction mixtures containing Mes*NPOTf and n equivalents (n = 1, 1.5, 2, 3, 4) of

DMAP; however, the data were difficult to interpret due to the small difference in chemical shift between [Mes*NP·DMAP]OTf (δ ^{31}P = 132 ppm) and [Mes*NP·(DMAP)$_2$]OTf (δ ^{31}P = 123 ppm). Addition of multiple equivalents of the less basic ligands 1,3-dimethyldiphenylurea (OU, **2.5**) and pyridine to Mes*NPOTf did not result in the formation of ligand-rich adducts; only [Mes*NP·OU]OTf (**2.8**) and [Mes*NP·pyridine]OTf (**1.43**) were observed in solution. In contrast, addition of two equivalents of the strong base 1,3-diisopropyl-4,5-dimethylimidazol-2-ylidene (Im, **2.6**) to Mes*NPOTf resulted in the observation of a single peak in the ^{31}P NMR spectrum at 61 ppm, which is dramatically different from the shift of the complex [Mes*NP·Im]OTf (**1.46**, δ ^{31}P = 339 ppm). Isolation of the speculated product, [Mes*NP·(Im)$_2$]OTf, was hampered by decomposition of the reaction mixture over time.

Ligand displacement reactions at dicoordinate phosphenium cations have been well characterized.[52] As demonstrated in Scheme 4.5, a more basic ligand will displace a less basic ligand, leading to clean formation of a new complex of the phosphenium cation. Although ligands bound to phosphadiazonium cations can also be displaced by more basic ligands, the reactions proceed in a less straightforward manner. The mono-coordinate phosphadiazonium cation can readily bind multiple ligands, and this, along with the ligand exchange behaviour noted above, leads to complicated product mixtures. For instance, addition of one equivalent of Im to [Mes*NP·DMAP]OTf results in the observation of several peaks in the ^{31}P NMR spectrum of the reaction mixture, which are assigned to [Mes*NP·(DMAP)$_2$]OTf , [Mes*NP·(Im)$_2$]OTf , and perhaps a mixed-ligand adduct. No change is observed in the ^{31}P NMR spectrum when the reverse reaction is undertaken between DMAP and the carbene complex [Mes*NP·Im]OTf.

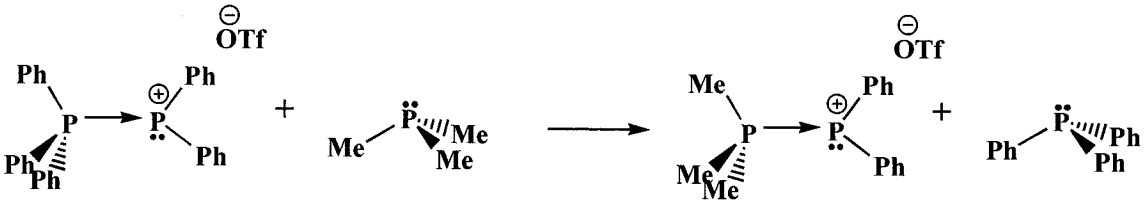

Scheme 4.5

4.2.2. Acceptor-Rich Phosphadiazonium Adducts

Two equivalents of Mes*NPOTf react rapidly at room temperature with one equivalent of 4,4'-bipyridine (4,4'-BIPY, **4.12**) to form the ligand-bridged adduct $[(Mes^*NP)_2{\cdot}(4,4'\text{-BIPY})][OTf]_2$ (**4.14**, $\delta\ ^{31}P = 61$ ppm). Addition of a stoichiometric amount of 4,4'-BIPY to Mes*NPOTf results in a product with a ^{31}P NMR chemical shift of 81 ppm, which is most likely the adduct [Mes*NP·(4,4'-BIPY)]OTf (**4.19**), where only one of the nitrogen donors of 4,4'-BIPY is interacting with a phosphadiazonium cation. Similarly, one equivalent of 1,4-diazabicyclo[2.2.2]octane (DABCO, **4.13**) reacts with two equivalents of Mes*NPOTf to form the ligand-bridged adduct $[(Mes^*NP)_2{\cdot}(DABCO)][OTf]_2$ (**4.20**, $\delta\ ^{31}P = 80$ ppm) in solution. Crystals grown from the reaction mixture had a ^{31}P chemical shift of 110 ppm, consistent with that observed in solutions where Mes*NPOTf and DABCO were combined in equivalent amounts to form [Mes*NP·DABCO]OTf (**4.21**). The shorter distance between the nitrogen donors in DABCO may destabilize the ligand-bridged adduct through unfavourable steric interactions.

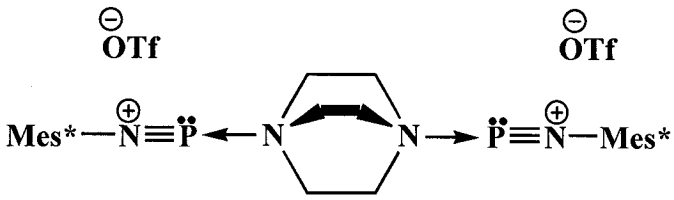

4.20

The acceptor-rich complex $[(Mes^*NP)_2{\cdot}(4,4'\text{-BIPY})][OTf]_2$ (Figure 4.3) exhibits similar structural features to those of the 1:1 adduct [Mes*NP·pyridine]OTf (**1.43**) (Table 4.1). The N(1)-P(1) bond lengths (4,4'-BIPY, N-P = 1.488(2), 1.489(2) Å; pyridine,[81] N-P = 1.472(8) Å) and C(1)-N(1)-P(1) bond angles (4,4'-BIPY, C-N-P = 165.6(2), 164.4(2)°; pyridine,[81] C-N-P = 161.7(7)°) in both complexes implicate retention of multiple N-P bonding, and indicate that the ligands impose few structural changes on the phosphadiazonium acceptor. Ignoring the weak contacts maintained between the phosphorus centres and the triflate anions, the low coordinate, hypervalent phosphorus(III) bonding environments in $[(Mes^*NP)_2{\cdot}(4,4'\text{-BIPY})][OTf]_2$ and [Mes*NP·pyridine]OTf can be assigned a **10-P-2** designation[133] (Scheme 4.6). The N→P coordinate bonds in the dication of $[(Mes^*NP)_2{\cdot}(4,4'\text{-BIPY})][OTf]_2$ (N→P = 1.984(2), 2.025(2) Å) are slightly longer than in **1.43** (N→P = 1.958(8) Å),[81] reflecting the reduction in basicity of the ligand on introduction of a greater cationic charge.

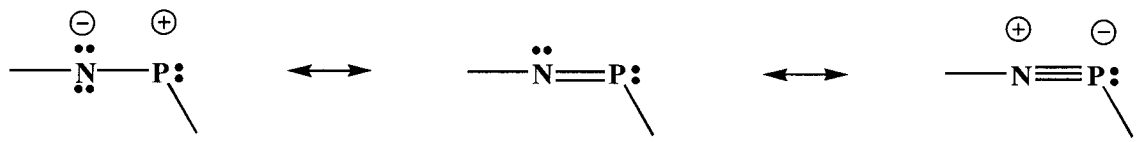

6-P-2 **8-P-2** **10-P-2**

Scheme 4.6

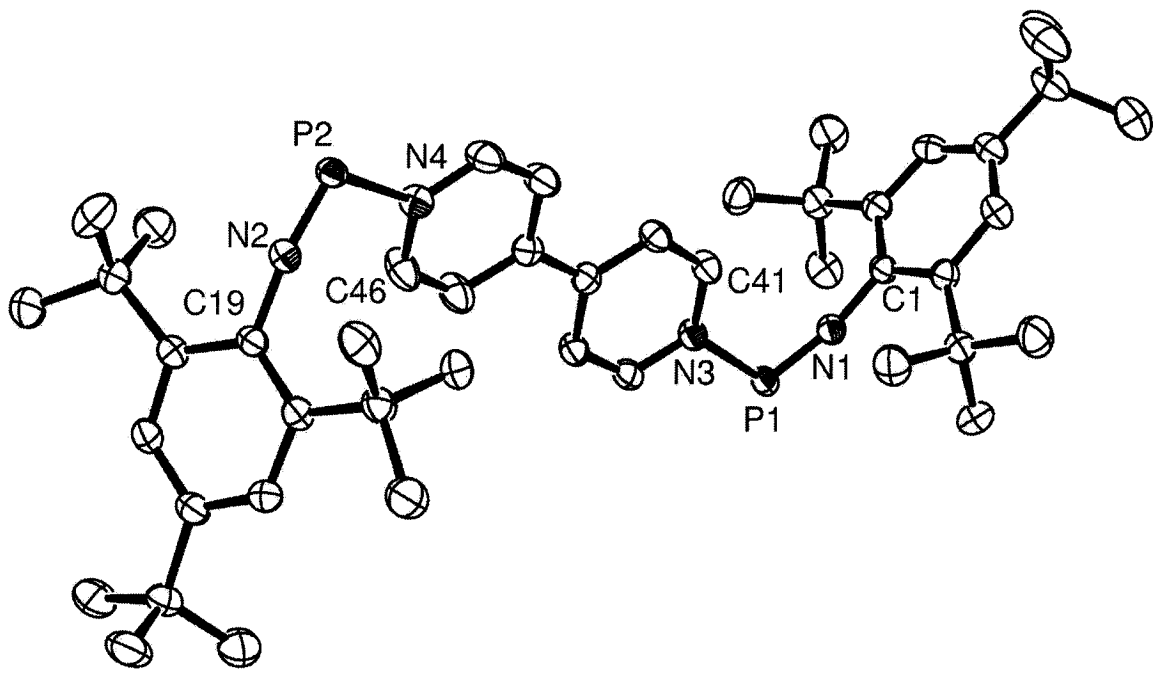

Figure 4.3 Solid state structure of the cation in $[(Mes^*NP)_2 \cdot (4,4'\text{-BIPY})][OTf]_2$ (**4.14**) drawn with 50% probability displacement ellipsoids. Hydrogen atoms and the anions have been omitted for clarity.

The two phosphadiazonium units in $[(Mes*NP)_2{\cdot}(4,4'\text{-BIPY})][OTf]_2$ are not related by crystallographic symmetry. The 4,4'-bipyridine ligand is slightly twisted (4°) about the central C-C bond, and the N→P coordinate bonds are inequivalent. Consequently, a single ^{31}P NMR signal is observed in solution (61 ppm), while two isotropic signals (60 and 63 ppm) are observed in the solid state CP-MAS ^{31}P NMR spectrum (Figure 4.4). By comparison, complexes of phosphines tethered by TMEDA (**4.10**)[81] or 1,4-dimethylpiperazine (**4.11**)[49] involve a crystallographic centre of symmetry. The anti-configuration of the phosphadiazonium units in $[(Mes*NP)_2{\cdot}(4,4'\text{-BIPY})][OTf]_2$ is consistent with structures observed for complexes representing phosphenium cations tethered by bis(diphosphino)ethane ligands (**3.7**, R = Me, Ph),[125] and the torsional angles N1-P1-N3-C41 (-0.7(2)°) and N2-P2-N4-C46 (21.3(2)°) indicate the possibility of conjugation between the phosphadiazonium and the π-system of the bipyridine donor.

4.3 Conclusions

Mes*NPOTf forms a complex with two DMAP ligands and two phosphadiazonium cations can be tethered by the 4,4'-BIPY ligand, highlighting the potential to diversify the coordination chemistry of phosphorus(III) as a Lewis acceptor despite the presence of a lone pair at the acceptor site. Moreover, the opportunity to implement aspects of transition metal coordination chemistry on the electron-rich (lone pair bearing) P(III) site offers potential for new directions in catalysis, supramolecular chemistry, and synthetic methods.

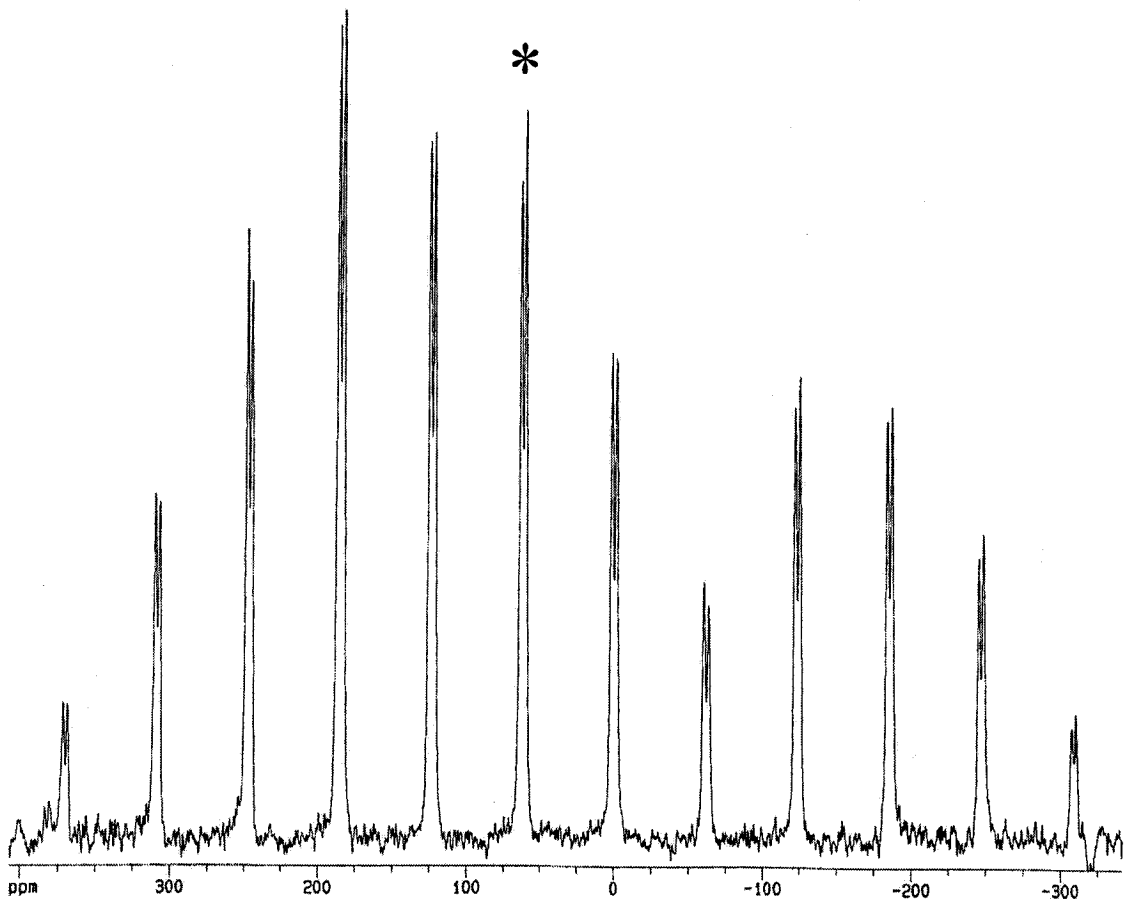

Figure 4.4 Solid state $^{31}P\{^{1}H\}$ CP-MAS NMR spectrum of $[(Mes^*NP)_2 \cdot (4,4'\text{-BIPY})][OTf]_2$ (**4.14**) showing the isotropic chemical shifts (*) of the two crystallographically distinct phosphorus centres.

Chapter 5: Ylidene-Iminophosphine Coordination Complexes

5.1 Introduction

The focus of the previous chapters was the nature of ligand-phosphorus interactions; here our focus shifts to the role of the leaving group in the coordination chemistry of the phosphadiazonium cation. To this effect, the spectroscopic and structural features of a series of complexes of halo-(2,4,6- tri-*tert*-butylphenyl-imino)phosphines, Mes*NPX (**5.1**, X = Cl, Br, I, OTf)[40;72] with the 1,3-diisopropyl-4,5-dimethylimidazol-2-ylidene ligand (Im, **2.6**)[98] were examined. The trifluoromethyl-sulfonyloxy (OTf, triflate) group is considered a pseudohalide for the purposes of this discussion. The imidazolylidene ligand Im is part of a well-known class of ligands, also referred to as *N*-heterocyclic (singlet) carbenes (NHC's), first isolated by Arduengo and coworkers in 1991.[148] *N*-heterocyclic carbenes are excellent donor ligands and have found widespread use in both main group and transition metal coordination chemistry.[149-152]

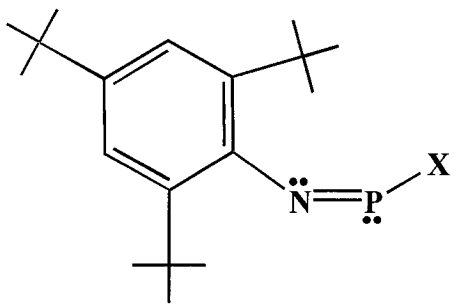

5.1, X = Cl, Br, I, OTf

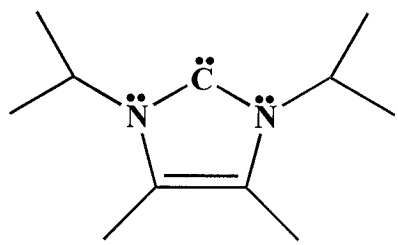

2.6

The first Im complexes of iminophosphines, Mes*NP(Im)Cl (**1.12**) and [Mes*NP·Im]OTf (**1.46**), were isolated by Andrew Phillips in 2000.[18;101] As discussed in

Section 1.4, Im effects nucleophilic displacement of the triflate anion leading to the formation of the $[Mes^*NP{\cdot}Im]^+$ cation, containing a dicoordinate phosphorus centre. In contrast, the displacement of Cl from phosphorus upon coordination of the ylidene ligand is less significant, and as such, Mes*NP(Im)Cl can be described as a neutral iminophosphide, containing a tri-coordinate phosphorus centre. Ylidene complexes of Mes*NPBr (**5.1**, X = Br)[40;153] and Mes*NPI (**5.1** X = I)[40;62] were prepared to see if the presence of a better halide leaving group at phosphorus would lead to the formation of a covalent compound or a salt.

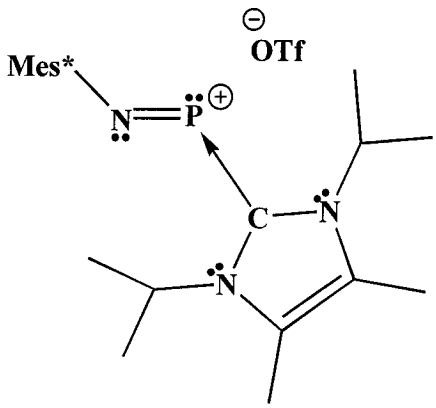

1.46

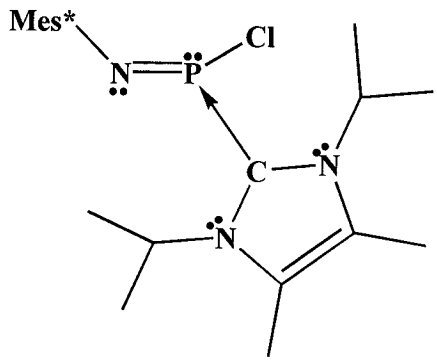

1.12

Imidazol-2-ylidene ligands are known to form complexes with several other phosphorus Lewis acceptors, and are effective stabilizers of highly reactive species. In 1999, Kuhn and coworkers isolated the complex formed between Im and the diphenyl-phosphenium cation (**5.2**).[154] The C→P coordinate bond in **5.2** (1.813(7) Å) is shorter than that observed in the Im complex of the phosphadiazonium cation, [Mes*NP·Im]OTf (C→P = 1.852(5) Å),[18] consistent with the trend observed for N→P and P→P bond lengths in pyridine and phosphine complexes of the two cations (Chapters 3 and 4).

Arduengo and coworkers have also isolated imidazol-2-ylidene complexes of tetrafluoro-phenylphosphorane (**5.3**)[155] and phosphinidenes (**5.4**).[44;156]

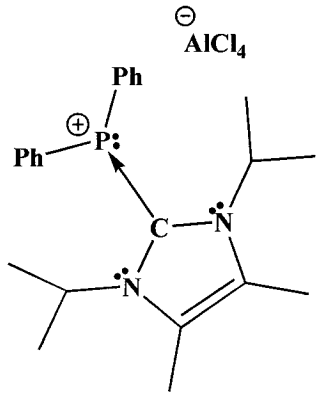

5.2

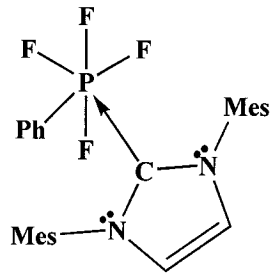

5.3

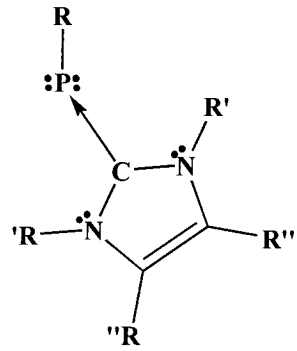

5.4

The stability of iminophosphine compounds usually depends on the presence of sterically bulky substituents, which counter the thermodynamic preference for N-P single bonds over N-P multiple bonds.[27] Some halo(imino)phosphines (RNPX) undergo reversible dimerization reactions (Scheme 5.1), and in one case (R = Mes*, X = OTf), both the mononer (**5.5**) and the dimer (**5.6**) have been isolated and structurally characterized.[69] The equilibrium in Scheme 5.1 lies to the right, favouring the 4-membered 1,3,2,4-diazadiphosphetidine ring, when the steric loading at nitrogen is insufficient. Adam Dyker, another graduate student in the Burford research group, has recently demonstrated that the phosphetidine $(DippNPCl)_2$ (**5.6**, R = 2,6-diisopropylphenyl (Dipp), X = Cl)[157] will dissociate upon introduction of the strong Lewis base Im to yield the coordination complex DippNP(Im)Cl (**5.7**).[82]

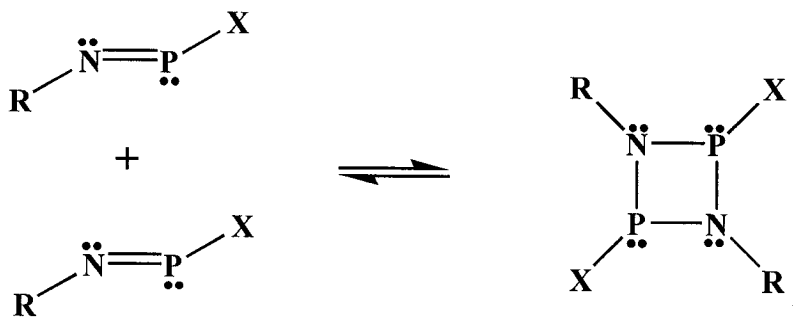

5.5 5.6

Scheme 5.1

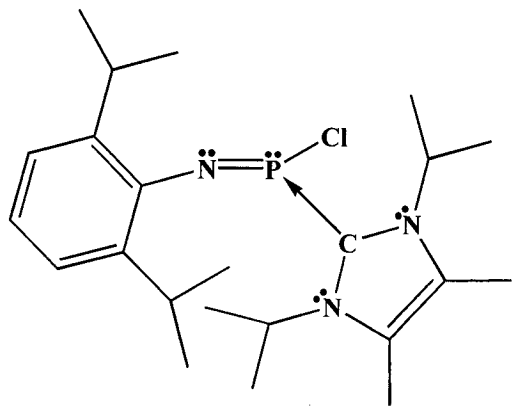

5.7

5.2 Results and Discussion

The bromo- and iodo-iminophosphines, Mes*NPBr and Mes*NPI (**5.1**, X = Br, I) react rapidly at room temperature with the imidazol-2-ylidene, Im (**2.6**). Solution ^{31}P NMR spectra of the reaction mixtures show primary components (> 90%) that correspond to the isolated products characterized as Mes*NP(Im)Br (**5.8**, X = Br) and Mes*NP(Im)I (**5.8**, X = I), respectively. Attempts to synthesize a similar coordination complex by

reaction of the pentamethylcyclopentadienyl-substituted iminophosphine (Mes*NPCp*, **5.1,** X = Cp*)[158] with Im were unsuccessful, and no reaction was observed between the species at room temperature. This contrasts ^{31}P NMR data reported by Phillips indicating the formation of a coordination complex between Im and the phenyl-substituted iminophosphine,[159] Mes*NPPh (**5.1**, X = Ph).[101]

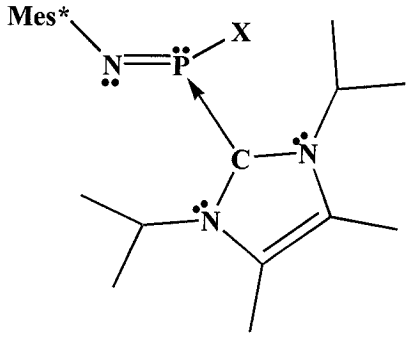

5.8, X = Br, I

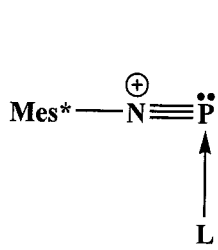

L = pyridine
quinuclidine
PPh_3
OU (**2.5**)
OIm (**2.4**, Ch = O)
SIm (**2.4**, Ch = S)
SeIm (**2.4**, Ch = Se)

5.9

The solid state structures of Mes*NP(Im)Br and Mes*NP(Im)I are illustrated in Figures 5.1 and 5.2, respectively. Selected structural parameters for all ylidene-iminophosphine complexes are presented in Table 5.1, along with analogous parameters for Mes*NPX and complexes **5.2 - 5.4**. Structural data from coordination complexes of the phosphadiazonium cation with nitrogen, phosphorus, and chalcogen ligands (**5.9**) have also been included in the table.

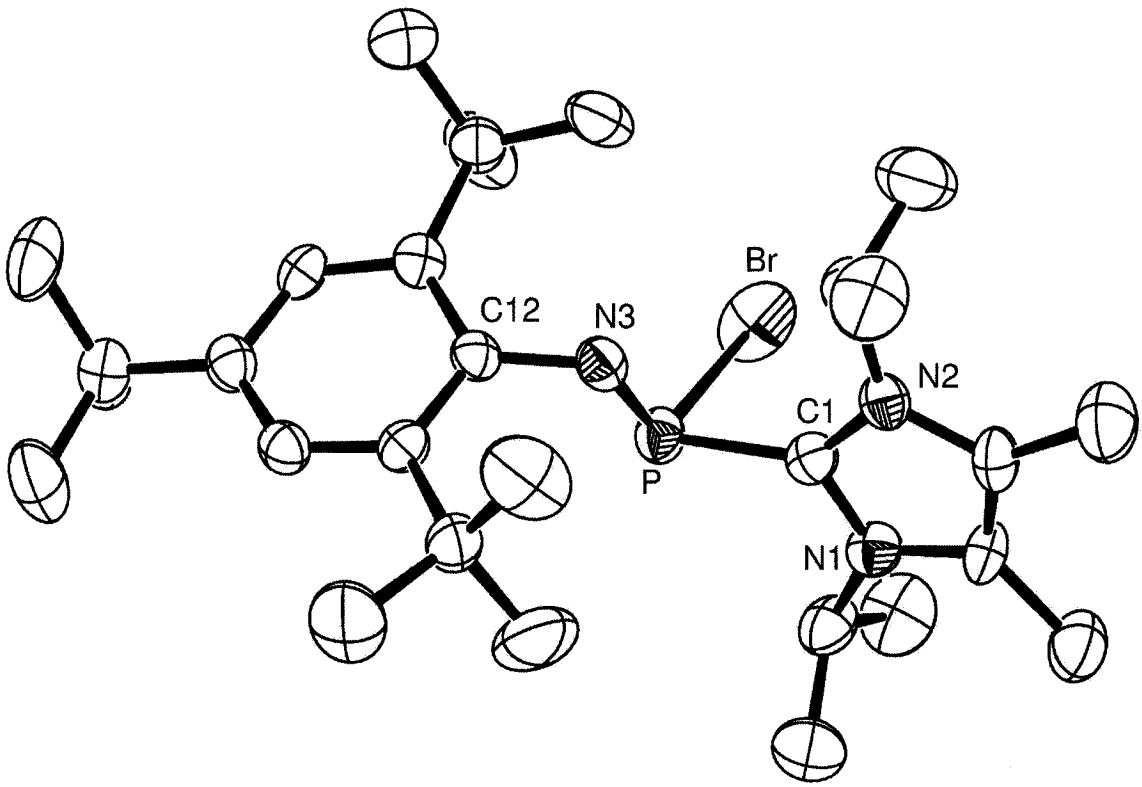

Figure 5.1 Solid state structure of Mes*NP(Im)Br (**5.8**, X = Br) drawn with 50% probability displacement ellipsoids. Hydrogen atoms have been omitted for clarity.

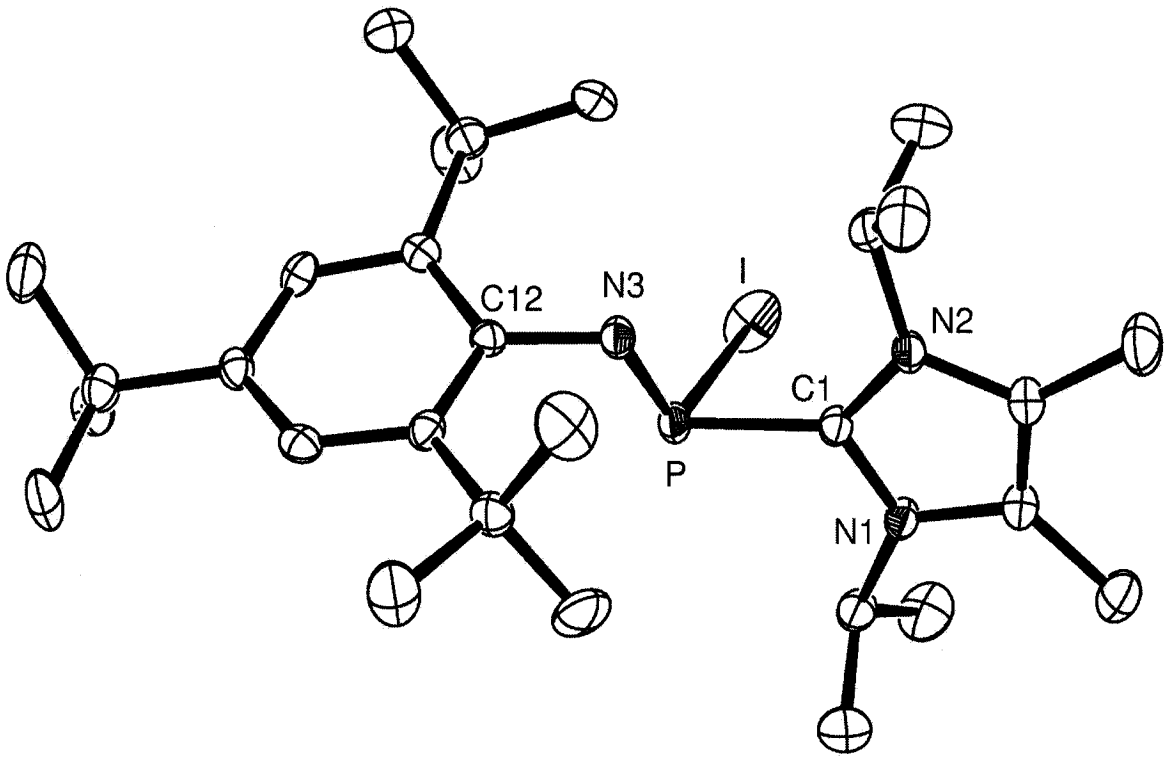

Figure 5.2 Solid state structure of Mes*NP(Im)I (**5.8**, X = I) drawn with 50% probability displacement ellipsoids. Hydrogen atoms have been omitted for clarity.

Table 5.1 ^{31}P NMR chemical shifts (ppm) in solution and selected structural parameters [bond lengths (Å), bond angles (°) and torsion angles (°)] for ylidene complexes of Mes*NPX and related compounds.

Compound	Label	$\delta\ ^{31}P$ [a]	C→P	N1-C-N2	N1-C-P	N2-C-P	P-X	N3-P	C-N3-P	C-N3-P-C	Σ<P	Ref.
Im	**2.6**	-	-	113.09(9)	-	-	-	-	-	-	-	[82]80
$(DippNPCl)_2$	**5.6**	211[a,b]	-	-	-	-	2.071(8) 2.085(8)	1.69(2) 1.73(1)	-	-	-	[157]55
DippNP(Im)Cl	**5.7**	128[b,c]	1.902(2)	106.6(2)	120.5(2)	132.6(2)	2.318(1)	1.543(2)	142.9(2)	-18.7(3)	310.5	[82]80
Mes*NPCl	**5.1**	132	-	-	-	-	2.142(4)	1.495(4)	154.8(4)	-	-	[40]38
Mes*NP(Im)Cl	**1.12**	172 154[b]	1.886(5)	106.7(4)	120.5(4)	132.8(4)	2.471(2)	1.585(5)	120.2(4)	-162.0(4)	301.2	[18;82]8 0
Mes*NPBr	**5.1**	146	-	-	-	-	2.337(2)	1.498(4)	159.5(4)	-	-	[153]51
Mes*NP(Im)Br	**5.8**	199	1.881(5)	106.1(4)	119.7(4)	134.2(4)	2.674(2)	1.578(4)	116.1(3)	-165.8(3)	304.2	[82]80
Mes*NPI	**5.1**	206	-	-	-	-	2.895(1)	1.480(3)	172.5(3)	-	-	[62]60
Mes*NP(Im)I	**5.8**	214 189[b]	1.874(3)	107.5(3)	119.1(2)	133.3(2)	2.907(1)	1.574(3)	116.2(2)	-166.6(2)	306.6	[82]80
Mes*NPOTf	**5.1**	50	-	-	-	-	1.923(3)	1.467(4)	176.4(3)	-	-	[72]70
[Mes*NP·Im]OTf	**1.46**	339 350[d]	1.852(5)	107.5(4)	119.7(3)	132.8(3)	2.951(5)	1.574(4)	116.2(3)	-170.1(4)	298.3[h]	[18;82]8 0
$[Mes*NP]AlCl_4$	**1.21**	79[d]	-	-	-	-	-	1.475(8)	177.0(7)	-	-	[40]38
$[Mes*NP·Im]AlCl_4$	**5.11**	331	-	-	-	-	-	-	-	-	-	[101]99
$[Ph_2P·Im]AlCl_4$	**5.2**	-27	1.813(7)	105.6(6)	122.7(5)	131.4(5)	-	-	-	-	310.1	[154]52
$PhF_4P·Im'$ [e]	**5.3**	-141	1.910(4)	105.0(3)	126.1(3)	128.9(3)	-	-	-	-	-	[155]53
PhP·Im'[e]	**5.4**	-54	1.794(3)	104.7(2)	124.7(2)	130.2(2)	-	-	-	-	-	[156]54
[Mes*NP·pyr]OTf	**1.43**	71	-	-	-	-	2.712(7)	1.472(8)	161.7(7)	-	307.3[h]	[81]79
[Mes*NP·quin]OTf	**1.44**	144	-	-	-	-	2.697(3)	1.519(2)	143.9(2)	-	302.2[h]	[81]79
$[Mes*NP·PPh_3]OTf$	**1.34**	-5, 52[f]	-	-	-	-	2.298(4)	1.486(4)	169.5(4)	-	305.9[h]	[59]57
[Mes*NP·OU]OTf	**2.8**	62	-	-	-	-	2.942(2)	1.486(2)	166.2(2)	-	308.6[h]	[83]81
[Mes*NP·OIm]OTf	**2.7**	77	-	-	-	-	2.774(4)	1.494(3)	159.7(3)	-	312.0[h]	[83]81
[Mes*NP·SIm]OTf	**2.7**	156	-	-	-	-	[g]	1.498(2)	174.4(2)	-	[g]	[83]81
[Mes*NP·SeIm]OTf	**2.7**	182	-	-	-	-	[g]	1.500(2)	175.5(2)	-	[g]	[83]81
$[Mes*NP·(DMAP)_2]OTf$	**4.2**	123	-	-	-	-	[g]	1.559(2)	125.2(2)	-	295.8	[145]45

[a] CH_2Cl_2; [b] Toluene; [c] Dynamic behaviour in solution; [d] Benzene; [e] Im' = 1,3-mesitylimidazol-2-ylidene; [f] Chemical shifts for fully dissociated acceptor and ligand; [g] P-O distance is greater than the sum of the van der Waals radii (P-O = 3.3 Å); [h] Weak contacts with triflate anion included in calculation.

The ylidene complexes of Mes*NP(Im)Br and Mes*NP(Im)I have been designated as complexes of iminophosphines (**5.8**, X = Br, I), rather than phosphadiazonium cations, on the basis of the length of their respective P-X bonds. Coordination of Im to Mes*NPBr results in an elongation in the P-Br bond of only 0.34 Å, similar to the change in P-Cl bond length observed in coordination of Im to Mes*NPCl (Δ P-Cl = 0.33 Å). The P-Br bond in Mes*NP(Im)Br (2.674(2) Å) is well within the sum of the van der Waals radii for phosphorus and bromine (3.7 Å),[51] although significantly longer than the P-Br bond in phosphorus tribromide (2.22 Å).[160] Coordination of Im to Mes*NPI results in no significant change to the P-I bond length (Δ P-I = 0.01 Å). This is likely a consequence of the differences in the solid state structure of Mes*NPI from those of Mes*NPCl and Mes*NPBr. Instead of discrete molecules, dimers (**5.10**) of Mes*NPI are present in the solid state, in which the two molecules are joined through relatively short I→P interactions (3.224 Å).[62] The Im ligand breaks up the dimers, substituting a C→P coordinate bond for an I→P coordinate bond, and as such coordination of a new donor effects little change. The P-I bond in Mes*NP(Im)I (2.907(1) Å) is well within the sum of the van der Waals radii for phosphorus and iodine (3.9 Å),[51] although longer than the P-I bond in phosphorus triiodide (2.52 Å).[160]

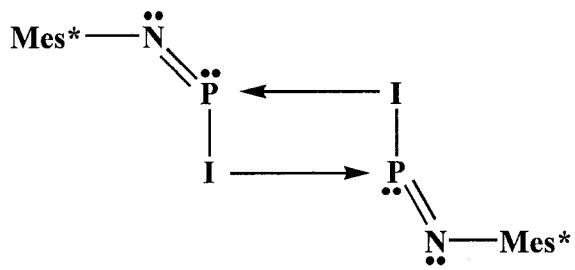

5.10

The (Mes*)N(3)-P bond lengths and (Mes*)C(12)-N(3)-P bond angles in complexes Mes*NP(Im)X (X = Cl, Br, I) and [Mes*NP·Im]OTf are equivalent in value (Table 5.1), irrespective of the identity of the leaving group X. This suggests that it is the ligand-phosphorus interaction, and not the P-X interaction, that determines the structural features of the Mes*NP fragment in coordination complexes of iminophosphines and the phosphadiazonium cation. Nevertheless, the identity of the leaving group does affect the electronic environment about phosphorus, as demonstrated by solution ^{31}P NMR data. In the iminophosphine complexes Mes*NP(Im)X (X = Cl, Br, I), in which P-X bonding is maintained, the ^{31}P chemical shifts range from 172-214 ppm. In contrast, the ^{31}P NMR chemical shift in [Mes*NP·Im]OTf (δ ^{31}P = 339 ppm) is similar to that observed in the reaction of Im with the phosphadiazonium salt [Mes*NP]$AlCl_4$ (**1.20**) to form [Mes*NP·Im]$AlCl_4$ (**5.11**, δ ^{31}P = 331 ppm), confirming its assignment as an ionic compound. The fact that the phosphorus centres in [Mes*NP·Im]OTf and [Mes*NP·Im]$AlCl_4$ are deshielded with respect to those in Mes*NP(Im)X (X = Cl, Br, I), indicates that there is a greater positive charge localized on phosphorus in the phosphadiazonium complexes. In Mes*NP(Im)X, the halogen substituents can act as π-donors, helping to delocalize any partial positive charge located on the phosphorus centres.

In all ylidene complexes of Mes*NPX (X = Cl, Br, I, OTf), the closest contact between the iminophosphine/phosphadiazonium and Im involves the phosphorus centre and the unique carbon centre, respectively. The C→P distances in Mes*NP(Im)X (X = Cl, 1.886(5) Å;[18] X = Br, 1.881(5) Å; X = I, 1.874(3) Å) are equivalent within experimental error, despite the variation in X, and are comparable in length with C-P

bonds in alkylphosphines (average, 1.855(19) Å).[106] The C→P distance in [Mes*NP·Im]OTf is slightly shorter (1.852(5) Å).[18] The uniformity in the C→P distances in the complexes again indicates that the leaving group does not play a large role in the ability of the phosphorus centre to accept electron density from a donor ligand. In contrast, a range of C→P distances is observed for imidazol-2-ylidene complexes of diphenylphosphenium **5.2** (1.813(7) Å),[154] tetrafluorophenylphosphorane **5.3** (1.910(4) Å),[155] and phosphinidenes **5.4** (R = Ph, R' = R'' = Me, 1.794(3) Å;[156] R = Ph, R' = Mes, R'' = H, 1.763(6) Å;[44] R = CF_3, R' = Mes, R'' = H, 1.784(2) Å[44]).

The (Mes*)N(3)-P distances in Mes*NP(Im)X (X = Cl, 1.585(4) Å; X = Br, 1.578(4) Å; X = I, 1.574(3) Å) and [Mes*NP·Im]OTf (1.574(4) Å) are comparable to those in alkyliminophosphines (e.g., Mes*NPCEt$_3$, N-P = 1.566(2) Å, C-N-P = 124.8(2)°)[144] and are longer than those in the corresponding free Lewis acceptors Mes*NPX. In addition, the (Mes*)C(12)-N(3)-P bond angles in the complexes (116 - 120°) are all substantially less than the almost linear C-N-P fragments in the corresponding halo(imino)phosphines. The elongation of (Mes*)N(3)-P on interaction with Im is significantly greater than that observed in complexes of Mes*NPOTf with pyridine,[81] quinuclidine,[81] triphenylphosphine,[59] and chalcogenourea[83] ligands (Table 5.1). The disruption of the N-P π-system in the acceptor upon coordination of Im is a consequence of the relatively high basicity of the ligand (cf. pK_a ImH^+ = 23,[104], $pyridineH^+$ = 5.2[105]). A similar arrangement is imposed by the two 4-dimethylaminopyridine (DMAP, **4.1**, pK_a $DMAPH^+$ = 9.2[161]) ligands in the donor-rich complex [Mes*NP·(DMAP)$_2$]OTf (**4.2**, (Mes*)N-P = 1.559(2) Å, C-N-P = 125.2(2)°).[145]

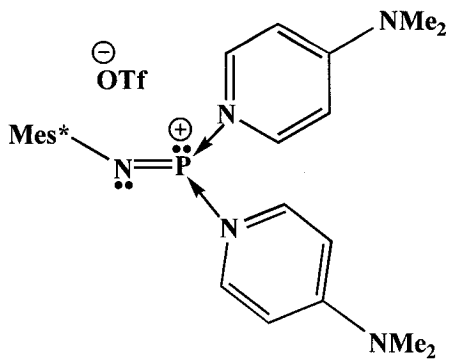

4.2

The planar five-membered ring of the Im unit in the complexes is structurally similar to that in the free ligand (Im), and contraction (6-7°) of the N(1)-C(1)-N(2) angle represents the only substantive adjustment within the ligand as a result of coordination. The orientation of the ligand with respect to the phosphorus acceptor is nonsymmetric. In all Im complexes of Mes*NPX, the N(1)-C(1)-P angle is uniformly smaller than the N(2)-C(1)-P angle (ΔN-C-P = difference between N(1)-C(1)-P and N(2)-C(1)-P = 12-15°; Table 5.1) due to steric repulsion arising from the eclipsed conformation of N(2) and N(3). A nonsymmetric interaction of the ylidene with phosphorus is also apparent in complexes **5.2** (ΔN-C-P = 8.7°)[154] and **5.4** (ΔN-C-P = 5.5°).[156]

All derivatives of Mes*NP(Im)X adopt a trans configuration of Mes* and Im about the P=N vector (torsion angles (Mes*)C(12)-N3-P-C(1) = 162-170°; Table 5.1). In contrast, Dipp and Im are observed in a cis configuration ((Mes*)C(12)-N(3)-P-C(1) = 18.7(3)°)[82] in the solid state structure of DippNP(Im)Cl (**5.7**, R = Dipp, X = Cl), likely due to the steric distinction between Mes* and Dipp substituents. Nevertheless, the steric strain imposed by Dipp is accommodated in the cis configuration by adjustment of

(Mes*)C(12)-N(3)-P, which is distinctly large for DippNP(Im)Cl (142.9(2)°) in comparison to the all trans-configured derivatives of Mes*NP(Im)X (116-120°).

5.3 Conclusions

The strong Lewis base Im forms coordination complexes with a series of halo(imino)phosphines Mes*NPX (X = Cl, Br, I, OTf) to give the iminophosphine complexes Mes*NP(Im)X (X = Cl, Br, I), and the phosphadiazonium complex [Mes*NP·Im]OTf. The complexes have identical structural parameters, with the exception of their P-X bond lengths, and yet have significantly different ^{31}P NMR chemical shifts. Thus, the identity of the leaving group X has an impact upon the electronic environment about phosphorus in the complexes, but does not affect the bonding of phosphorus to any other elements.

Chapter 6: Spectroscopic Studies of Coordination Complexes of the Phosphadiazonium Cation

6.1 Introduction

Phosphorus-31 NMR spectroscopy is, second to X-ray crystallography, the most important and widely used analytical technique for the characterization of structure and bonding in low-coordinate phosphorus-nitrogen compounds.[162] With the increased number of ligand-phosphadiazonium complexes now isolated, an examination of the trends in the spectroscopic features of these compounds is warranted. Phosphorus-31 NMR chemical shifts of the complexes [Mes*NP·L]OTf (Mes* = 2,4,6-tri-*tert*-butylphenyl, OTf = trifluoromethylsulfonyloxy or triflate), both in solution and in the solid state, will be discussed in context of the basicity of the donor ligand, L. In addition to exhibiting a range of ^{31}P NMR chemical shifts, the complexes exhibit a range of colours in solution (Figure 6.1). This has prompted studies of the electronic spectra of these compounds, and these will also be related to trends in ligand basicity.

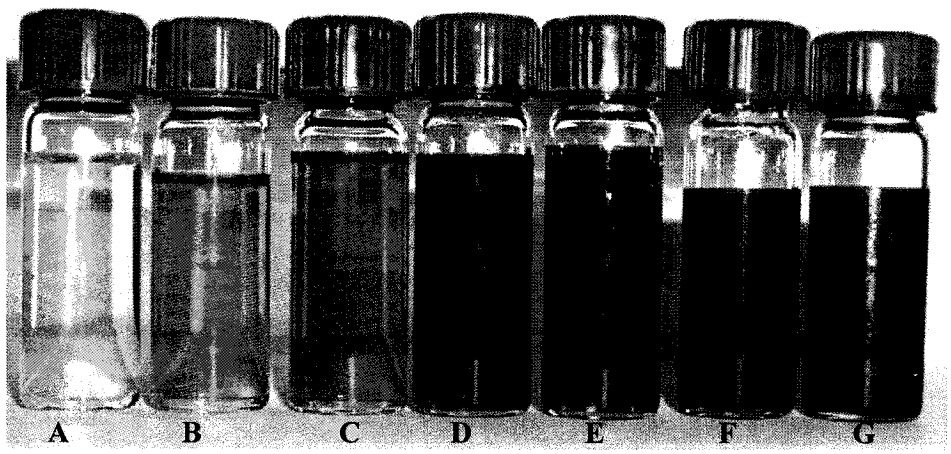

Figure 6.1 Solutions of (**A**) Mes*NPOTf (**1.33**), (**B**) [Mes*NP·DABCO]OTf (**4.21**), (**C**) [(Mes*NP)$_2$·(4,4'-BIPY)][OTf]$_2$ (**4.14**) (**D**) [Mes*NP·SIm]OTf (**2.7**, Ch = S), (**E**) [Mes*NP·DMAP]OTf (**4.16**), (**F**) [Mes*NP·SeIm]OTf (**2.7**, Ch = Se), and (**G**) [Mes*NP·Im]OTf (**1.46**) in CH_2Cl_2.

Niecke and coworkers have surveyed the ^{31}P NMR chemical shifts of iminophosphines (R'NPR) in both solution and in the solid state, and generally they appear in the range of 600 to 50 ppm (data for selected compounds are presented in Table 6.1).[162;163] Like the solid state structural features of iminophosphines, the ^{31}P NMR chemical shifts are highly sensitive to substituent effects: *P*-Aryl-, *P*-alkyl- and *P*-phosphino-substituted iminophosphines appear at lower field, while *P*-halo- and *P*-oxy-substituted iminophosphines appear at higher field. The iminophosphine Mes*NPOTf (**1.33**), used extensively in the coordination chemistry studies in this thesis, exhibits the lowest chemical shift of all known iminophosphine compounds (52 ppm).[72] The shielding of the phosphorus nucleus in Mes*NPOTf has been explained by the relative importance of the phosphadiazonium resonance contributor (**1.33b**) in this compound (Scheme 6.1).[162]

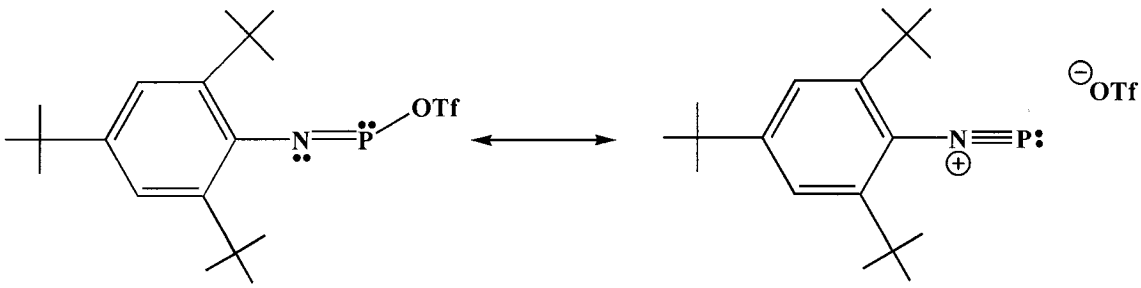

1.33 **1.33b**

Scheme 6.1

Table 6.1 Solution ^{31}P NMR chemical shifts (ppm) and UV-visible n-π^* transitions (λ_{max} / nm) for iminophosphines Mes*NPR (reproduced from reference 62).

Substituent (R)	δ ^{31}P	λ(n-π^*)[a]
P^tBu_2	580	570
CEt_3	520	544
^iPr	491	533
^tBu	490	525
$CH(SiMe_3)_2$	476	532
Ph	415	576
Mes*	396	568
$N(SiMe_3)_2$	327	416
$N(SiMe_3)^tBu$	313	401
O^tBu	179	340
OMe	156	335

[a] Extinction coefficients not reported for these transitions.

The UV-visible spectra of iminophosphines, also surveyed by Niecke, show two well separated bands, one of high intensity, and the other of low intensity, referring to π-π^*, and n-π^* transitions, respectively (Table 6.2).[64] The n-π^* band generally exhibits a low molar extinction coefficient. In iminophosphines of the type Mes*NPR a large variation in the energies of the n-π^* transitions is observed, indicating that the energy of the LUMO in these compounds is strongly affected by the substituents located at phosphorus (Table 6.1).[64] The ^{31}P NMR data and the UV-visible data are correlated, and a plot of λ_{max} (n-π^*) vs. δ ^{31}P reveals a linear relationship (Figure 6.2).

As the ^{31}P NMR chemical shift of the iminophosphine increases, the n-π^* transition of the compound is observed at longer wavelengths.

Table 6.2 UV-visible π-π* transitions (λ_{max} / nm) and n-π* transitions (λ_{max} / nm), for iminophosphines R'NPR. The extinction coefficients (ε / $M^{-1}cm^{-1}$) for each transition are located in the columns to the right of those listing λ_{max}.

R	R'	λ(π-π*)	ε	λ(n-π*)	ε	Reference
CEt_3	^tBu	230	11700	440	250	64
^tBu	CEt_3	235	10800	448	210	64
^tBu	^tBu	233	12000	431	210	66
$N(SiMe_3)_2$	^tBu	267	5600	348	200	66
^tBu	NMe_2	310	4700	345	500	64
Cp*	NMe_2	264	2700	346	500	64
Cp*	$N(SiMe_3)_2$	271	2600	341	500	64

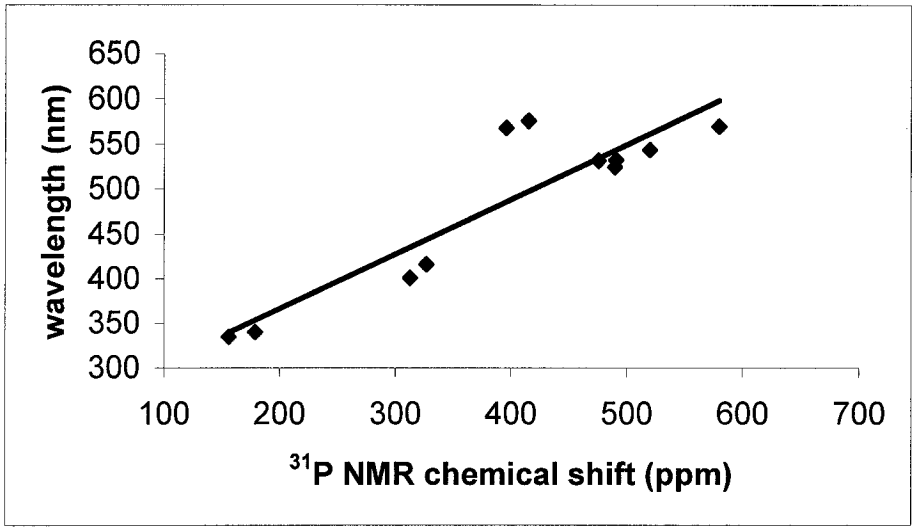

Figure 6.2 Relationship between ^{31}P NMR chemical shifts and electron excitations λ_{max}(n-π*) in the iminophosphines Mes*NPR (reproduced from reference 62).

As discussed in Section 1.3, theoretical calculations have revealed that the energetically high-lying orbitals in iminophosphines are the π- and π*-orbitals of the P-N π-bond, and the σ_n-orbital from the lone pair at the phosphorus atom.[65;66] Depending on the substituents present at phosphorus and nitrogen, there are two possible frontier orbital arrangements (Figure 6.3). Arrangement (**1**), where the HOMO is a σ-orbital and the LUMO is a π*-orbital, is present in the majority of substituted-iminophosphine

compounds, whereas arrangement (**2**) (π HOMO, π^* LUMO) is present in iminophosphines with π-donor substituents bound to phosphorus or nitrogen.

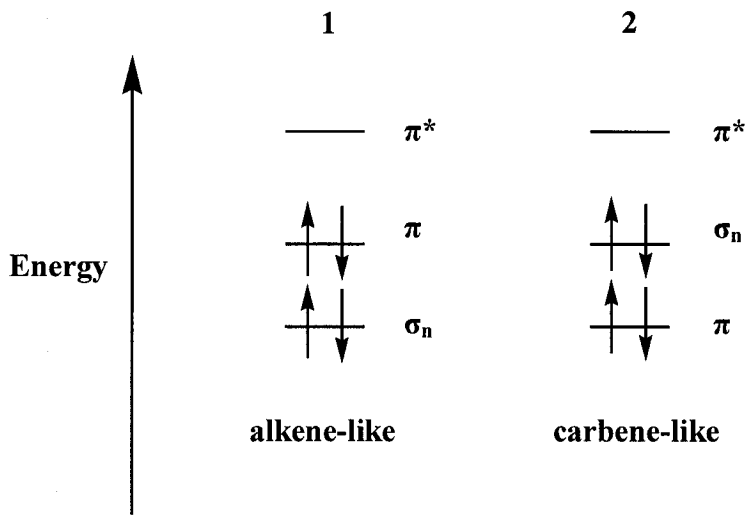

Figure 6.3 Possible frontier orbital energy sequences for iminophosphines.

6.2 Results and Discussion

6.2.1 ^{31}P NMR Spectroscopy

The ^{31}P NMR chemical shifts of the Lewis acceptor phosphorus centres in coordination complexes [Mes*NP·L]OTf vary between 36 and 339 ppm in CD_2Cl_2 (Table 6.3). Generally, coordination of a ligand causes a downfield shift in the ^{31}P NMR spectrum from that of the free Lewis acceptor Mes*NPOTf (the complexes containing the weakly coordinating PPh_3 and DIPHOS ligands are an exception).

Table 6.3 Solution ^{31}P NMR chemical shifts in CD_2Cl_2 (ppm), solid state ^{31}P NMR isotropic chemical shifts (ppm), and solution colour for complexes [Mes*NP·L]OTf.

Ligand (L)	Label	δ $^{31}P^c$	δ_{iso} $^{31}P^c$	Colour[i]	Ref.
None	**1.33**	52	49	yellow	72
DIPHOS	**3.15, R = Ph**	10, **48**[d] 10, **36**[e]	-17, 12, **35**	orange	130
PPh_3	**1.34**	-5, **52**[f]	-1, **71**	orange	59
DEPE	**3.15, R = Et**	27, **53**	**32**, 32, 49	red-orange	130
2,2'-BIPY	**1.45**	54	67	red-orange	80;130
4,4'-BIPY[a]	**4.14**	61	**60, 63**[g]	red	145
DMPE	**3.15, R = Me**	16, **62**	-	red	130
OU	**2.8**	62	73	orange	83
pyridine	**1.43**	71	65	red-orange	81
OIm	**2.7, Ch = O**	77	-	orange	83
DABCO[a]	**4.20**	80	-	red-brown	this work
4,4'-BIPY[b]	**4.19**	81	-	red	this work
PMDETA	**3.16**	89	**93, 103**[h]	yellow[j]	130
DABCO[b]	**4.21**	110	-	red-brown	this work
TMEDA	**3.14**	110	146	yellow[j]	130
2DMAP	**4.2**	123	147	red-brown	145
DMAP	**4.16**	132	-	pink-purple	145
quinuclidine	**1.44**	144	-	red	81
SIm	**2.7, Ch = S**	156	165	red	83
SeIm	**2.7, Ch = Se**	182	195	red-purple	83
Im	**1.46**	339	366	blue	82

[a] Ligand-bridged adduct; [b] 1:1 Adduct; [c] Signal corresponding to phosphadiazonium centre is in bold; [d] 298K, temperature dependence; [e] 193 K; [f] Dissociated in solution; [g] Two crystallographically distinct phosphorus centres in ligand-bridged adduct; [h] Two isomers present in powdered form; [i] Colour at high concentrations used for NMR studies; red-brown solutions appear orange at lower concentrations; [j] Turns red over time in solution.

In solution, ligand-phosphorus interactions result in nucleophilic displacement of the triflate group from phosphorus. Introduction of positive charge in the Mes*NP·L fragment results in a deshielding of the phosphorus nucleus, and as a result its chemical shift is observed at lower field. Coordination of the ligands to the phosphadiazonium

cation in solution is reversible (Scheme 6.2), and as such the ligand and the triflate group compete for interaction with the phosphorus centre. The right side of the equilibrium is favoured as the donor strength of the ligand increases, leading to a greater charge separation in the complexes and a downfield shift in the ^{31}P NMR resonances.

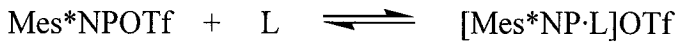

Scheme 6.2

The ^{31}P NMR chemical shifts of complexes [Mes*NP·L]OTf can be used to assess the relative donor abilities (or basicities) of the ligands, L, with respect to the phosphadiazonium cation. According to the data in Table 6.3, the PPh_3 and DIPHOS ligands are the weakest donors because the ^{31}P NMR chemical shifts of the Lewis acceptor phosphorus centres in [Mes*NP·PPh_3]OTf and [Mes*NP·DIPHOS]OTf complexes appear at highest field. Likewise, the SeIm and Im ligands are the strongest donors because the ^{31}P NMR chemical shifts of the Lewis acceptor phosphorus centres in [Mes*NP·SeIm]OTf and [Mes*NP·Im]OTf appear at lowest field. The relative basicities of the ligands increase from top to bottom in the table. The bidentate and tridentate ligands, TMEDA and PMDETA, are weaker donors than the monodentate amine ligand, quinuclidine, reflecting the reduction in basicity of multidentate ligands upon introduction of a greater cationic charge. Nevertheless, the more shielded phosphorus nuclei in [Mes*NP·TMEDA]OTf (**3.14**) and [Mes*NP·PMDETA]OTf (**3.16**) could also be a consequence of the increased coordination number at phosphorus. The ^{31}P NMR

chemical shift of the ligand-rich adduct [Mes*NP·$(DMAP)_2$]OTf (**4.2**) is also located at slightly higher field than that of the corresponding 1:1 adduct [Mes*NP·DMAP]OTf (**4.16**).

One way to quantify relative ligand basicities is to compare the pK_a values of their conjugate acids: the higher the pK_a of the conjugate acid, the stronger the base. For instance, the pK_a of the conjugate acid of the weak base PPh_3 is 2.7, while the pKa of the conjugate acid of dimethylimidazol-2-ylidene (a model for the strong base Im) is 23.[104] The acidity constants (pK_a) of several protonated Lewis bases in aqueous media are presented in Table 6.4. Although acidity constants for protonated chalcogeno-ureas in aqueous solution were not available, calculated gas phase proton affinities indicate that the basicity of the ligands increases in the following manner: urea < thiourea < selenourea.[164;165] The pK_a of *O*-protonated *N,N*-dimethylbenzamide is only –1,[166] but the presence of the additional amino group in ureas should increase the donor ability of the carbonyl oxygen.

A plot of the pK_a values of several protonated ligands vs. the solution ^{31}P NMR chemical shifts of complexes [Mes*NP·L]OTf yields a satisfactory linear relationship (Figure 6.4), despite the fact that the chemical shifts were not measured in aqueous media. The correlation between the pK_a values and ^{31}P NMR chemical shifts supports the assignment of a relative ligand basicity scale based upon ^{31}P NMR spectroscopy. (Note: The average of the pK_a values for singly- and doubly-protonated ethylenediamine were used to model the donor ability of TMEDA, while the average of the pK_a values for singly- and doubly-protonated DABCO were used to model the donor ability of DABCO in the bridged-ligand complex.)

Table 6.4 pK_a values in aqueous solution of protonated ligands

Ligand·H^+	pK_a	Reference
Ph_3PH^+	2.7	167
Et_3PH^+	8.7	168
Me_3PH^+	8.7	168
$[PhC(OH)NMe_2]^+$	-1.0	166
pyridine·H^+	5.2	105
DMAP·H^+	9.2	161
NH_4^+	9.2	161
ethylenediamine·H^+	10.0	161
ethylenediamine·$2H^{2+}$	6.9	161
Me_3NH^+	9.8	169
quinuclidine·H^+	11.0	169
DABCO·H^+	8.8	170
DABCO·$2H^{2+}$	3.0	170
1,3-dimethylimidazolium (DMI)	23.0	104

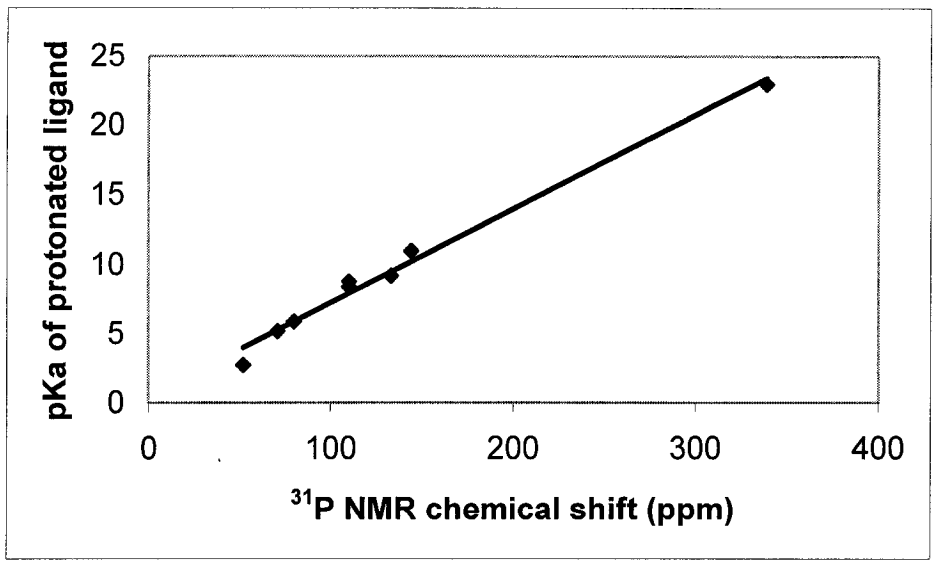

Figure 6.4 Relationship between ^{31}P NMR chemical shifts and pK_a of protonated ligands in coordination complexes [Mes*·L]OTf.

In arene solvents (benzene, toluene) the ^{31}P NMR chemical shifts of the complexes are located 10-20 ppm downfield with respect to those measured in dichloromethane (Table 6.3), indicating that solvent plays an important role in the equilibrium process depicted in Scheme 6.2. Dichloromethane is a more polar solvent than benzene or toluene, and intuitively, one would expect greater charge separation in species [Mes*NP·L]OTf in this solvent. The deshielded signals of the complexes in benzene and toluene may be a consequence of their abilities to act as π-donor ligands. Benzene and toluene molecules have been observed to coordinate to the phosphadiazonium cation through their respective π-systems in the solid state (Section 1.4)[79] and their solvation of the phosphadiazonium cation in solution could result in greater dissociation of the triflate group.

The solid state ^{31}P NMR isotropic chemical shifts (δ_{iso} ^{31}P) of [Mes*NP·L]OTf are similar to the ^{31}P chemical shifts observed in solution, indicating that few structural differences exist between the complexes in solution and in the solid state. In the majority of complexes, the solid state ^{31}P resonances are located 10-30 ppm downfield with respect to those in solution, although there are some exceptions (Table 6.3). For example, δ_{iso} ^{31}P is observed at higher field in [Mes*NP·pyridine]OTf (**1.43**) and [Mes*NP·DEPE]OTf (**3.15**, R = Et). The solid state ^{31}P NMR isotropic chemical shifts of iminophosphines (R'NPR) are also very similar in value to the corresponding chemical shifts observed in solution;[163] however, the differences between δ_{iso} ^{31}P and δ ^{31}P are generally smaller in these compounds.

6.2.2 UV-Visible Spectroscopy

The UV-visible spectrum of the yellow compound Mes*NPOTf exhibits an absorption maximum at 360 nm with an extinction coefficient of 11 000 $M^{-1}cm^{-1}$. Another more intense absorption is visible in the UV region of the spectrum at 221 nm; however, the extinction coefficient for this absorption has not been calculated due to the reduced transparency of CH_2Cl_2 below 250 nm. The wavelength of the lowest energy transition in Mes*NPOTf (360 nm) agrees well with those reported by Niecke for the iminophosphines Mes*NPO^{t}Bu (340 nm) and Mes*NPOMe (335 nm), which have been assigned as n-π^* transitions.[64] Nevertheless, the extinction coefficient for the lowest energy transition in Mes*NPOTf is much larger than those typically observed for n-π^* transitions in iminophosphines (Table 6.2). The relative importance of the phosphadiazonium resonance contributor (**1.33b**, Scheme 6.1) in Mes*NPOTf could result in the compound having a different sequence of frontier orbitals than other iminophosphines.

Experimental difficulties were encountered in measuring UV-visible spectra of the coordination complexes [Mes*NP·L]OTf. Typically, samples for ^{31}P NMR spectroscopy were run at concentrations of approximately 0.05 M, while much lower concentrations were needed for UV-visible spectroscopy. For the more weakly coordinating ligands (e.g., pyridine, OU), dilution resulted in complete dissociation of the ligands from the acceptor species. The orange or red-orange solutions became yellow, and the resulting UV-visible spectra were identical to that of Mes*NPOTf.

The more basic ligands, SIm, DMAP, SeIm, and Im, remain coordinated to the phosphadiazonium cation at concentrations as low as 4.0×10^{-4} M, indicated by the red,

pink-purple, red-purple, and blue colours of their respective solutions. Nevertheless, some ligand dissociation may still be occurring in these solutions and the accuracy of the calculated concentrations is unknown. The UV-visible spectra of these complexes show two absorption maxima in the visible region (Table 6.5). The transition of longer wavelength is of lesser intensity, and has a small extinction coefficient (assuming the calculated concentration of the solution is accurate). Based upon Niecke's work with iminophosphines,[64] this transition has been assigned as an n-π^* excitation. In general, the wavelengths of the n-π^* transitions in [Mes*NP·L]OTf increase with the basicity of the ligand, L.

The transitions of shorter wavelength in the UV-visible spectra of [Mes*NP·L]OTf are of significantly greater intensity, and have tentatively been assigned as π-π^* transitions. At the solution concentrations needed to observe the n-π^* transitions in the complexes, the π-π^* transitions have intensities greater than three absorbance units. At lower concentrations, the absorption maxima of the n-π^* transitions disappear, and the solutions become virtually colourless. The ligands may not be coordinated to the phosphadiazonium cation in these dilute solutions, and as such, the extinction coefficients of the π-π^* transitions cannot be accurately determined.

In general, as the wavelength of the n-π^* transition in the complexes becomes longer, the value of the ^{31}P NMR chemical shift increases (Figure 6.5); however, the value of λ_{max} is actually greater in [Mes*NP·DMAP]OTf (**4.16**, δ ^{31}P = 132 ppm) than in [Mes*NP·SIm]OTf (**2.7**, Ch = S, δ ^{31}P = 156 ppm). The wavelength of the n-π^* transition in [Mes*NP·Im]OTf (**1.46**, blue solution, λ_{max} = 600 nm) is longer than any observed in iminophosphines Mes*NPR, but the ^{31}P NMR chemical shift of the complex is

substantially less than that of the iminophosphine Mes*NP^{t}Bu (λ_{max} = 570 nm, δ ^{31}P = 580 ppm).[64]

Table 6.5 UV-visible transitions (λ_{max} / nm), extinction coefficients (ε / $M^{-1}cm^{-1}$), and colours of solutions of complexes of the phosphadiazonium cation [Mes*NP·L]OTf.

Ligand	λ_{max}	ε	Colour
None	361	11000	yellow
	221	-	
SIm	492	1300	red
	394	-	
DMAP	510	400	pink-purple
	341	-	
SeIm	518	800	red-purple
	404	-	
Im	603	600	blue
	360	-	

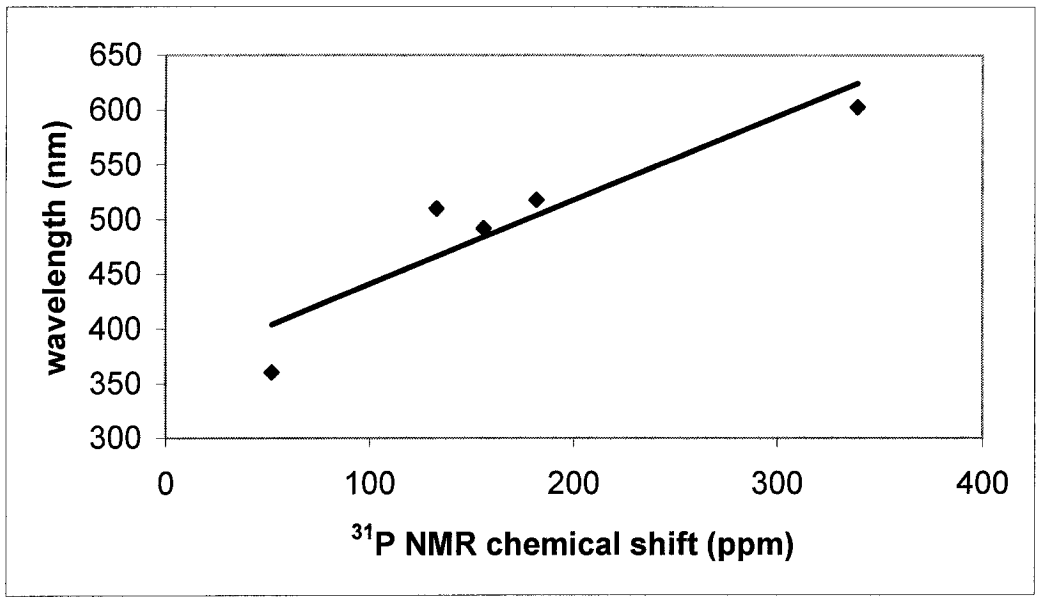

Figure 6.5 Relationship between ^{31}P NMR chemical shifts and electron excitations λ_{max} in complexes of the phosphadiazonium cation [Mes*NP·L]OTf.

Evidently, coordination of a ligand has a substantial effect on the electronic structure of the phosphadiazonium Lewis acceptor. The HOMO-LUMO energy gap in the complexes is markedly smaller than that in the free acceptor species Mes*NPOTf, and as the basicity of the coordinating the ligand increases, the difference in energy between the HOMO and LUMO in the complexes decreases. At present, the reasons for the changes in the electronic structure of Mes*NPOTf upon complexation of a ligand are not well understood. Theoretical calculations are currently underway to better elucidate the electronic structure of these species. Previous theoretical studies of low coordinate phosphine Lewis acids have examined the relative energies of the HOMO and LUMO in the free acceptor species, but not in the coordination complexes.[171;172]

6.3 Conclusions

As the basicity of the ligand coordinating to the phosphadiazonium cation increases, the chemical shift of the resulting complex moves to lower field and the colour of the complex shifts from yellow to red to blue. Lower energy transitions are observed in the UV-visible spectra of the complexes than in the spectrum of the free acceptor species Mes*NPOTf, indicating that coordination of a ligand reduces the energy gap between the HOMO and LUMO in the phosphadiazonium cation. The solid state ^{31}P NMR isotropic chemical shifts of the complexes are comparable to the ^{31}P NMR chemical shifts observed in solution, suggesting that the structures of the complexes in solution are similar to those viewed in the solid state.

Chapter 7: Conclusions and Future Work

7.1 Most Significant Contributions to Scientific Development From This Thesis

The coordination complexes presented in this thesis highlight the potential for electron-rich centres to behave as Lewis acids in spite of the presence of a lone pair of electrons at the acceptor site. In addition, the coordination of neutral donors to the phosphadiazonium cation represents a new synthetic methodology in phosphorus chemistry, where phosphorus-element (element = main group element) bonds are formed through donor-acceptor interactions. The general applicability of this method to all main group donor atoms is supported by the isolation of Ch→P(III) (Ch = O, S, Se) bonds in the complexes [Mes*NP·ChIm]OTf (**2.7**, Ch = O, S, Se) and [Mes*NP·OU]OTf (**2.8**). Examples of C→P(III), N→P(III), and P→P(III) bonds have also been isolated using this synthetic strategy.

The coordination chemistry of the phosphadiazonium cation has been diversified beyond the initial observations of mono-ligand (**7.1**) and bidentate-ligand complexes (**7.2**) to include a tridentate ligand complex (**7.3**), a donor-rich complex (**7.4**), and an acceptor-rich complex (**7.5**). The isolation of the donor-rich complex [Mes*NP·$(DMAP)_2$]OTf (**4.2**) represents the first example of multiple ligands coordinating to one phosphorus(III) Lewis acid. Spectroscopic studies of all known complexes of the phosphadiazonium cation have revealed a link between ligand basicity, ^{31}P NMR chemical shifts, and absorptions in the visible region of electronic spectra.

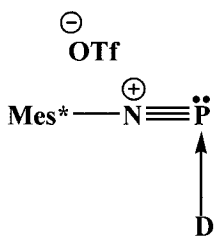

7.1

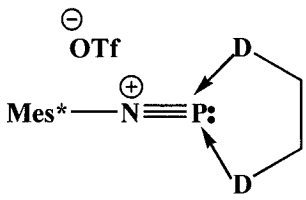

7.2

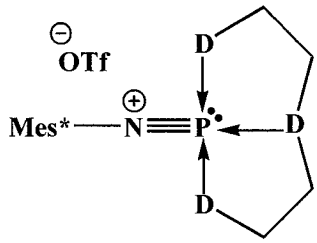

7.3

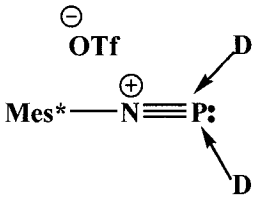

7.4

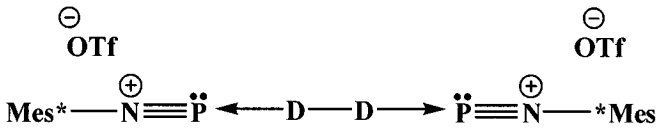

7.5

D = Donor Atom

In all complexes, both P-N π-bonding and the stereochemically active lone pair at phosphorus are retained, highlighting rare hypervalent bonding environments for phosphorus(III). In the context of the phosphorus bonding environments described throughout the introductory chapter, coordination complexes of the phosphadiazonium cation contain examples of bonding environments **M**, **X**, **Y**, and **Z**. Typically, high valence electron counts at phosphorus are accompanied by high coordination numbers (e.g., PF_5, PF_6^-). The coordination complexes in this thesis are significant in that they combine a relatively high electron count at phosphorus with a relatively low coordination number. Most importantly, these bonding environments are synthetically accessible only *via* the coordination chemistry of phosphorus(III) as a Lewis acceptor.

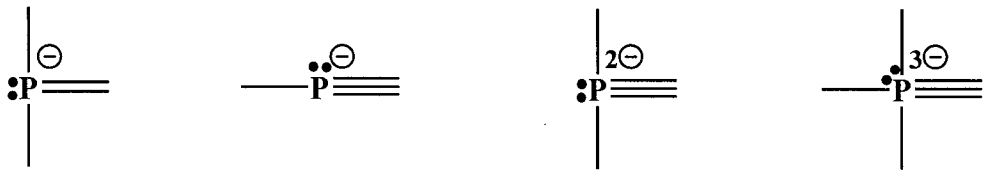

M X Y Z

7.2 Future Work

7.2.1 Coordination of Heavy Main Group Element Donors to the Phosphadiazonium Cation

Although the coordination chemistry of the phosphadiazonium cation has already been used to isolate examples of E→P(III) (E = C, N, O, P, S, Se) coordinate bonds, a wide variety of different element donors are still available to offer new bond forming possibilities to this phosphine Lewis acid. Of particular interest is the coordination of heavier Group 13 and 14 elements to phosphorus. A series of low valent aluminum(I),[173] gallium(I),[174] indium(I),[175] and thallium(I)[176] carbene analogues (**7.6**, E = Al, Ga, In, Tl) have recently been isolated using the β-diketiminate ligand $(NDippCMe)_2CH$ (Dipp = 2,6-diisopropylphenyl). The gallium analogue has already been observed to coordinate to the diphenylphosphenium cation, $[PPh_2]^+$ (**7.7**), and the resulting complex represents an interesting example of "coordination chemistry umpolung": a metal atom donor coordinating to a non-metal acceptor.[94] Heavier Group 14 carbene analogues (**7.8**, E = Si, Ge, Sn),[177-179] which are isovalent with the imidazol-2-ylidene ligand used in Chapter 5, have also been synthesized and should provide an easy route to the formation of Group14 element-phosphorus bonds.

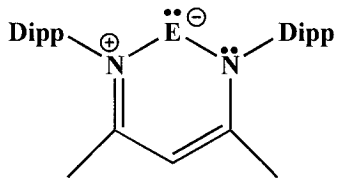

7.6, E = Al, Ga, In, Tl

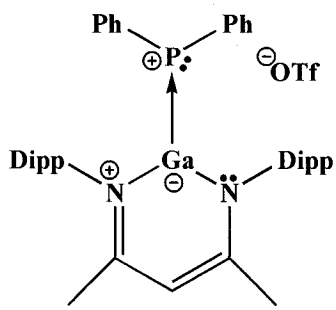

7.7

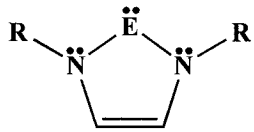

7.8, E = Si, Ge, Sn

Coordination of the heavier Group 15 elements, arsenic and antimony, to the phosphadiazonium cation may also be achievable through a slightly different synthetic strategy. Unlike the diphenylphosphenium cation, $[PPh_2]^+$, the phosphadiazonium cation demonstrates a marked preference for the formation of chelate complexes over tethered complexes (Chapter 3). In the presence of TMEDA or 1,2-bis(diphosphino)ethane ligands, chelate complexes (**7.2**) of the phosphadiazonium cation are formed exclusively, independent of the reaction stoichiometry. The use of mixed-donor chelating ligands incorporating a nitrogen anchor, may allow for coordination of less basic donor atoms, such as As or Sb, to the phosphadiazonium cation. Representative examples of these ligands (**7.9 – 7.11**),[180;181] which have already been used in transition metal coordination chemistry, are pictured below.

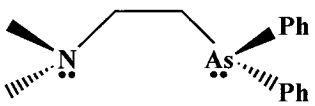

7.9

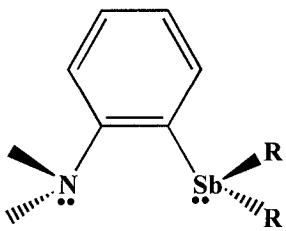

7.10, R = Me, Ph

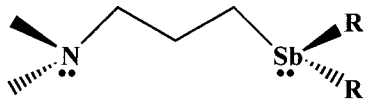

7.11, R = Me, Ph

7.2.2 Supramolecular Chemistry

The ability of the phosphadiazonium cation to bind multiple ligands, along with the ability of bridging ligands to link multiple phosphadiazonium moieties, may allow for the construction of large, supramolecular structures through coordination chemistry. For example, reaction of three equivalents of Mes*NPOTf with 1,3,5-tripyridylbenzene should yield the trication **7.12**. Additional donor molecules could then be reacted with the phosphorus centres in **7.12** to build out from the centre, creating a dendrimer-like molecule. Phosphorus-containing dendrimers possess unique properties and are finding numerous applications in materials science and catalysis.[182]

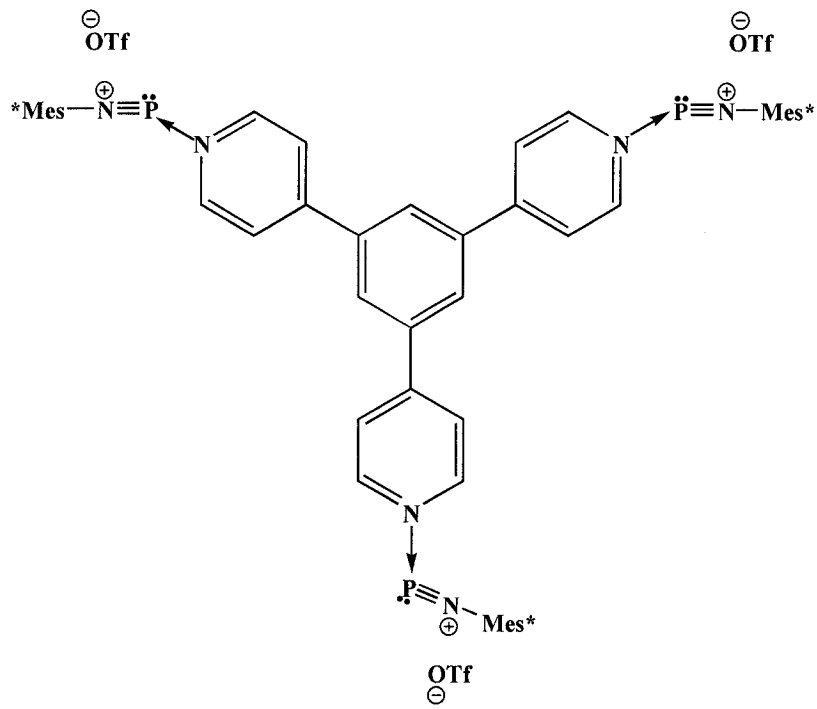

7.12

A molecule with two iminophosphine groups connected by a linker unit (**7.13**) offers another route to the synthesis of high-molecular weight coordination complexes.

Reaction of **7.13** with bridging ligands like 4,4'bipyridine could yield coordination polymers (**7.14**) or molecular squares (**7.15**). Should the molecular species **7.15** be accessible, its cavity could be used as a host for a variety of guest molecules. Changing the linker unit in **7.13** would allow for variation in the shape and size of the cavities in complexes similar to **7.15**.

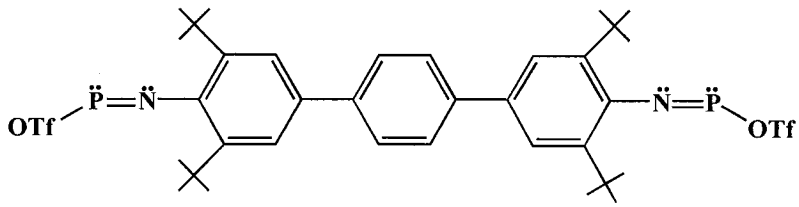

7.13

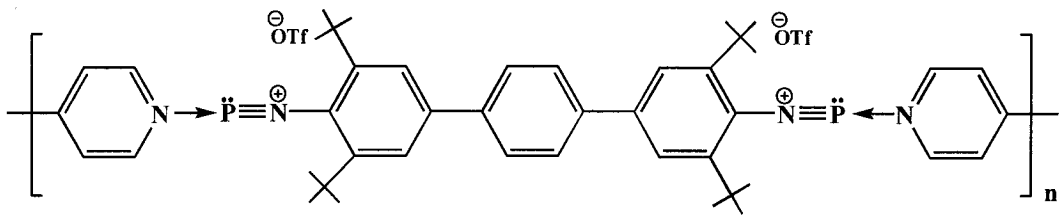

7.14

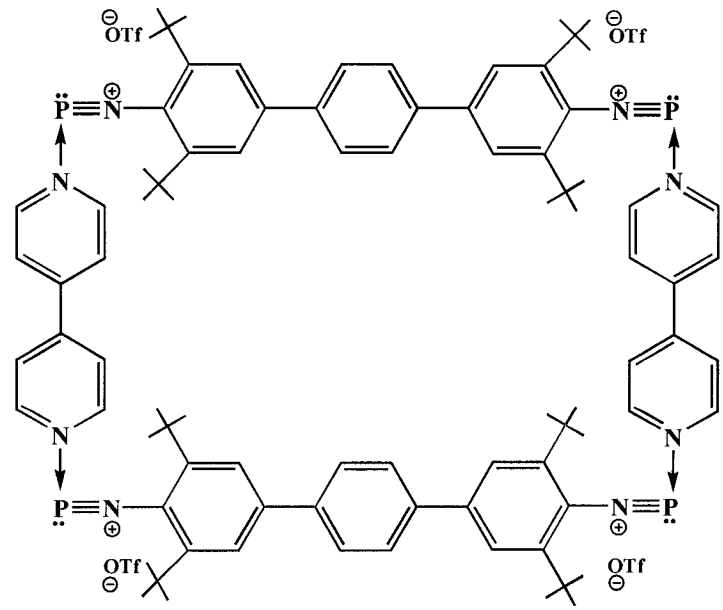

7.15

7.2.3 Host-Guest Chemistry

Another synthetic target is to maximize the number of donor atoms interacting with the phosphadiazonium cation in order to impose an even greater degree of hypervalency on the phosphorus centre. One way to accomplish this is to incorporate the phosphadiazonium cation as a guest in a donor-rich host molecule. Crown ethers (**7.16**) are often used as hosts for metal cation guests, yet ethers are very weak bases and do not coordinate to the phosphadiazonium cation in solution. The amine analogues of crown ethers, **7.17** and **7.18**, are commercially available, and should complex the phosphadiazonium cation efficiently. The concept of putting an electron-rich (lone pair bearing) guest in a crown ring is not unprecedented. Mulvey and coworkers have synthesized a series of "inverse" crown ether complexes, where metal atoms are incorporated into the host ring, and an oxygen atom acts as a guest (**7.19**).[183] The inclusion of the phosphadiazonium cation in either **7.17** or **7.18** would offer a unique example of an electron-rich guest sitting inside an electron-rich host.

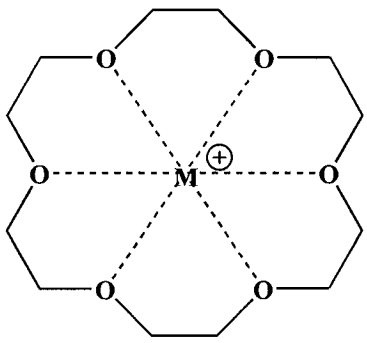

7.16

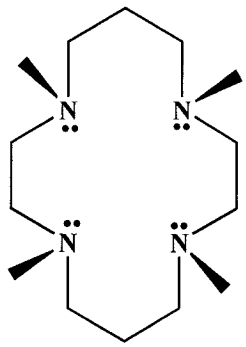

7.17

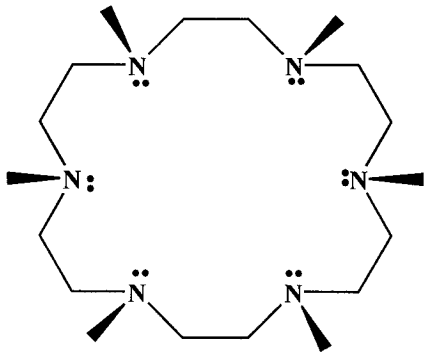

7.18

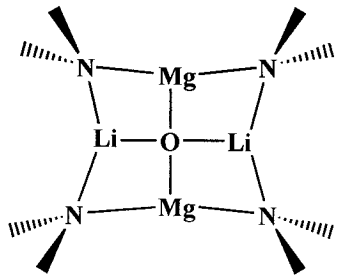

7.19

Chapter 8: Experimental Procedures

8.1 General Procedures

The synthesis, manipulation and storage of the compounds described in this thesis were performed using an inert gas atmosphere (N_2 or Ar) or a reduced pressure environment, unless otherwise indicated. Schlenk techniques were primarily used in the synthesis of starting materials and for recrystallization.[184] All glassware was flame-dried under dynamic vacuum prior to use, and experiments were performed in an evacuated (10^{-3} Torr) reactor (Figure 7.1).[185] Alternatively, reactions were performed in 4 dram (20 mL) glass vials (sealed with Teflon-lined caps) in a glove box with a nitrogen atmosphere (Braun; O_2, H_2O < 0.1 ppm). Solids were also manipulated in a glove box with a nitrogen atmosphere and stored in sealed Pyrex glass tubes. Solvents and liquid reagents were transferred by reduced pressure distillation, or using a syringe.

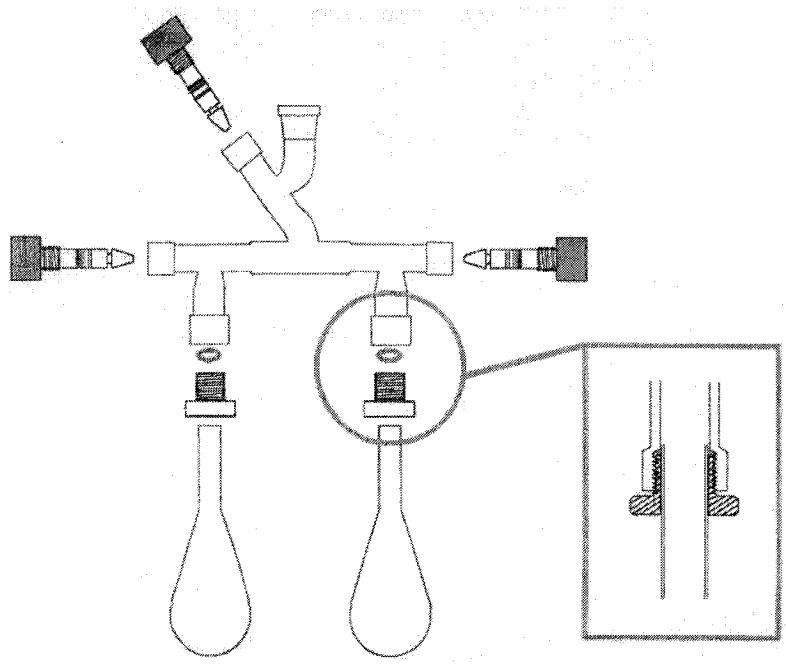

Figure 8.1 Glass reactor used in many reactions, including Teflon taps, bushings, and o-rings. Adapted from reference 185.

Solvents were dried and degassed using three freeze-pump-thaw cycles prior to use. Benzene, toluene, and *n*-hexane, were dried at reflux over potassium. Dichloromethane was first set to reflux over calcium hydride, then over phosphorus pentoxide, and again over calcium hydride. Diethyl ether was dried at reflux over sodium-benzophenone, while n-pentane was dried by reflux over sodium-benzophenone with 5% tetraethylene glycol dimethyl ether. d_2-Dichloro-methane and d_6-benzene were dried by stirring over calcium hydride for seven days.

Chemicals and reagents were obtained from Aldrich Chemical Company and used as received, unless otherwise stated. 1,2- Bis(diphenylphosphino)ethane (DIPHOS), 1,2-bis(diethylphosphino)ethane (DEPE), and 1,2-bis(dimethylphosphino)ethane (DMPE) were obtained from Strem Chemical Co. and used as received. Phosphorus trichloride was distilled prior to use. Triethylamine was purified by fractional distillation from potassium hydroxide and then calcium hydride. N,N,N',N'-Tetramethylethylenediamine (TMEDA) was stirred over potassium hydroxide and then distilled prior to use. The following compounds were synthesized according to literature procedures: trifluoromethylsulfonyloxy-(2,4,6-tri-*tert*-butylphenylimino)phosphine (Mes*NPOTf),[72] chloro-(2,4,6-tri-*tert*-butylphenylimino)phosphine (Mes*NPCl),[40] bromo-(2,4,6-tri-*tert*-butylphenylimino)phosphine (Mes*NPBr),[40] iodo-(2,4,6-tri-*tert*-butylphenylimino)phosphine (Mes*NPI),[40] pentamethylcyclopentadienyl-(2,4,6-tri-*tert*-butylphenylimino)phosphine (Mes*NPCp*),[158] 1,3-diisopropyl-4,5-dimethylimidazol-2-ylidene (Im),[98] 1,3-diisopropyl-4,5-dimethylimidazole-2(3*H*)-thione (SIm),[98] and 1,3-diisopropyl-4,5-dimethylimidazole-2(3*H*)-selenone (SeIm).[99]

Melting points were obtained on samples sealed in glass capillaries under dry nitrogen by using an Electrothermal apparatus. Chemical analyses were performed by Beller Laboratories, Göttingen, Germany or by Desert Analytics, Tucson, Arizona. Samples for chemical analyses were evacuated for a minimum of 8 hours under dynamic vacuum and then flame-sealed in Pyrex tubes.

8.2 NMR Spectroscopy

Samples for analysis by solution NMR spectroscopy were prepared in 5 mm (o.d.) flame-sealed Pyrex NMR tubes and ^{1}H, ^{13}C, ^{19}F, and ^{31}P NMR data were collected at 298 K on Bruker AC-250 or Bruker Avance 500 NMR spectrometers. Chemical shifts are reported in ppm relative to $SiMe_4$ for ^{1}H and ^{13}C, 10% CCl_3F for ^{19}F, and 85% H_3PO_4 for ^{31}P. In the case of both ^{31}P and ^{19}F, chemical shifts were calibrated by first running a sample of the primary reference compound and then setting the observed peak to 0 ppm. For ^{1}H and ^{13}C spectra, the solvent signal was used as a secondary reference (^{1}H: $CHDCl_2$, 5.32 ppm; ^{13}C: CD_2Cl_2, 54.00 ppm,). NMR spectra of reaction mixtures were obtained by transferring an aliquot of the bulk solution to a 5 mm NMR tube, which was subsequently flame-sealed (or sealed with a plastic cap and parafilm). Spectra were obtained within one day of sample preparation.

Solid state $^{31}P\{^{1}H\}$ NMR spectra were obtained on ground crystalline solids. The samples were packed in zirconium oxide rotors fitted with Vespel or Kel-Fcaps (4 mm o.d.). Chemical shifts are reported in ppm and referenced to external 85% aqueous H_3PO_4 by setting the isotropic peak of external solid $[NH_4][H_2PO_4]$ to 0.81 ppm. Solid state $^{31}P\{^{1}H\}$ NMR spectra were obtained by Dr. Michael Lumsden with a 4 mm Bruker

double-resonance MAS probe using a combination of cross-polarization, magic-angle spinning, and high-power ^{1}H decoupling on a Bruker AMX 400 MHz spectrometer (**2.7** (Ch = S, Se), **2.8**, **3.15** (R = Ph), and **4.14**). All other solid state ^{31}P NMR spectra were obtained by Dr. Ulrike Werner-Zwanziger with a similar probe, using direct excitation with proton decoupling, under magic-angle spinning, on a Bruker Avance 400 MHz spectrometer. Typically, a contact time of 5 ms and spinning speeds of 10-12 kHz were used to collect data over a period of 128 scans. In order to determine the isotropic chemical shift, spectra at different spinning speeds were acquired to distinguish the spinning sidebands from the centreband.

Simulation of the solution $^{31}P\{^{1}H\}$ NMR spectra of [Mes*NP·DMPE]OTf [Mes*NP·DEPE]OTf, and [Mes*NP·DIPHOS]OTf was performed by Dr. Michael Lumsden using g-NMR Version 4.0 by Cherwell Scientific.

8.3 Vibrational Spectroscopy

Infrared spectra were collected on samples prepared as Nujol mulls on CsI plates using Nicolet 510P FT-IR or Bruker Vector FT-IR spectrometers. Raman spectra were collected on powdered samples, sealed in glass capillaries under dry nitrogen, using a Bruker RFS 100 FT-Raman spectrometer. Vibrational spectra are reported in wavenumbers (cm^{-1}) followed by ranked intensities in parentheses, where a value of one corresponds to the most intense peak in the spectrum.

8.4 UV-Visible Spectroscopy

Samples for UV-visible spectroscopy were prepared in a glove box with a nitrogen atmosphere. A stoichiometric amount of the ligand and Mes*NPOTf were weighed into a 4 dram vial, and dissolved in CH_2Cl_2. The resulting solution was quantitatively transferred to a 10 mL volumetric flask, which was subsequently filled to the mark with CH_2Cl_2. Standard analytical pipetting techniques were too cumbersome to attempt in the glove box. As a result, dilutions were performed by drawing up an aliquot of the solution in a 1 mL syringe, and adding the necessary volume to an empty 10 mL volumetric flask, which was afterward filled to the mark with CH_2Cl_2.

The solution samples were loaded into 2 mm quartz cells, which were subsequently sealed with Teflon stoppers. As an added precaution, parafilm was wrapped around the stopper to improve the seal. The UV-visible spectra were collected using a Cary 100 Bio UV-visible spectrophotometer, immediately after removing the samples from the glove box. Dried and degassed CH_2Cl_2 was used as the reference sample. Data processing was done using the Win-UV software package.

8.5 Crystal Growing Methods and X-ray Crystallography

Crystals for single crystal X-ray diffraction were obtained by a variety of methods; however, the two methods most commonly used are noted here. **Liquid-liquid diffusion:** Approximately 50-100 mg of sample was dissolved in a small amount of solvent (CH_2Cl_2 or C_6H_6, 2-4 mL) in a 150 mm (14 mm o.d.) Pyrex tube. A second solvent (hexane, 20-30 mL) was layered on to the solution using a syringe. The sealed tube (Ar) was left undisturbed for several weeks at room temperature. After deposition

of crystals, the solution was carefully removed using a syringe, and the crystals were coated with perfluoropolyether 216 (Riedel-de Haën). **Vapour diffusion:** Approximately 50-100 mg of sample was dissolved in 2-3 mL of solvent (CH_2Cl_2 or C_6H_6) in a 4 dram vial. A smaller vial (1 dram) was placed inside the larger vial (4 dram), and filled with approximately 3 mL of solvent in which the sample is insoluble (hexane or pentane). The larger vial was capped tightly and the system was allowed to stand at room temperature until crystals of suitable quality were formed. After formation of crystals, the supernatant solution was removed with a syringe, and the crystals were coated with perfluoropolyether 216 or paratone oil.

Unless otherwise stated, all single crystal X-ray data collection, structure solution, and refinement was performed by Dr. Robert McDonald or Dr. Michael Ferguson at the X-ray Crystallography Laboratory, Department of Chemistry, University of Alberta. The only exception is the structure of Mes*NP(Im)Br (**5.8**, X = Br), which was obtained by Paul Ragogna and Dr. Douglas Stephan at the University of Windsor. All data were collected using Siemens/Bruker PLATFORM diffractometers fitted with Bruker SMART CCD detectors, and all measurements were made with graphite monochromated Mo-Kα radiation at 193(2) K. The data were corrected for Lorentz and polarization effects. Absorption corrections were also applied to each structure. Decay corrections were not necessary. The structures were solved by direct methods and expanded using Fourier techniques. Full matrix least squares refinement was carried out on F^2 data using the program *SHELX97*.[186] Non-hydrogen atoms were refined anisotropically. Hydrogen atoms were included in geometrically calculated positions, but were not refined. In the case of the [Mes*NP·PMDETA]OTf (**3.16**) and [(Mes*NP)$_2$·(4,4'-BIPY)][OTf]$_2$ (**4.14**),

the data were corrected for electron density due to disordered solvent molecules through the use of the *SQUEEZE*[187] procedure as implemented in *PLATON*.[188]

8.6 Isolation Procedures and Characterization Data

The reaction procedures and spectroscopic characterization data for the new compounds (**2.7** (Ch = S, Se), **2.8**, **3.14**, **3.15** (R = Me, Et, Ph), **3.16**, **4.2**, **4.14**, **4.16**, **4.18**, **4.19**, **4.20**, and **5.8** (X = Br, I) presented in this thesis are described in the following sections. For compounds that have been characterized by single crystal X-ray diffraction studies, relevant crystallographic information is provided in Tables 8.1 to 8.4. Please note that CD_2Cl_2 was used as the solvent for all solution NMR data reported below.

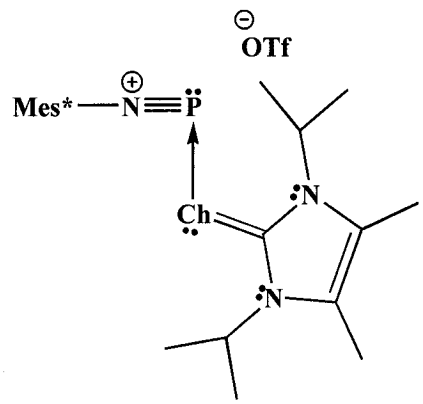

2.7, Ch = S, Se

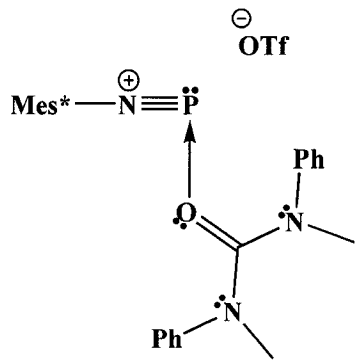

2.8

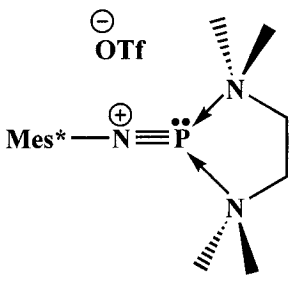

3.14

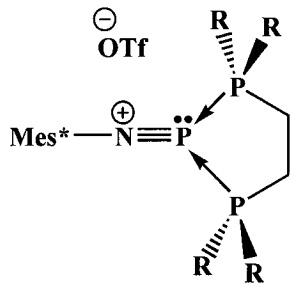

3.15, R = Me, Et, Ph

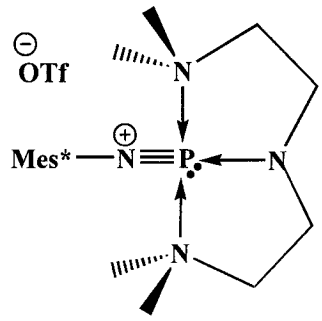

3.16

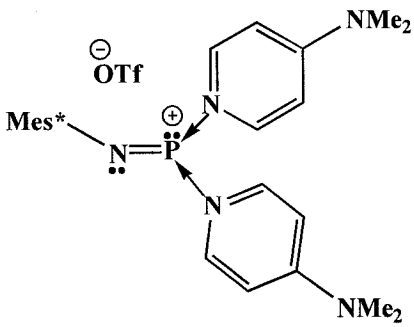

4.2

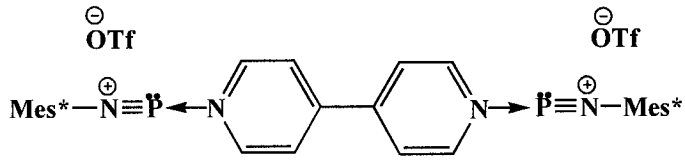

4.14

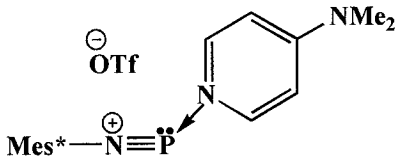

4.16

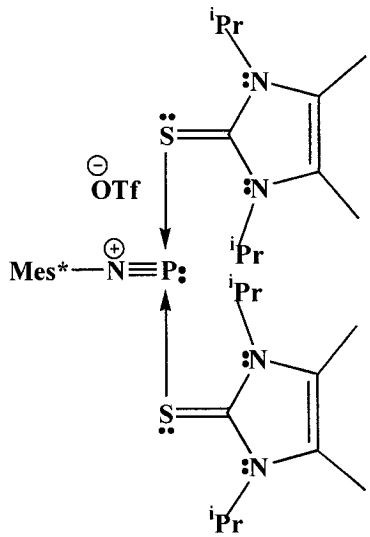

4.18

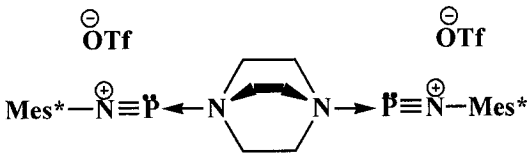

4.20

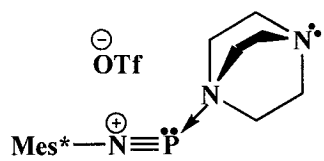

4.21

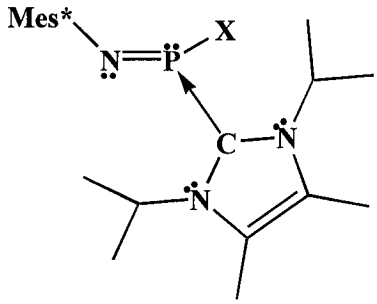

5.8, X = Br, I

8.6.1 Preparation of [Mes*NP·SIm]OTf (2.7, Ch = S)

A solution of SIm (0.14 g, 0.68 mmol) in benzene (10 mL) was added to a solution of Mes*NPOTf (0.30 g, 0.68 mmol) in benzene (20 mL), in an evacuated reactor, over a period of 40 minutes with stirring. The solvent was removed from the red solution *in vacuo* giving a pink solid, which was separated by decanting, washed with benzene (20 mL) and characterized as $C_{30}H_{49}F_3N_3O_3PS_2$ (0.23 g, 0.35 mmol, 52 %), 651.84 g/mol, m.p. 161°C.

Elemental Analysis (%): Calculated: C, 55.3, H, 7.6, N, 6.5

Found: C, 54.2, H, 7.5, N, 6.2

Raman: 2969(6), 2931(7), 1597(2), 1452(1), 1412(4), 1363(3), 1292(5), 1136(8), 1061(9), 117(10).

UV-vis: λ_{max} = 492 nm, ε = 1300 $M^{-1}cm^{-1}$.

NMR (solid state): CP-MAS δ_{iso} $^{31}P\{^1H\}$ 165 (s).

8.6.2 Preparation of [Mes*NP·SeIm]OTf (2.7, Ch = Se)

A solution of SeIm (0.18 g, 0.69 mmol) in benzene (15 mL) was added to a solution of Mes*NPOTf (0.30 g, 0.68 mmol) in benzene (20 mL), in an evacuated reactor, over a period of 25 minutes with stirring. The solvent was removed from the red solution *in vacuo* giving a pink solid, which was separated by decanting, washed with benzene (20 mL) and characterized as $C_{30}H_{49}F_3N_3O_3PSSe$ (0.23 g, 0.33 mmol, 48 %), 698.73 g/mol, m p. 139 °C.

Elemental Analysis (%): Calculated: C, 51.6, H, 7.1, N, 6.0

Found: C, 51.9, H, 6.8, N, 6.0

Raman: 2995(8), 2970(3), 2932(4), 2882(9), 1597(2), 1451(1), 1412(7), 1376(11), 1357(5), 1284(6), 1204(12), 1136(9), 1061(10), 1031(13), 286(14).

UV-vis: λ_{max} = 518 nm, ε = 800 $M^{-1}cm^{-1}$.

NMR (solid state): CP-MAS δ_{iso} $^{31}P\{^1H\}$ 195 (s).

8.6.3 Preparation of [Mes*NP·OU]OTf (2.8)

A solution of OU (0.24 g, 1.0 mmol) in benzene (15 mL) was added to a solution of Mes*NPOTf (0.44 g, 1.0 mmol) in benzene (20 mL), in an evacuated reactor, over a period of 5 minutes with stirring. The solvent was removed from the orange solution *in vacuo* leaving an orange oil. Addition of n-hexane (20 mL) resulted in precipitation of an orange solid, which was separated by decanting, washed with n-hexane (20 mL) and characterized as $C_{34}H_{45}F_3N_3O_4PS$ (0.41 g, 0.61 mmol, 61 %), 679.79 g/mol, m.p. 147°C.

Elemental Analysis (%): Calculated: C, 60.1, H, 6.7, N, 6.2

Found: C, 58.6, H, 6.8, N, 5.8

IR: 1673(15), 1600 (12), 1563(11), 1495(6), 1405(5), 1300(8), 1280(2), 1247(1), 1224(7), 1174(10), 1157(4); 1129(14), 1109(16), 1079 (19), 1029(3), 1003(22), 941(20), 879(23), 753(21), 740(17), 712(13), 694(18), 638(9), 517(24).

Raman: 3067(3), 3007(11), 2964(2), 2929(4), 2907(5), 2879(7), 1600(6), 1513(1), 1481(9), 1294(13), 1029(12), 1003(8), 123(10).

NMR (solution): ^{1}H 1.3 (s, 9H, *p*-C($C\underline{H}_3$)$_3$), 1.4 (s, 18H, *o*-C($C\underline{H}_3$)$_3$), 3.3 (s, 6H, N($C\underline{H}_3$)), 7.3-7.5 (m, 12H, *m*-C$\underline{H}$, N($C_6\underline{H}_5$); $^{13}C\{^{1}H\}$ 30 (s, *p*-C($\underline{C}H_3$)$_3$), 31 (s, *o*-C($\underline{C}H_3$)$_3$), 34 (s, impurity), 35.8 (s, *p*-$\underline{C}$(CH$_3$)$_3$), 36.2 (s, impurity), 37 (s, *o*-$\underline{C}$(CH$_3$)$_3$), 43 (s, N($\underline{C}H_3$)), 121 (q, $^{1}J_{FC}$ = 320 Hz, $\underline{C}F_3$), 123 (s, *m*-$\underline{C}$H), 124 (s, N($\underline{C}_6H_5$)), 127 (s, N($\underline{C}_6H_5$)), 129 (s, N($\underline{C}_6H_5$)), 131 (s, N($\underline{C}_6H_5$)), 134 (d, $^{2}J_{PC}$ = 42 Hz, *i*-$\underline{C}$NP), 143 (s, N($\underline{C}_6H_5$)), 147 (d, $^{3}J_{PC}$ = 10 Hz, *o*-$\underline{C}$C(CH$_3$)$_3$), 152 (d, $^{5}J_{PC}$ = 7 Hz, *p*-$\underline{C}$C(CH$_3$)$_3$), 160 (s, $\underline{C}$=O); $^{19}F\{^{1}H\}$ -78.6 (s); $^{31}P\{^{1}H\}$ 62 (s).

NMR (solid state): CP-MAS δ_{iso} $^{31}P\{^{1}H\}$ 73 (s).

Crystallography: Crystals were obtained by liquid-liquid diffusion of CH_2Cl_2 and hexane, and were spectroscopically identical to the powder. Crystallographic data are provided in Table 8.1.

8.6.4 Preparation of [Mes*NP·TMEDA]OTf (3.14)

TMEDA (17 μL, 0.11 mmol) was added to a solution of Mes*NPOTf (0.050 g, 0.11 mmol) in toluene (1.5 mL), in a 4 dram vial. The resulting yellow solution was stirred for 10 minutes at RT. The solution was subsequently placed in the freezer at –35 °C, and X-ray quality, pale yellow, needle-like crystals deposited after a period of three days. The supernatant solution was separated from the crystals by decantation and the

crystals were washed with 1 mL of n-hexane, and characterized as $C_{25}H_{45}N_3O_3F_3PS$ (0.040 g, 0.07 mmol, 64%), 555.69 g/mol, d. p. 120-122°C.

Elemental Analysis: The crystals were unstable at room temperature and decomposed to a bright orange solid upon standing for several days, and as such reliable and reproducible chemical analyses could not be obtained and an accurate yield cannot be reported. The decomposition product was evident in the baseline of the solution NMR spectra ($^{31}P\{^1H\}$ 137 (s))

IR: 1603(18), 1361(7), 1263(1), 1224(6), 1158(5), 1143(4), 1101(15), 1030(2), 1004(12), 943(9), 929(16), 880(13), 774(8), 752(11), 637(3), 571(17), 517(10), 488(14).

Raman: 2962(1), 2926(3), 1604(5), 1456(4), 1428(2), 1392(6), 1377(7), 1292(8), 1193(10), 1029(9).

NMR (solution): ^1H 1.3 (s, 9H, *p*-C($C\underline{H}_3$)$_3$), 1.5 (s, 18H, *p*-C($C\underline{H}_3$)$_3$), 2.8 (s, 12H, N($C\underline{H}_3$)), 3.3 (s, 4H, N$C\underline{H}_2$), 7.4 (s, 2H, *m*-C$\underline{H}$); $^{13}C\{^1H\}$ 31 (s, *p*-C($\underline{C}H_3$)$_3$), 32 (s, *o*-C($\underline{C}H_3$)$_3$), 35 (s, *p*-$\underline{C}$(CH$_3$)$_3$), 37 (s, *o*-$\underline{C}$(CH$_3$)$_3$), 46 (d, $^2J_{PC}$ = 12 Hz, N($\underline{C}H_3$)), 58 (s, N$\underline{C}H_2$), 121 (q, $^1J_{FC}$ = 321 Hz, $\underline{C}F_3$), 123 (s, *m*-$\underline{C}$H), 135 (d, $^2J_{PC}$ = 39 Hz, *i*-$\underline{C}$NP), 144 (d, $^3J_{PC}$ = 10 Hz, *o*-$\underline{C}$C(CH$_3$)$_3$), 148 (s, *p*-$\underline{C}$C(CH$_3$)$_3$); $^{19}F\{^1H\}$ –80(s); $^{31}P\{^1H\}$ 107(s).

NMR (solid state): MAS δ_{iso} $^{31}P\{^1H\}$146 (s).

Crystallography: Crystals were obtained as noted above. Crystallographic data are provided in Table 8.1.

8.6.5 Identification of [Mes*NP·DMPE]OTf (3.15, R = Me) in solution

DMPE (19 μL, 0.11 mmol) was added to a solution of Mes*NPOTf (0.050 g, 0.11 mmol) in benzene (3 mL), in a 4 dram vial. The resulting red solution was stirred for 30

minutes at RT. $^{31}P\{^{1}H\}$ solution NMR spectra of the reaction mixture indicate the formation of [Mes*NP·DMPE]OTf [$^{31}P\{^{1}H\}$ AB_2 spin system: $\delta_A = 62$ (Mes*N<u>P</u>), $\delta_B = 16$ ($(CH_3)_2\underline{P}CH_2CH_2\underline{P}(CH_3)_2$), $^{1}J_{AB} = 520$ Hz] in approximately 50% yield, along with several other phosphorus-containing products which have not been identified. The mixture of products could not be separated.

8.6.6 Preparation of [Mes*NP·DEPE]OTf (3.15, R = Et)

DEPE (53 μL, 0.23 mmol) was added to a solution of Mes*NPOTf (0.100 g, 0.23 mmol) in benzene (3 mL), in a 4 dram vial. The resulting red-orange solution was stirred for 30 minutes at RT. Approximately 15 mL of n-hexane was added to the solution, and fine, yellow, needle-like crystals formed over a period of two hours. The supernatant solution was separated from the crystals by decantation and the crystals were washed with 1.5 mL of n-hexane, and characterized as $C_{29}H_{53}NO_3F_3P_3S$ (0.121 g, 0.19 mmol, 82 %), 645.73 g/mol, d. p. 97–131 °C.

Elemental Analysis (%): Calculated: C, 53.9, H, 8.3, N, 2.2

Found: C, 53.8, H, 7.9, N, 2.1

IR: 1411(8), 1367(7), 1274(3), 1259(1), 1222(6), 1151(5), 1102(15), 1031(2), 982(16), 878(11), 805(17), 780(12), 761(10), 735(9), 639(4), 571(14), 517(13).

Raman: 2951(3), 2914(2), 1597(4), 1446(1), 1396(5), 1292(7), 1031(6).

NMR (solution): ^{1}H 1.23 (m, 12H, $PCH_2C\underline{H}_3$), 1.27 (s, 9H, *p*-$C(C\underline{H}_3)_3$), 1.4 (s, 18H, *o*-$C(C\underline{H}_3)_3$), 2.1 (m, 8H, $PC\underline{H}_2CH_3$), 2.5 (d, $^{2}J_{PH} = 8$ Hz, 4H, $PC\underline{H}_2C\underline{H}_2P$), 7.3 (d, $^{5}J_{PH} = 2$ Hz, 2H, *m*-C<u>H</u>); $^{13}C\{^{1}H\}$ 8 (s, $PCH_2\underline{C}H_3$), 16 (s, $P\underline{C}H_2CH_3$), 19 (t, $^{1}J_{PC} = 9$ Hz, $P\underline{C}H_2\underline{C}H_2P$), 30 (s, *p*-$C(\underline{C}H_3)_3$), 31 (s, *o*-$C(\underline{C}H_3)_3$), 35 (s, *p*-$\underline{C}(CH_3)_3$), 37 (s, *o*-$\underline{C}(CH_3)_3$),

122 (q, $^1J_{FC}$ = 321 Hz, $\underline{C}F_3$), 123 (s, *m*-$\underline{C}$H), 138 (d, $^2J_{PC}$ = 41 Hz, *i*-$\underline{C}$NP), 142 (d, $^3J_{PC}$ = 15 Hz, *o*-$\underline{C}C(CH_3)_3$), 145 (s, *p*-$\underline{C}C(CH_3)_3$); $^{19}F\{^1H\}$ –80 (s); $^{31}P\{^1H\}$ AB_2 spin system: δ_A = 53 (Mes*N$\underline{P}$), δ_B = 27 ($(C_2H_5)_2\underline{P}CH_2CH_2\underline{P}(C_2H_5)_2$), $^1J_{AB}$ = 528 Hz. Small amounts of other phosphorus-containing compounds (> 10 % intensity of peaks assigned to [Mes*NP·DEPE]OTf) were invariably observed in the solution NMR spectra upon dissolution of analytically pure material. These compounds, which have not been identified, were most likely produced as a result of solution isomerization or solvent activation. Compound a): $^{31}P\{^1H\}$: 30 (dd, $^1J_{PP}$ = 354 Hz, $^1J_{PP}$ = 411 Hz) 53.2 (d, $^1J_{PP}$ = 354 Hz), 53.3 (d, $^1J_{PP}$ = 411 Hz); Compound b): $^{31}P\{^1H\}$ 81 (d, $^1J_{PP}$ = 443 Hz).

NMR (solid state): MAS δ_{iso} $^{31}P\{^1H\}$ 32 (d, $^1J_{PP}$ = 599 Hz), 32 (unresolved multiplet hidden under doublet), 49 (d, $^1J_{PP}$ = 477 Hz).

Crystallography: Crystals suitable for X-ray diffraction could not be obtained.

8.6.7 Preparation of [Mes*NP·DIPHOS]OTf (3.15, R = Ph)

Mes*NPOTf (0.050 g, 0.11 mmol) and DIPHOS (0.045 g, 0.11 mmol) were weighed into the same 4 dram vial and dissolved in benzene (3 mL) to give an orange solution, which was stirred for 30 minutes at RT. A 1 dram vial containing pentane (3 mL) was placed inside the larger vial, which was then capped. Large orange, block-like crystals suitable for X-ray diffraction deposited after 2 days at room temperature. The supernatant solution was separated from the crystals by decantation and the crystals were washed with 0.5 mL of benzene, and characterized as $C_{45}H_{53}NO_3F_3P_3S$ (0.046 g, 0.05 mmol, 48 %), 837.91 g/mol, m. p. 100–101 °C.

Elemental Analysis (%): Calculated: C, 64.5, H, 6.4, N, 1.7

Found: C, 64.8, H, 6.1, N, 1.7

IR: 3056(14), 1598(24), 1418(13), 1362(9), 1310(18), 1255(1), 1222(6), 1153(3), 1101(10), 1072(16), 1027(2), 998(12), 926(23), 879(15), 747(7), 695(8), 684(5), 660(22), 636(4), 615(19), 571(20), 518(11), 509(17), 468(21).

Raman: 3061(3), 2948(6), 2907(7), 1599(4), 1584(2), 1496(1), 1096(8), 1027(9). 999(5).

NMR (solution): ^{1}H 1.1 (s, 18H, *o*-C(C$\underline{H}_3$)$_3$), 1.3 (s, 9H, *p*-C(C$\underline{H}_3$)$_3$), 3.1 (d, $^{2}J_{PH}$ = 1Hz, 4H, PC$\underline{H}_2$) 7.2 (s, 2H, *m*-C$\underline{H}$), 7.3-7.6 (m, 20H, P(C$_6\underline{H}_5$)); $^{13}C\{^{1}H\}$ 24 (s, P$\underline{C}H_2$), 31 (s, *p*-C($\underline{C}H_3$)$_3$), 32 (s, *o*-C($\underline{C}H_3$)$_3$), 35.5 (s, *p*-$\underline{C}$(CH$_3$)$_3$), 36.4 (s, *o*-$\underline{C}$(CH$_3$)$_3$), 122 (q, $^{1}J_{FC}$ = 321 Hz, $\underline{C}F_3$), 123 (s, *m*-$\underline{C}$H), 128 (s, P($\underline{C}_6H_5$)), 129 (s, P($\underline{C}_6H_5$)), 130 (s, P($\underline{C}_6H_5$)), 132.7 (s, P($\underline{C}_6H_5$)), 133.1 (s, P($\underline{C}_6H_5$)), 136 (d, $^{1}J_{PC}$ = 197 Hz, P($\underline{C}_6H_5$)), 145 (s, *o*-$\underline{C}$C(CH$_3$)$_3$), 148 (s, *p*-$\underline{C}$C(CH$_3$)$_3$); $^{19}F\{^{1}H\}$ –80(s); $^{31}P\{^{1}H\}$(298 K) AB_2 spin system: δ_A = 36 (Mes*N$\underline{P}$), δ_B = 10 ((C$_6$H$_5$)$_2\underline{P}$CH$_2$CH$_2\underline{P}$(C$_6$H$_5$)$_2$), $^{1}J_{AB}$ = 453 Hz **or** ABB' spin system: δ_A = 36 (Mes*N$\underline{P}$), δ_B = 10 ((C$_6$H$_5$)$_2\underline{P}$CH$_2$CH$_2\underline{P}$(C$_6$H$_5$)$_2$), $^{1}J_{AB}$ = 466 Hz, $^{1}J_{AB'}$ = 441 Hz, $^{2}J_{BB'}$ = 163 Hz. Small amounts of other phosphorus-containing compounds (> 10 % intensity of peaks assigned to [Mes*NP·DIPHOS]OTf) were invariably observed in the solution NMR spectra upon dissolution of analytically pure material. These compounds, which have not been identified, were most likely produced as a result of solution isomerization or solvent activation. Compound a): $^{31}P\{^{1}H\}$: 18 (dd, $^{1}J_{PP}$ = 351 Hz, $^{1}J_{PP}$ = 410 Hz), 43.0 (d, $^{1}J_{PP}$ = 351 Hz), 43.1 (d, $^{1}J_{PP}$ = 410 Hz); Compound b): $^{31}P\{^{1}H\}$ 65 (d, $^{1}J_{PP}$ = 452 Hz).

NMR (solid state): CP-MAS δ_{iso} $^{31}P\{^{1}H\}$ –17 (d, $^{1}J_{PP}$ = 469 Hz), 12 (d, $^{1}J_{PP}$ = 360 Hz), 35 (unresolved multiplet).

Crystallography: Crystals were obtained as noted above. Crystallographic data are provided in Table 8.2.

8.6.8 Preparation of [Mes*NP·PMDETA]OTf (3.16)

PMDETA (48 μL, 0.23 mmol) was added to a solution of Mes*NPOTf (0.100 g, 0.23 mmol) in n-hexane (5 mL), in a 4 dram vial. There was immediate formation of a yellow solution and an off-white solid, and these were stirred for 30 minutes at RT. The supernatant solution was separated from the powder by decantation and the powder was washed with 2 × 4 mL portions of n-hexane, and characterized as $C_{28}H_{52}N_4O_3F_3PS$ (0.116g, 0.19 mmol, 82 %), 612.78 g/mol, d. p. 116 °C.

Elemental Analysis: The powder was unstable at room temperature, and decomposed to a bright yellow solid upon standing for several days, and as such reliable and reproducible chemical analyses could not be obtained and an accurate yield cannot be reported. The decomposition product was evident in the baseline of the solution NMR spectra ($^{31}P\{^1H\}$137 (s)).

IR: 1602(20), 1488(3), 1422(9), 1363(8), 1273(1), 1265(2), 1226(7), 1156(5), 1099(13), 1076(21), 1031(4), 968(12), 943(15), 929(14), 891(18), 878(19), 785(11), 764(10), 748(16), 638(6), 573(22), 518(17), 279(23).

Raman: 3090(8), 2962(2), 2926(3), 2892(4), 2875(5), 2796(10), 2773(11), 1602(6), 1485(1), 1361(7), 1291(9), 1031(9), 350(12).

NMR (solution): ^1H 1.3 (s, 9H, *p*-C(C$\underline{H}_3$)$_3$), 1.5 (s, 18H, *o*-C(C$\underline{H}_3$)$_3$), 2.4 (s, 12H, N(C$\underline{H}_3$)$_2$), 2.6-2.8 (m, 4H, C$\underline{H}_2$N(CH$_3$)$_2$), 2.8 (d, $^3J_{PH}$ = 2.5 Hz, 3H, N(C$\underline{H}_3$)), 3.0-3.2 (m, 4H, C$\underline{H}_2$N(CH$_3$)), 7.3 (d, $^5J_{PH}$ = 1 Hz, 2H, *m*-C$\underline{H}$); $^{13}C\{^1H\}$ 31 (s, *p*-C($\underline{C}$H$_3$)$_3$), 32 (s, *o*-

$C(\underline{C}H_3)_3$), 35 (s, *p*-$\underline{C}(CH_3)_3$), 37 (s, *o*-$\underline{C}(CH_3)_3$), 44 (s, $N(\underline{C}H_3)_2$), 46 (s, $N(\underline{C}H_3)$), 57.0 (s, $\underline{C}H_2N(CH_3)_2$), 57.2 (s, $\underline{C}H_2N(CH_3)$), 122 (q, $^1J_{FC}$ = 321 Hz, $\underline{C}F_3$), 123 (s, *m*-$\underline{C}H$), 135 (d, $^2J_{PC}$ = 46 Hz, *i*-$\underline{C}NP$), 142 (d, $^3J_{PC}$ = 12 Hz, *o*-$\underline{C}C(CH_3)_3$), 147 (s, *p*-$\underline{C}C(CH_3)_3$); $^{19}F\{^1H\}$ – 80 (s); $^{31}P\{^1H\}$ 89(s).

NMR (solid state): MAS δ_{iso} $^{31}P\{^1H\}$ 93 (s), 103 (s).

Crystallography: Crystals suitable for X-ray diffraction were obtained by dissolving 70 mg of complex in a 50/50 mixture of ether and toluene (4 mL), and placing the solution in a freezer at –35 °C for one week. The crystals were spectroscopically identical to the powder. Crystallographic data are provided in Table 8.2.

8.6.9 Preparation of [Mes*NP·(DMAP)$_2$]OTf (4.2)

Mes*NPOTf (0.100 g, 0.23 mmol) and DMAP (0.056 g, 0.46 mmol) were weighed into the same 4 dram vial and dissolved in CH_2Cl_2 (3 mL) to give a red-brown solution, which was stirred for 30 minutes at RT. Addition of n-pentane (15 mL) gave a yellow microcrystalline solid, which was separated by decanting, washed with n-pentane (4 mL), and characterized as $C_{33}H_{49}N_5O_3F_3PS$ (0.12 g, 0.18 mmol, 78%), 683.82 g/mol, m.p. 186 – 188 °C.

Elemental Analysis (%): Calculated: C, 58.0, H, 7.2, N, 10.2

Found: C, 58.3, H, 7.0, N, 9.7

IR: 1624(2), 1560(11), 1525(17), 1417(10), 1399(13), 1331(20), 1293(5), 1264(1), 1223(6), 1212(7), 1148(8), 1051(9), 1035(3), 1010(4), 822(14), 728(19), 639(12), 568(15), 540(16), 518(18).

Raman: 3080(5), 2965(1), 2926(1), 2819(7), 1626(6), 1601(3), 1560(5), 1445(6), 1417(5), 1386(7), 1293(2), 1224(7), 1051(3), 1034(4), 943(7), 766(6).

NMR (solution): ^{1}H 1.3 (s, 27H, *o*-C(C$\underline{H}_3$)$_3$, *p*-C(C$\underline{H}_3$)$_3$), 3.2 (s, 12H, N(C$\underline{H}_3$)$_2$), 6.8 (d, $^{3}J_{HH}$ = 7.5 Hz, 4H, *m*-C$\underline{H}$(DMAP)), 7.3 (d, $^{5}J_{PH}$ = 0.5 Hz, 2H, *m*-C$\underline{H}$(Mes*)), 8.2 (d, $^{3}J_{HH}$ = 7.3 Hz, 4H, *o*-C$\underline{H}$(DMAP)); ^{13}C{^{1}H} 31.6 (s, *o/p*-C(C$\underline{H}_3$)$_3$), 31. 7 (s, *o/p*-C(C$\underline{H}_3$)$_3$), 31.9 (s, *o/p*-C(C$\underline{H}_3$)$_3$), 35 (s, *p*-$\underline{C}$(CH$_3$)$_3$), 36 (s, *o*-$\underline{C}$(CH$_3$)$_3$), 40 (s, N($\underline{C}$H$_3$)$_2$), 108 (s, *m*-$\underline{C}$H(DMAP)), 122 (q, $^{1}J_{FC}$ = 321 Hz, $\underline{C}$F$_3$), 123 (s, *m*-$\underline{C}$H(Mes*)), 140 (d, $^{2}J_{PC}$ = 7 Hz, *i*-$\underline{C}$NP), 141 (s, *o*-$\underline{C}$C(CH$_3$)$_3$), 142 (s, *o*-$\underline{C}$H(DMAP)), 143 (s, *p*-$\underline{C}$C(CH$_3$)$_3$), 158 (s, $\underline{C}$N(CH$_3$)$_2$); ^{19}F{^{1}H} –80 (s); ^{31}P{^{1}H} 123 (s).

NMR (solid state): MAS δ_{iso} ^{31}P{^{1}H} 147 (s).

Crystallography: Crystals suitable for X-ray diffraction were obtained by vapour diffusion. The complex (80 mg) was dissolved in 1.5 mL of CH_2Cl_2 in a 4 dram vial, and then a 1 dram vial containing n-hexane (3 mL) was introduced. The crystals were spectroscopically identical to the powder. Crystallographic data are provided in Table 8.3.

8.6.10 Preparation of [(Mes*NP)$_2$·(4,4'-BIPY)][OTf]$_2$ (4.14)

Mes*NPOTf (0.050 g, 0.11 mmol) and 4,4'-BIPY (0.009 g, 0.06 mmol) were weighed into the same 4 dram vial and dissolved in CH_2Cl_2 (3 mL) to give a deep red solution, which was stirred for 30 minutes at RT. A 5mL vial containing n-hexane (3 mL) was placed inside the larger vial, which was then capped. Large red-purple, block-like crystals suitable for X-ray diffraction deposited overnight at room temperature. The supernatant solution was separated from the crystals by decantation and the crystals were

washed with 0.5 mL of CH_2Cl_2, and characterized as $C_{48}H_{66}N_4O_6F_6P_2S_2$ (0.034g, 0.03 mmol, 57%) 1035.14 g/mol, m.p. 161 – 163 °C.

Elemental Analysis (%): Calculated: C, 55.7, H, 6.4, N, 5.4

Found: C, 54.2, H, 6.4, N, 5.0

IR: 3103(15), 3055(18), 1609(11), 1499(9), 1365(7), 1275(1), 1244(2), 1221(4), 1159(6), 1061(10), 1027(3), 1001(8), 880(16), 829(12), 817(17), 759(19), 738(14), 638(5), 576(20), 518(13).

Raman: 3090(14), 2967(7), 2930(8), 2907(10), 1618(2), 1599(5), 1522(4), 1498(1), 1288(3), 1240(11), 1201(14), 1135(11), 1071(11), 1063(11), 1027(9), 1018(6), 822(15), 567(13), 349(16), 273(12), 155(11).

NMR (solution): ^{1}H 1.3 (s, 18H, *p*-C(C$\underline{H}_3$)$_3$), 1.4 (s, 36H, *o*-C(C$\underline{H}_3$)$_3$), 7.4 (d, $^5J_{PH}$ = 1 Hz, 4H, *m*-C$\underline{H}$(Mes*)), 7.9 (d, $^3J_{HH}$ = 6 Hz, 4H, *m*-C$\underline{H}$(BIPY)), 8.9 (d, $^3J_{HH}$ = 6 Hz, 4H, *o*-C$\underline{H}$(BIPY)); ^{13}C{^{1}H} 30 (s, *p*-C($\underline{C}$H$_3$)$_3$), 31 (s, *o*-C($\underline{C}$H$_3$)$_3$), 35 (s, *p*-$\underline{C}$(CH$_3$)$_3$), 36 (s, *o*-$\underline{C}$(CH$_3$)$_3$), 120 (q, $^1J_{FC}$ = 320 Hz, $\underline{C}$F$_3$), 123 (s, *m*-$\underline{C}$H(BIPY)), 124 (s, *m*-$\underline{C}$H(Mes*)), 134 (d, $^2J_{PC}$ = 42 Hz, *i*-$\underline{C}$NP), 145 (d, $^3J_{PC}$ = 9 Hz, *o*-$\underline{C}$C(CH$_3$)$_3$), 147 (s, *o*-$\underline{C}$H(BIPY)), 149 (s, *p*-$\underline{C}$C(CH$_3$)$_3$), 152 (s, $\underline{C}$-$\underline{C}$(BIPY)); ^{19}F{^{1}H} –80 (s); ^{31}P{^{1}H} 61 (s).

NMR (solid state): CP-MAS δ_{iso} ^{31}P{^{1}H}: 60 (s), 63 (s).

Crystallography: Crystals were obtained as noted above. Crystallographic data are provided in Table 8.3.

8.6.11 Preparation of [Mes*NP·DMAP]OTf (4.16)

Mes*NPOTf (0.100 g, 0.23 mmol) and DMAP (0.028 g, 0.23 mmol) were weighed into the same 4 dram vial and dissolved in C_6H_6 (6 mL). There was immediate

formation of a purple-pink solution and a pink solid, and these were stirred for 30 minutes at RT. The solid was separated by decantation, washed with n-pentane (4 mL), and characterized as $C_{26}H_{39}N_3O_3F_3PS$ (0.12 g, 0.20 mmol, 90%), 561.65 g/mol, m.p. 164 – 165 °C.

Elemental Analysis (%): Calculated: C, 55.6, H, 7.0, N, 7.5

Found: C, 57.0, H, 7.2, N, 7.5

IR: 3086(17), 1631(2), 1601(18), 1575(13), 1502(12), 1407(9), 1364(7), 1318(15), 1279(4), 1246(1), 1157(6), 1061(21), 1028(5), 1011(3), 880(22), 833(11), 758(16), 687(19), 636(8), 573(10), 517(14), 451(20).

Raman: 3091(9), 3062(7), 2964(1), 2926(3), 2906(3), 2877(6), 1629(9), 1601(6), 1572(7), 1466(2), 1447(1), 1399(8), 1029(5), 991(7), 822(9), 763(8).

UV-vis: λ_{max} = 510 nm, ε = 400 $M^{-1}cm^{-1}$.

NMR (solution): ^{1}H 1.3 (s, 9H, *p*-C(C$\underline{H}_3$)$_3$), 1.4 (s, 18H, *o*-C(C$\underline{H}_3$)$_3$), 3.3 (s, 6H, N(C$\underline{H}_3$)$_2$), 6.9 (d, $^3J_{HH}$ = 8 Hz, 2H, *m*-C$\underline{H}$(DMAP)), 7.4 (d, $^5J_{PH}$ = 1 Hz, 2H, *m*-C$\underline{H}$(Mes*)), 8.2 (d, $^3J_{HH}$ = 8 Hz, 2H, *o*-C$\underline{H}$(DMAP)); ^{13}C{^{1}H} 31 (s, *p*-C($\underline{C}$H$_3$)$_3$), 32 (s, *o*-C($\underline{C}$H$_3$)$_3$), 35 (s, *p*-$\underline{C}$(CH$_3$)$_3$), 36 (s, *o*-$\underline{C}$(CH$_3$)$_3$), 41 (s, N($\underline{C}$H$_3$)$_2$), 108 (s, *m*-$\underline{C}$H(DMAP)), 122 (q, $^1J_{FC}$ = 321 Hz, $\underline{C}$F$_3$), 123 (s, *m*-$\underline{C}$H(Mes*)), 136 (d, $^3J_{PC}$ = 8 Hz, *o*-$\underline{C}$C(CH$_3$)$_3$), 139 (d, $^2J_{PC}$ = 30 Hz, *i*-$\underline{C}$NP), 140 (d, $^2J_{PC}$ = 8 Hz, *o*-$\underline{C}$H(DMAP)), 147 (s, *p*-$\underline{C}$C(CH$_3$)$_3$), 158 (s, $\underline{C}$N(CH$_3$)$_2$); ^{19}F{^{1}H} –80 (s) ; ^{31}P{^{1}H} 132 (s).

Crystallography: Crystals suitable for X-ray diffraction could not be obtained.

8.6.12 Identification of [Mes*NP·(SIm)$_2$]OTf (4.18) in solution

SIm (0.048, 0.22 mmol) and Mes*NPOTf (0.050 g, 0.11 mmol) were weighed into the same 4 dram vial and dissolved in CH_2Cl_2 (1.5 mL). The resulting red solution was stirred for 10 minutes at RT. $^{31}P\{^1H\}$ solution NMR spectra of the reaction mixture indicate the formation of [Mes*NP·(SIm)$_2$]OTf in quantitative yield.

NMR (solution): $^{31}P\{^1H\}$(298 K) 99 (s); $^{31}P\{^1H\}$(203 K) 71 (s).

Low temperature $^{31}P\{^1H\}$ solution NMR spectra indicate that rapid ligand exchange is occurring between phosphorus centres at room temperature. It is speculated that a mixture of the mono-adduct [Mes*NP·SIm]OTf and the bis-adduct [Mes*NP·(SIm)$_2$]OTf is present at room temperature, while only [Mes*NP·(SIm)$_2$]OTf is present at lower temperatures.

Other reaction mixtures were prepared in the same manner with 0.033 mmol and 0.044 mmol of SIm, respectively.

NMR (solution) Mes*NPOTf + 3SIm: $^{31}P\{^1H\}$(298 K) 86 (s); $^{31}P\{^1H\}$(203 K) 73 (s).

NMR (solution) Mes*NPOTf + 4SIm: $^{31}P\{^1H\}$(298 K) 83 (s); $^{31}P\{^1H\}$(203 K) 72 (s).

All attempts to isolate solid or crystalline material from the reaction mixtures resulted in the production of a red oil.

8.6.13 Identification of [(Mes*NP)$_2$·DABCO][OTf]$_2$ (4.20) in solution

Mes*NPOTf (0.10 g, 0.23 mmol) and DABCO (0.013 g, 0.11 mmol) were weighed into the same 4 dram vial and dissolved in CH_2Cl_2 (3 mL) to give a red-brown solution, which was stirred for 30 minutes at RT. The solution was removed in vacuo, yielding a red-brown powder (0.098 g), d.p. 127 – 130 °C. The powder redissolved to

yield the ligand-bridged adduct in solution; however, ^{31}P solid state NMR spectra of the powder revealed that it was not a pure material, but a mixture of Mes*NPOTf and another compound, possibly **4.21**.

Raman: 2968(5), 2928(6), 2909(7), 1599(2), 1475(1), 1412(3), 1394(5), 1366(4), 1293(9), 1134(8), 1070(10).

NMR (solution): ^{1}H 1.3 (s, 18H, *p*-C(C$\underline{H}_3$)$_3$), 1.5 (s, 36H, *o*-C(C$\underline{H}_3$)$_3$), 3.2 (s, 12H, NC$\underline{H}_2$C$\underline{H}_2$N), 7.4 (d, $^{5}J_{PH}$ = 1 Hz, 4H, *m*-C$\underline{H}$); $^{31}P\{^{1}H\}$ 80 (s).

NMR (solid state): CP-MAS δ_{iso} $^{31}P\{^{1}H\}$: 50 (s, Mes*N$\underline{P}$OTf), 190 (s).

Crystallography: Large, red block-like crystals were obtained by liquid-liquid diffusion of CH_2Cl_2 and hexane, and were spectroscopically identical to the powder characterized as [Mes*NP·DABCO]OTf (**4.21**, see next section). The crystals were not suitable for X-ray diffraction.

8.6.14 Preparation of [Mes*NP·DABCO]OTf (4.21)

Mes*NPOTf (0.10 g, 0.23 mmol) and DABCO (0.013 g, 0.11 mmol) were weighed into the same 4 dram vial and dissolved in CH_2Cl_2 (3 mL) to give a red-brown solution, which was stirred for 30 minutes at RT. Approximately 15 mL of n-hexane was added to the solution, resulting in precipitation of red-brown powder. The supernatant solution was separated from the powder by decantation and the powder was washed with 2 × 4 mL portions of n-hexane, and characterized as $C_{25}H_{41}N_3O_3F_3PS$ (0.050 g, 0.09 mmol, 78 %), 551.66 g/mol, m.p. 161 – 162 °C.

Raman: 2964(6), 2928(8), 2905(9), 1598(4), 1454(7), 1412(1), 1393(5), 1376(3), 1366(2), 1294(10), 1201(15), 1134(13), 1055(12), 1029(11), 147(14).

NMR (solution): $^{31}P\{^{1}H\}$ 110 (s).

8.6.15 Preparation of Mes*NP(Im)Br (5.8, X = Br)

A solution of Im (0.15 g, 0.81 mmol) in benzene (5 mL) was added dropwise to a stirred solution of Mes*NPBr (0.30 g, 0.81 mmol) in benzene (4 mL) over a period of five minutes in a 4 dram vial. The reaction mixture was stirred for 45 minutes and the solvent was removed *in vacuo* to a volume of approximately 3 mL. The orange powder was separated from the red supernatant solution using a needle and syringe, washed with 2 × 4 mL portions of hexane, dried under dynamic vacuum, and characterized as $C_{29}H_{49}BrN_3P$ (0.35 g, 0.63 mmol, 78%), 550.60 g/mol, d.p. 170°C.

Elemental Analysis (%): Calculated: C, 63.2, H, 9.0, N, 7.6

Found: C, 62.8, H, 8.5, N, 7.7

IR: 3049(22), 1621(13), 1418(2), 1395(6), 1375(3), 1361(5), 1285(14), 1266(8), 1238(1), 1214(4), 1188(10), 1171(19), 1155(16), 1139(12), 1121(7), 1082(21), 1018(15), 905(17), 878(18), 795(9), 756(20), 697(11) 397(23).

Raman: 3052(11), 2968(1), 2924(2), 2765(11), 1622(9), 1596(6), 1452(5), 1363(7), 1293(4), 1243(3), 1147(10), 1020(11), 822(11), 264(12), 143(11), 124(8).

NMR (solution): ^{1}H 1.3 (s, 9H, *p*-C(C$\underline{H}_3$)$_3$), 1.4 (s, 18H, *o*-C(C$\underline{H}_3$)$_3$), 1.6 (d, 12H, $^{3}J_{HH}$ = 8 Hz, CH(C$\underline{H}_3$)$_2$), 2.4 (s, 6H, C=C(C$\underline{H}_3$)), 6.0 (m, 2H, $^{3}J_{HH}$ = 8 Hz, C$\underline{H}$(CH$_3$)$_2$), 7.3 (d, 2H, $^{5}J_{PH}$ = 1 Hz, *m*-C$\underline{H}$); $^{13}C\{^{1}H\}$ 11 (s, C=C(C$\underline{H}_3$)), 21 (s, CH(C$\underline{H}_3$)$_2$), 23 (s, CH(C$\underline{H}_3$)$_2$), 32 (s, *p*-C(C$\underline{H}_3$)$_3$), 33 (s, *o*-C(C$\underline{H}_3$)$_3$), 35(s, *p*-C(CH$_3$)$_3$), 37(s, *o*-C(CH$_3$)$_3$), 51 (d, $^{4}J_{PC}$ = 18

Hz, C$H(CH_3)_2$), 123 (s, *m*-CH), 126 (s, C=C(CH_3)), 128 (s, unassigned), 129 (s, unassigned), 139 (d, $^3J_{PC}$ = 12 Hz, *o*-C$C(CH_3)_3$), 142 (s, *p*-C$C(CH_3)_3$), 147 (d, $^2J_{PC}$ = 20 Hz, *i*-CNP), 152 (d, $^1J_{PC}$ = 123 Hz, PC); $^{31}P\{^1H\}$ 199 (s).

NMR (solid state): MAS δ_{iso} $^{31}P\{^1H\}$ 212 (s), 215 (s).

Crystallography: Crystals were obtained by liquid-liquid diffusion of benzene and n-hexane, and were spectroscopically identical to the powder. Crystallographic data are provided in Table 8.4.

8.6.16 Preparation of Mes*NP(Im)I (5.8, X = I)

A solution of Im (0.11 g, 0.61 mmol) in benzene (5 mL) was added dropwise to a stirred solution of Mes*NPI (0.27 g, 0.61 mmol) in benzene (4 mL) over a period of five minutes in a 4 dram vial. The reaction mixture was stirred for 45 minutes, and the solvent was removed *in vacuo* to a volume of approximately 3 mL. The red powder was separated from the red supernatant solution using a needle and syringe, washed with 2 × 4 mL portions of hexane, dried under dynamic vacuum, and characterized as $C_{29}H_{49}N_3PI$ (0.32 g, 0.54 mmol, 89%), 597.60 g/mol, m.p. 209-210°C.

Elemental Analysis (%): Calculated: C, 58.3, H, 8.3, N, 7.0

Found: C, 58.5, H, 8.3, N, 7.1

IR: 1620(12), 1411(2), 1377(3), 1361(4), 1307 (19), 1285(16), 1265(7), 1234(1), 1214(5), 1153(13), 1136(8), 1119(6), 1081(15), 1012(10), 903(17), 878(14), 794(9), 770(20), 756(18), 694(11), 396(21).

Raman: 3049(15), 2968(1), 2930(2), 1621(8), 1597(7), 1473(5), 1451(6), 1422(6), 1399(12), 1360(7), 1291(4), 1265(10), 1237(3), 1198(11), 1146(9), 1121(15), 1012(10), 822(14), 262(15), 223(14), 161(14), 145(13), 123(8).

NMR (solution): ^{1}H 1.3 (s, 9H, *p*-C(C$\underline{H}_3$)$_3$), 1.4 (s, 18H, *o*-C(C$\underline{H}_3$)$_3$), 1.6 (d, 12H, $^{3}J_{HH}$ = 7 Hz, CH(C$\underline{H}_3$)$_2$), 2.4 (s, 6H, C=C(C$\underline{H}_3$)), 5.9 (m, 2H, $^{3}J_{HH}$ = 7 Hz, C$\underline{H}$(CH$_3$)$_2$), 7.3 (d, 2H, $^{5}J_{PH}$ = 1Hz, *m*-C$\underline{H}$); ^{13}C{^{1}H} 11 (s, C=C(C$\underline{H}_3$)), 21 (s, CH(C$\underline{H}_3$)$_2$), 23 (s, CH(C$\underline{H}_3$)$_2$), 32 (s, *p*-C(C$\underline{H}_3$)$_3$), 33 (s, *o*-C(C$\underline{H}_3$)$_3$), 35 (s, *p*-C$\underline{C}$(CH$_3$)$_3$), 37 (s, *o*-C$\underline{C}$(CH$_3$)$_3$), 51 (d, $^{4}J_{PC}$ = 17 Hz, C$\underline{H}$(CH$_3$)$_2$), 123 (s, *m*-C$\underline{H}$), 127 (s, C=C$\underline{C}$(CH$_3$)), 128 (s, unassigned), 129 (s, unassigned), 132 (s, unassigned), 138 (d, $^{3}J_{PC}$ = 13 Hz, *o*-C$\underline{C}$C(CH$_3$)$_3$), 142 (s, *p*-C$\underline{C}$C(CH$_3$)$_3$), 146 (d, $^{2}J_{PC}$ = 16 Hz, *i*-C$\underline{C}$NP), 151 (d, $^{1}J_{PC}$ = 129 Hz, P$\underline{C}$); ^{31}P{^{1}H} 214.

NMR (solid state): MAS δ_{iso} ^{31}P{^{1}H} 223 (s).

Crystallography: Crystals were obtained by liquid-liquid diffusion of benzene and n-hexane, and were spectroscopically identical to the powder. Crystallographic data are provided in Table 8.4.

Table 8.1 Summary of crystal data, data collection, and refinement conditions for [Mes*NP·OU]OTf (**2.8**), and [Mes*NP·TMEDA]OTf (**3.14**).

	[Mes*NP·OU]OTf	**[Mes*NP·TMEDA]OTf**
formula	$C_{34}H_{45}F_3N_3O_4PS$	$C_{25}H_{45}N_3O_3F_3PS$
molar mass	679.76	555.67
crystal system	monoclinic	monoclinic
space group	$P2_1/n$	$P2_1/c$
colour	orange	colourless
a /Å	24.569(2)	19.2943(16)
b /Å	11.2697(10)	10.5163(9)
c /Å	13.5349(12)	15.1501(13)
α /deg	90	90
β /deg	103.611(2)	104.1370(16)
γ /deg	90	90
V / Å^3	3642.4(6)	2980.9(4)
T /K	193(2)	193(2)
Z	4	4
R^a (I >2σ(I))	0.0491	0.0725
wR_2^b (all data)	0.1445	0.1929
GOF^c (all data)	1.020	1.044
Δρ max and min /e Å^{-3}	+ 0.530, -0.365	+1.10, -0.83

[a] $R = (3*F_o*-*F_c*) / (3*F_o*)$. [b] $wR_2 = [(3w(F_o^2 - F_c^2)^2) / (3w(F_o^2)^2)]^{1/2}$.
[c] GOF = $[(3w(F_o^2 -F_c^2) / (n - p)]^{1/2}$, where n = number of reflections, and p = number of parameters.

Table 8.2 Summary of crystal data, data collection, and refinement conditions for [Mes*NP·DIPHOS]OTf (**3.15**, R = Ph), and [Mes*NP·PMDETA]OTf (**3.16**).

	[Mes*NP·DIPHOS]OTf ·(C_6H_6)[d]	**[Mes*NP·PMDETA]OTf ·(C_7H_8)·($C_4H_{10}O$)$_{0.5}$**[e]
formula	$C_{51}H_{59}NO_3F_3P_3S$	$C_{37}H_{65}N_4O_{3.5}F_3PS$
molar mass	915.96	741.96
crystal system	monoclinic	triclinic
space group	$P2_1/c$	$P\bar{1}$
colour	orange	colourless
a /Å	17.4920(8)	10.0330(5)
b /Å	14.7170(7)	12.5898(6)
c /Å	19.1407(9)	18.1171(9)
α /deg	90	106.4874(8)
β /deg	101.3930(10)	100.8079(8)
γ /deg	90	98.1714(8)
V / Å^3	4830.3(4)	2108.54(18)
T /K	193(2)	193(2)
Z	4	2
R^a (I >2σ(I))	0.0548	0.0667
wR_2^b (all data)	0.1369	0.2003
GOF[c] (all data)	1.038	1.091
Δρ max and min /e Å^{-3}	+0.63, -0.38	+0.84, -0.54

[a] $R = (3*F_o*-*F_c*) / (3*F_o*)$. [b] $wR_2 = [(3w(F_o^2 - F_c^2)^2) / (3w(F_o^2)^2)]^{1/2}$.
[c] GOF = $[(3w(F_o^2 -F_c^2) / (n - p)]^{1/2}$, where n = number of reflections, and p = number of parameters. [d] Asymmetric unit includes one molecule of benzene as solvate. [e] Asymmetric unit includes one molecule of toluene and one half molecule of diethylether as solvate.

Table 8.3 Summary of crystal data, data collection, and refinement conditions for [Mes*NP·(DMAP)$_2$]OTf (**4.2**), and [(Mes*NP)$_2$·(4,4'-BIPY)][OTf]$_2$ (**4.14**).

	[Mes*NP·(DMAP)$_2$]OTf	**[(Mes*NP)$_2$·(4,4'-BIPY)][OTf]$_2$ ·(CH$_2$Cl$_2$)$_{1.5}$**[d]
formula	$C_{33}H_{49}N_5O_3F_3PS$	$C_{49.5}H_{69}N_4O_6F_6P_2S_2Cl_3$
molar mass	683.80	1162.50
crystal system	triclinic	triclinic
space group	$P\bar{1}$	$P\bar{1}$
colour	pale yellow	red
a /Å	9.6256(8)	10.1616(4)
b /Å	10.3665(8)	16.9451(6)
c /Å	19.7482(16)	18.9324(7)
α /deg	92.2375(16)	110.8114(7)
β /deg	98.4811(15)	91.4223(7)
γ /deg	113.4698(15)	90.1012(7)
V / Å^3	1777.3(2)	3046.1(2)
T /K	193(2)	193(2)
Z	2	2
R[a] (I >2σ(I))	0.0580	0.0489
wR_2[b] (all data)	0.1550	0.1406
GOF[c] (all data)	1.021	1.052
Δρ max and min /e Å^{-3}	+0.535, -0.348	+1.338, -0.846

[a] $R = (3*F_o*-*F_c*) / (3*F_o*)$. [b] $wR_2 = [(3w(F_o^2 - F_c^2)^2) / (3w(F_o^2)^2)]^{1/2}$.
[c] GOF = $[(3w(F_o^2 -F_c^2) / (n - p)]^{1/2}$, where n = number of reflections, and p = number of parameters. [d] Asymmetric unit includes one and a half molecules of dichloromethane as solvate.

Table 8.4 Summary of crystal data, data collection, and refinement conditions for Mes*NP(Im)Br (**5.8**, X = Br) and Mes*NP(Im)I (**5.8**, X = I).

	Mes*NP(Im)Br	**Mes*NP(Im)I**
formula	$C_{29}H_{49}N_3PBr$	$C_{29}H_{49}N_3PI$
molar mass	550.59	597.58
crystal system	triclinic	triclinic
space group	$P\bar{1}$	$P\bar{1}$
colour	orange	orange
a /Å	8.531(5)	8.4383(5)
b /Å	9.659(5)	9.5486(6)
c /Å	21.359(11)	21.455(1)
α /deg	77.668(11)	77.177(1)
β /deg	79.791(10)	80.761(1)
γ /deg	64.430(10)	65.159(1)
V / Å^3	1543.7(14)	1525.2(2)
T /K	293(2)	193(2)
Z	2	2
R^a (I >2σ(I))	0.0623	0.0420
wR_2^b (all data)	0.1529	0.0957
GOF^c (all data)	0.958	1.049
Δρ max and min /e Å^{-3}	+ 0.644, - 0.692	+ 1.060, - 0.705

[a] $R = (3*F_o*-*F_c*) / (3*F_o*)$. [b] $wR_2 = [(3w(F_o^2 - F_c^2)^2) / (3w(F_o^2)^2)]^{1/2}$.
[c] GOF = $[(3w(F_o^2 -F_c^2) / (n - p)]^{1/2}$, where n = number of reflections, and p = number of parameters.

Reference List

(1) Emsley, J. *The 13th Element: The Sordid Tale of Murder, Fire, and Phosphorus*; John Wiley & Sons, Inc.: New York, 2000.

(2) Dillon, K. B.; Mathey, F.; Nixon, J. F. *Phosphorus: The Carbon Copy*; John Wiley & Sons: 1997.

(3) Manners, I. *Angew. Chem. Int. Ed. Engl.* **1996**, *35*, 1602-1621.

(4) Burford, N.; Ragogna, P. J. *Dalton Trans.* **2002**, 4307-4315.

(5) Massey, A. G. *Main Group Chemistry, Second Edition*; John Wiley & Sons, Ltd.: Chichester, 2000.

(6) Check, C. E.; Lobring, K. C.; Keating, P. R.; Gilbert, T. M.; Sunderlin, L. S. *J. Phys. Chem. A* **2003**, *107*, 8961-8967.

(7) Niecke, E.; Flick, W. *Angew. Chem. Int. Ed. Engl.* **1974**, *13*, 134.

(8) Scherer, O. J.; Kuhn, N. *Chem .Ber.* **1974**, *107*, 2123-2125.

(9) Niecke, E.; Gudat, D. Bis(imino)phosphoranes; In *Multiple Bonds and Low Coordination in Phosphorus Chemistry*; Regitz, M., Scherer, O. J., eds. Georg Thieme Verlag: New York, 1990; pp 392-404.

(10) Meisel, M. Dioxo- and Dithioxophosphoranes including the Metaphosphate Anion; In *Multiple Bonds and Low Coordination in Phosphorus Chemistry*; Regitz, M., Scherer, O. J., eds. Georg Thieme Verlag: New York, 1990; pp 415-442.

(11) Niecke, E.; Gudat, D. Iminooxo-, Iminothioxo-, and Iminoselenoxophosphoranes; In *Multiple Bonds and Low Coordination in Phosphorus Chemistry*; Regitz, M., Scherer, O. J., eds. Georg Thieme Verlag: New York, 1990; pp 405-410.

(12) Yoshifuji, M. Phophinylidene-methylene(imino, oxo, thioxo, or selenoxo)phosphoranes; In *Multiple Bonds and Low Coordination in Phosphorus Chemistry*; Regitz, M., Scherer, O. J., eds. Georg Thieme Verlag: New York, 1990; pp 411-414.

(13) Igau, A.; Grutzmacher, H.; Baceiredo, A.; Bertrand, G. *J. Am. Chem. Soc.* **1988**, *110*, 6463-6466.

(14) Bertrand, G. λ^5-Phosphaalkynes (Alkylidynephosphoranes); In *Multiple Bonds and Low Coordination in Phosphorus Chemistry*; Regitz, M., Scherer, O. J., eds. Georg Thieme Verlag: New York, 1990; pp 443-454.

(15) Majoral, J.-P. σ^3,λ^5-Phosphonitriles (Nitrilophosphoranes); In *Multiple Bonds and Low Coordination in Phosphorus Chemistry*; Regitz, M., Scherer, O. J., eds. Georg Thieme Verlag: New York, 1990; pp 455-461.

(16) Igau, A.; Baceiredo, A.; Grützmacher, H.; Pritzkow, H.; Bertrand, G. *J. Am. Chem. Soc.* **1989**, *111*, 6853-6854.

(17) Guerret, O.; Bertrand, G. *Acc. Chem. Res.* **1997**, *30*, 486-493.

(18) Burford, N.; Cameron, T. S.; LeBlanc, D. J.; Phillips, A. D.; Concolino, T. E.; Lam, K. C.; Rheingold, A. L. *J. Am. Chem. Soc.* **2000**, *122*, 5413-5414.

(19) Pitzer, K. S. *J. Am. Chem. Soc.* **1948**, *70*, 2140-2145.

(20) Mulliken, R. S. *J. Am. Chem. Soc.* **1950**, *72*, 4493-4503.

(21) Gier, T. E. *J. Am. Chem. Soc.* **1961**, *83*, 1769-1770.

(22) Dasent, W. E. *Nonexistent Compounds, Compounds of Low Stability*; Marcel Dekker: New York, 1965.

(23) Dimroth, K.; Hoffmann, P. *Angew. Chem. Int. Ed. Engl.* **1964**, *3*, 384-385.

(24) Allmann, R. *Angew. Chem. Int. Ed. Engl.* **1965**, *4*, 150-151.

(25) Ashe III, A. J. *J. Am. Chem. Soc.* **1971**, *93*, 3293-3295.

(26) Niecke, E.; Flick, W. *Angew. Chem. Int. Ed.Engl.* **1973**, *12*, 585-586.

(27) Burford, N.; Clyburne, J. A. C.; Chan, M. S. W. *Inorg. Chem.* **1997**, *36*, 3204-3206.

(28) Norman, N. C. *Polyhedron* **1993**, *12*, 2431-2446.

(29) Becker, G. *Z. Anorg. Allg. Chem.* **1976**, *423*, 242-254.

(30) Becker, G.; Gresser, G.; Uhl, W. *Z. Naturforsch.* **1981**, *36B*, 16-19.

(31) Yoshifuji, M.; Shima, I.; Inamoto, N.; Hirotsu, K.; Higuchi, T. *J. Am. Chem. Soc.* **1981**, *103*, 4587-4589.

(32) Appel, R.; Knoll, F.; Ruppert, I. *Angew. Chem. Int. Ed. Engl.* **1981**, *20*, 731-744.

(33) Cowley, A. H. *Acc. Chem. Res.* **1984**, *17*, 386-392.

(34) Power, P. P. *Chem. Rev.* **1999**, *99*, 3463-3503.

(35) Sasamori, T.; Takeda, N.; Fujio, M.; Kimura, M.; Nagase, S.; Tokitoh, N. *Angew. Chem. Int. Ed.* **2002**, *41*, 139-141.

(36) Cowley, A. H.; Kemp, R. A. *Chem. Rev.* **1985**, *85*, 367-382.

(37) Gudat, D. *Coord. Chem. Rev.* **1997**, *163*, 71-106.

(38) Kopp, R. W.; Bond, A. C.; Parry, R. W. *Inorg. Chem.* **1976**, *15*, 3042-3046.

(39) Schmidpeter, A.; Lochschmidt, S.; Sheldrick, W. S. *Angew. Chem. Int. Ed. Engl.* **1985**, *24*, 226-227.

(40) Niecke, E.; Nieger, M.; Reichert, F. *Angew.Chem. Int. Ed. Engl.*. **1988**, *27*, 1715-1716.

(41) Zollinger, H. *Diazo Chemistry I*; VCH: New York, 1994.

(42) Mathey, F. Phosphinidenes; In *Multiple Bonds and Low Coordination in Phosphorus Chemistry*; Regitz, M., Scherer, O. J., eds. Georg Thieme Verlag: New York, 1990; pp 33-57.

(43) Cowley, A. H. *Acc. Chem. Res.* **1997**, *30*, 445-451.

(44) Arduengo, A. J.; Calabrese, J. C.; Cowley, A. H.; Dias, H. V. R.; Goerlich, J. R.; Marshall, W. J.; Riegel, B. *Inorg. Chem.* **1997**, *36*, 2151-2158.

(45) Arduengo, A. J.; Carmalt, C. J.; Clyburne, J. A. C.; Cowley, A. H.; Pyati, R. *Chem. Commun.* **1997**, 981-982.

(46) Dillon, K. B.; Waddington, T. C. *Chem. Commun.* **1969**, 1317.

(47) Sheldrick, W. S.; Schmidpeter, A.; Zwaschka, F.; Dillon, K. B.; Platt, A. W. G.; Waddington, T. C. *Dalton Trans.* **1981**, 413-418.

(48) Dillon, K. B. *Chem. Rev.* **1994**, *94*, 1441-1456.

(49) Muller, G.; Brand, J.; Jetter, S. E. *Z. Naturforsch.* **2001**, *56b*, 1163-1171.

(50) Muller, G.; Hans-Joachim, M.; Winkler, M. *Z. Naturforsch.* **2001**, *56b*, 1155-1162.

(51) Bondi, A. *J. Phys. Chem.* **1964**, *68*, 441-451.

(52) Burford, N.; Ragogna, P. J.; McDonald, R.; Ferguson, M. *J. Am. Chem. Soc.* **2003**, *125*, 14404-14410.

(53) Burford, N.; Parks, T. M.; Royan, B. W.; Borecka, B.; Cameron, T. S.; Richardson, J. F.; Gabe, E. J.; Hynes, R. *J. Am. Chem. Soc.* **1992**, *114*, 8147-8153.

(54) Burford, N.; Parks, T. M.; Bakshi, P. K.; Cameron, T. S. *Angew .Chem. Int. Ed. Engl.* **1994**, *33*, 1267-1268.

(55) Althaus, H.; Breunig, H. J.; Lork, E. *Chem.Commun.* **1999**, 1971-1972.

(56) Reed, R.; Réau, R.; Dahan, F.; Bertrand, G. *Angew. Chem. Int. Ed. Engl.*. **1993**, *32*, 399-401.

(57) Burford, N.; Cameron, T. S.; LeBlanc, D. J.; Losier, P.; Sereda, S.; Wu, G. *Organometallics* **1997**, *16*, 4712-4717.

(58) David, G.; Niecke, E.; Nieger, M.; Radseck, J.; Schoeller, W. W. *J. Am. Chem. Soc.* **1994**, *116*, 2191-2192.

(59) Burford, N.; Cameron, T. S.; Clyburne, J. A. C.; Eichele, K.; Robertson, K. N.; Sereda, S.; Wasylishen, R. E.; Whitla, W. A. *Inorg. Chem.* **1996**, *35*, 5460-5467.

(60) Romanenko, V. D.; Rudzevich, V. L.; Rusanov, E. B.; Chernega, A. N.; Senio, A.; Sotiropoulos, J. M.; Pfister-Guillouzo, G.; Sanchez, M. *Chem. Commun.* **1995**, 1383-1385.

(61) Niecke, E. Iminophosphines; In *Multiple Bonds and Low Coordination in Phosphorus Chemistry*; Regitz, M., Scherer, O. J., eds. Georg Thieme Verlag: New York, 1990; pp 293-320.

(62) Niecke, E.; Gudat, D. *Angew. Chem. Int. Ed.* **1991**, *30*, 217-237.

(63) Gonbeau, D.; Pfister-Guillouzo, G.; Barrans, J. *Can. J. Chem.* **1983**, *61*, 1371-1378.

(64) David, G.; von der Gönna, V.; Niecke, E.; Busch, T.; Schoeller, W. W.; Rademacher, P. *Faraday Trans.* **1994**, *90*, 2611-2616.

(65) Schoeller, W. W.; Niecke, E. *Chem. Commun.* **1982**, 569-570.

(66) Niecke, E.; Gudat, D.; Schoeller, W. W.; Rademacher, P. *Chem. Commun.* **1985**, 1050.

(67) Niecke, E.; Rüger, R.; Schoeller, W. W. *Angew. Chem. Int. Ed. Engl.* **1981**, *20*, 1034-1036.

(68) Burford, N.; Clyburne, J. A. C.; Losier, P.; Parks, T. M. Group 15 carbene analogues: cationic bis(amino)phosphenium and -arsenium compounds-; In *Brauer-Herrmann: Synthetic Methods of Organometallic and Inorganic Chemistry Volume 3, Phosphorus, Arsenic, Antimony and Bismuth*; Karsch, H. H., ed. Thieme: 1996; pp 21-27.

(69) Burford, N.; Cameron, T. S.; Conroy, K. D.; Ellis, B.; Lumsden, M. D.; Macdonald, C. L. B.; McDonald, R.; Phillips, A. D.; Ragogna, P. J.; Schurko, R. W.; Walsh, D.; Wasylishen, R. E. *J. Am. Chem. Soc.* **2002**, *124*, 14012-14013.

(70) Cowley, A. H.; Kemp, R. A. *Chem. Commun.* **1982**, 319-320.

(71) Cowley, A. H.; Kemp, R. A. *Inorg. Chem.* **1983**, *22*, 547-550.

(72) Niecke, E.; Detsch, R.; Nieger, M.; Reichert, F.; Schoeller, W. W. *Bull. Soc. Chim. Fr.* **1993**, *130*, 25-31.

(73) Altmeyer, O.; Niecke, E.; Nieger, M.; Busch, T.; Schoeller, W. W.; Stalke, D. *Heteroat.Chem.* **1990**, *1*, 191-194.

(74) Schoeller, W. W.; Busch, T.; Niecke, E. *Chem. Ber.* **1990**, *123*, 1653-1654.

(75) Schoeller, W. W.; Busch, T.; Haug, W. *Phosphor. Sulfur Silicon* **1990**, *49/50*, 285-288.

(76) Romanenko, V. D.; Ruban, A. V.; Reitel, G. V.; Povolotskii, M. I.; Chernega, A. N.; Markovskii, L. N. *Zh. Obshch. Khim.* **1989**, *59*, 2780-2781.

(77) Huheey, J. E.; Keiter, E. A.; Keiter, R. L. *Inorganic Chemistry*; Harper Collins College: New York, 1993; p A-31.

(78) Burford, N.; Clyburne, J. A. C.; Bakshi, P. K.; Cameron, T. S. *J. Am. Chem. Soc.* **1993**, *115*, 8829-8830.

(79) Burford, N.; Clyburne, J. A. C.; Bakshi, P. K.; Cameron, T. S. *Organometallics* **1995**, *14*, 1578-1585.

(80) Burford, N.; Cameron, T. S.; Robertson, K. N.; Phillips, A. D.; Jenkins, H. A. *Chem. Commun.* **2000**, 2087-2088.

(81) Burford, N.; Losier, P.; Phillips, A. D.; Ragogna, P. J.; Cameron, T. S. *Inorg. Chem.* **2003**, *42*, 1087-1091.

(82) Burford, N.; Dyker, C. A.; Phillips, A. D.; Spinney, H. A.; Decken, A.; McDonald, R.; Ragogna, P. J.; Rheingold, A. L. *Inorg. Chem.* **2004**, *43*, 7502-7507.

(83) Burford, N.; Phillips, A. D.; Spinney, H. A.; Robertson, K. N.; Cameron, T. S.; McDonald, R. *Inorg. Chem.* **2003**, *42*, 4949-4954.

(84) Kaukorat, T.; Neda, I.; Schmutzler, R. *Coord. Chem. Rev.* **1994**, *137*, 53-107.

(85) Bouhadir, G.; Reed, R. W.; Réau, R.; Bertrand, G. *Heteroat. Chem.* **1995**, *6*, 371-375.

(86) Jones, V. A.; Sriprang, S.; Thornton-Pett, M.; Kee, T. P. *J. Organomet. Chem.* **1998**, *567*, 199-218.

(87) Schultz, C. W.; Parry, R. W. *Inorg. Chem.* **1976**, *15*, 3046-3050.

(88) Thomas, M. G.; Schultz, C. W.; Parry, R. W. *Inorg. Chem.* **1977**, *16*, 994-1001.

(89) Schmidpeter, A.; Lochschmidt, S.; Sheldrick, W. S. *Angew. Chem. Int. Ed. Engl.* **1982**, *21*, 63-64.

(90) Shagvaleev, F. Sh.; Zykova, T. V.; Tarasova, R. I.; Sitdikova, T. Sh.; Moskva, V. V. *Zh. Obshch. Khim.* **1990**, *60*, 1775-1779.

(91) Burford, N.; LeBlanc, D. J. *Inorg. Chem.* **1999**, *38*, 2248-2249.

(92) Abrams, M. B.; Scott, B. L.; Baker, R. T. *Organometallics* **2000**, *19*, 4944-4956.

(93) Burford, N.; Ragogna, P. J.; McDonald, R.; Ferguson, M. J. *Chem. Commun.* **2003**, 2066-2067.

(94) Burford, N.; Ragogna, P. J.; Robertson, K. N.; Cameron, T. S.; Hardman, N. J.; Power, P. P. *J. Am. Chem. Soc.* **2002**, *124*, 382-383.

(95) Timosheva, N. V.; Chandrasekaran, A.; Day, R. O.; Holmes, R. R. *Inorg. Chem.* **1998**, *37*, 3862-3867.

(96) Sood, P.; Chandrasekaran, A.; Day, R. O.; Holmes, R. R. *Inorg. Chem.* **1998**, *37*, 6329-6336.

(97) Sherlock, D. J.; Chandrasekaran, A.; Day, R. O.; Holmes, R. R. *Inorg. Chem.* **1997**, *36*, 5082-5089.

(98) Kuhn, N.; Kratz, T. *Synthesis* **1993**, 561-562.

(99) Kuhn, N.; Henkel, G.; Kratz, T. *Z. Naturforsch.* **1993**, *48b*, 973-977.

(100) Kuhn, N.; Henkel, G.; Kratz, T. *Chem. Ber.* **1993**, *126*, 2047-2049.

(101) Phillips, A. D. Synthesis and Characterization of Complexes Involving Phosphino-Centres as Lewis Acids. 2001.
Ref Type: Thesis/Dissertation

(102) Niecke, E.; Nieger, M.; Reichert, F.; Schoeller, W. W. *Angew. Chem. Int. Ed. Engl.* **1988**, *27*, 1713-1716.

(103) Burford, N.; Clyburne, J. A. C.; Silvert, D.; Warner, S.; Whitla, W. A.; Darvesh, K. V. *Inorg. Chem.* **1997**, *36*, 482-484.

(104) Amyes, T. L.; Diver, S. T.; Richard, J. P.; Rivas, F. M.; Toth, K. *J. Am. Chem. Soc.* **2004**, *126*, 4366-4374.

(105) Sacconi, L.; Paoletti, P.; Ciampolini, M. *J. Am. Chem. Soc.* **1960**, *82*, 3828-3831.

(106) Allen, F. H.; Kennard, O.; Watson, D. G.; Brammer, L.; Orpen, A. G.; Taylor, R. *Perkin.Trans.II* **1987**, S1-S19.

(107) Kuhn, N.; Fawzi, R.; Kratz, T.; Steimann, M.; Henkel, G. *Phosphor. Sulfur Silicon* **1996**, *108*, 107-119.

(108) Frampton, C. S.; Parkes, K. E. B. *Acta Cryst.* **1996**, *C52*, 3246-3248.

(109) Ganis, P.; Avitabile, G.; Benedetti, E.; Pedone, C.; Goodman, M. *Proc. Nat. Acad. Sci. U.S.* **1970**, *67*, 426-433.

(110) Kapon, M.; Reisner, G. M. *Acta Cryst.* **1989**, *C45*, 780-782.

(111) Ueda, H.; Onishi, H.; Nagai, T. *Acta Cryst.* **1986**, *C42*, 462-464.

(112) Bittner, A.; Männig, D.; Nöth, H. *Z. Naturforsch.* **1986**, *41b*, 587-591.

(113) Bagnall, K. W.; Al-Daher, A. G. M.; Bombieri, G.; Benetollo, F. *Inorg. Chim. Acta* **1986**, *115*, 229-236.

(114) de Wet, J. F.; Caira, M. R. *Dalton Trans.* **1986**, 2035-2041.

(115) Baker, M. J.; Harrison, K. N.; Orpen, A. G.; Pringle, P. G.; Shaw, G. *Dalton Trans.* **1992**, 2607-2614.

(116) Burford, N.; Royan, B. W.; White, P. S. *Acta Cryst.* **1990**, *C46*, 274-276.

(117) Keder, N. L.; Shibao, R. K.; Eckert, H. *Acta Cryst.* **1992**, *C48*, 1670-1671.

(118) Chernega, A. N.; Ruban, A. V.; Romanenko, V. D. *Zh. Strukt. Khim* **1991**, *32*, 158-160.

(119) Markovskii, L. N.; Romanenko, V. D.; Ruban, A. V.; Drapailo, A. B.; Chernega, A. N.; Antipin, M. Y.; Struchkov, Y. T. *Zh. Obshch. Khim.* **1988**, *58*, 291-295.

(120) Pötschke, N.; Nieger, M.; Niecke, E. *Acta. Chem. Scand.* **1997**, *51*, 337-339.

(121) Pötschke, N.; Barion, D.; Nieger, M.; Niecke, E. *Tetrahedron* **1995**, *51*, 8993-8996.

(122) Chernega, A. I.; Antipin, M. Y.; Struchkov, Y. T.; Ruban, A. V.; Romanenko, V. D. *Zh. Strukt. Khim* **1990**, *31*, 134-140.

(123) Chernega, A. N.; Antipin, M. Y.; Struchkov, Y. T.; Ruban, A. V.; Romanenko, V. D.; Markovskii, L. N. *Doklady Akademii Nauk SSSR* **1989**, *307*, 610-612.

(124) Burford, N. *Coord. Chem. Rev.* **1992**, *112*, 1-18.

(125) Burford, N.; Herbert, D. E.; Ragogna, P. J.; McDonald, R.; Ferguson, M. J. *J. Am. Chem. Soc.* **2004**, *126*, 17067-17073.

(126) Ellis, B.; Carlesimo, M.; Macdonald, C. *Chem. Commun.* **2003**, 1946-1947.

(127) Bettermann, G.; Schomburg, D.; Schmutzler, R. *Phosphorus and Sulfur* **1986**, *28*, 327-336.

(128) Balitzky, Y. V.; Pipko, S. E.; Sinitsa, A. D.; Chernega, A. N.; Gololobov, Y. G. *Phosphor. Sulfur Silicon* **1993**, *75*, 167-170.

(129) Pipko, S. E.; Balitzky, Y. V.; Sinitsa, A. D.; Gololobov, Y. G. *Tetrahedron Lett.* **1994**, *35*, 165-168.

(130) Burford, N.; Phillips, A. D.; Spinney, H. A.; Lumsden, M.; Werner-Zwanziger, U.; Ferguson, M. J.; McDonald, R. *J. Am. Chem. Soc.* **2005**, *127*, 3921-3927.

(131) Atwood, J. L.; Robinson, K. D.; Jones, C.; Raston, C. L. *Chem. Commun.* **1991**, 1697-1699.

(132) Jegier, J. A.; Atwood, D. A. *Inorg. Chem.* **1997**, *36*, 2034-2039.

(133) Perkins, C. W.; Martin, J. C.; Arduengo III, A. J.; Lau, W.; Algeria, A.; Kochi, J. K. *J. Am Chem. Soc.* **1980**, *102*, 7753-7759.

(134) Ashby, M. T.; Li, Z. *Inorg. Chem.* **1992**, *31*, 1321-1322.

(135) Trinquier, G.; Ashby, M. T. *Inorg. Chem.* **1994**, *33*, 1306-1313.

(136) Poetschke, N.; Nieger, M.; Khan, M. A.; Niecke, E.; Ashby, M. T. *Inorg. Chem.* **1997**, *36*, 4087-4093.

(137) Arduengo III, A. J.; Stewart, C. A. *Chem. Rev.* **1994**, *94*, 1215-1237.

(138) Cotton, F. A.; Wilkinson, G. *Advanced Inorganic Chemistry, Fifth Edition*; John Wiley & Sons: New York, 1988.

(139) Rivard, E.; Huynh, K.; Lough, A. J.; Manners, I. *J. Am. Chem. Soc.* **2004**, *126*, 2286-2287.

(140) Blättner, M.; Nieger, M.; Ruban, A.; Schoeller, W. W.; Niecke, E. *Angew. Chem. Int. Ed.* **2000**, *39*, 2768-2771.

(141) Averbuch-Pouchot, M. T.; Meisel, M. *Acta Cryst.* **1989**, *C45*, 1937-1939.

(142) Meisel, M.; Lönnecke, P.; Grimmer, A. R.; Wulff-Molder, D. *Angew. Chem. Int. Ed.* **1997**, *36*, 1869-1870.

(143) Burford, N.; Losier, P.; Bakshi, P. K.; Cameron, T. S. *Chem. Commun.* **1996**, 307-308.

(144) Barion, D.; Gärtner-Winkhaus, C.; Link, M.; Nieger, M.; Niecke, E. *Chem. Ber.* **1993**, *126*, 2187-2195.

(145) Burford, N.; Spinney, H. A.; Ferguson, M. J.; McDonald, R. *Chem. Commun.* **2004**, 2696-2697.

(146) Sheldrick, W. S. *Dalton Trans.* **1974**, 1402-1405.

(147) Cameron, T. S.; Chan, C.; Chute, W. J. *Acta Cryst.* **1980**, *B36*, 2391-2393.

(148) Arduengo III, A. J.; Harlow, R. L.; Kline, M. *J. Am. Chem. Soc.* **1991**, *113*, 361-363.

(149) Arduengo, A. J. *Acc. Chem. Res.* **1999**, *32*, 913-921.

(150) Bourissou, D.; Guerret, O.; Gabbaï, F. P.; Bertrand, G. *Chem. Rev.* **2000**, *100*, 39-91.

(151) Herrmann, W. A.; Köcher, C. *Angew. Chem. Int. Ed.* **1997**, *36*, 2162-2187.

(152) Kirmse, W. *Angew. Chem. Int. Ed.* **2004**, *43*, 1767-1769.

(153) Chernega, A. N.; Korkin, A. A.; Aksinenko, N. E.; Ruban, A. V.; Romanenko, V. D. *Zh. Obshch. Khim.* **1990**, *60*, 2462-2469.

(154) Kuhn, N.; Fahl, J.; Bläser, D.; Boese, R. *Z. Anorg. Allg. Chem.* **1999**, *625*, 729-734.

(155) Arduengo, A. J.; Krafczyk, R.; Marshall, W. J.; Schmutzler, R. *J. Am. Chem. Soc.* **1997**, *119*, 3381-3382.

(156) Arduengo, A. J.; Dias, H. V. R.; Calabrese, J. C. *Chem. Lett.* **1997**, 143-145.

(157) Burford, N.; Cameron, T. S.; Conroy, K. D.; Ellis, B.; Macdonald, C. L. B.; Ovans, R.; Phillips, A. D.; Ragogna, P. J.; Walsh, D. *Can.. J. Chem.* **2002**, *80*, 1404-1409.

(158) Gudat, D.; Schiffner, H. M.; Nieger, M.; Stalke, D.; Blake, A. J.; Grondey, H.; Niecke, E. *J. Am. Chem. Soc.* **1992**, *114*, 8857-8862.

(159) Niecke, E.; Lysek, M.; Symalla, E. *Chimia* **1986**, *40*, 202-205.

(160) Corbridge, D. E. C. *The Structural Chemistry of Phosphorus*; Elsevier: New York, 1974.

(161) March, J. *Advanced Organic Chemistry: Reactions, Mechanisms and Structure*; John Wiley and Sons: New York, 1992.

(162) Niecke, E.; Gudat, D. P^{31} NMR spectroscopic investigations of low-coordinated multiple bonded PN systems; In *Phosphorus-31 NMR spectral properties in compound in characterization and structural analysis*; Quin, L. D., Verkade, J. G., eds. 1994; pp 159-174.

(163) Gudat, D.; Hoffbauer, W.; Niecke, E.; Schoeller, W. W.; Fleischer, U.; Kutzelnigg, W. *J. Am. Chem. Soc.* **1994**, *116*, 7325-7331.

(164) Abboud, J. L. M.; Mo, O.; de Paz, J. L. G.; Yanez, M.; Esseffar, M.; Bouab, W.; El-Mouhtadi, M.; Mokhlisse, R.; Ballesteros, E.; Herreros, M.; Homan, H.; Lopez-Mardomingo, C.; Notario, R. *J. Am. Chem. Soc.* **1993**, *115*, 12468-12476.

(165) Gonzalez, A. I.; Otilia, M.; Yanez, M. *J. Phys. Chem. A* **1999**, *103*, 1662-1668.

(166) Cox, R. A.; Druet, L. M.; Klausner, A. E.; Modro, T. A.; Wan, P.; Yates, K. *Can. J. Chem.* **1981**, *59*, 1568-1573.

(167) Allman, T.; Goel, R. G. *Can. J. Chem.* **1982**, *60*, 716-722.

(168) Streuli, C. A. *Anal. Chem.* **1960**, *32*, 985-987.

(169) Benoit, R. L.; Lefebvre, D.; Fréchette, M. *Can. J. Chem.* **1987**, *65*, 996-1001.

(170) Paoletti, P.; Stern, J. H.; Vacca, A. *J. Phys. Chem.* **1965**, *69*, 3759-3762.

(171) Gudat, D. *Eur.J.Inorg. Chem.* **1998**, 1087-1094.

(172) Ellis, B. D.; Ragogna, P. J.; Macdonald, C. L. B. *Inorg. Chem.* **2004**, *43*, 7857-7867.

(173) Cui, C.; Roesky, H. W.; Schmidt, H.-G.; Noltemeyer, M.; Hao, H.; Cimpoesu, F. *Angew. Chem. Int. Ed.* **2000**, *39*, 4274-4276.

(174) Hardman, N. J.; Eichler, B. E.; Power, P. P. *Chem. Commun.* **2000**, 1991-1992.

(175) Hill, M. S.; Hitchcock, P. B. *Chem. Commun.* **2004**, 1818-1819.

(176) Hill, M. S.; Hitchcock, P. B.; Pongtavornpinyo, R. *Dalton Trans.* **2005**, 273-277.

(177) Haaf, M.; Schmedake, T. A.; West, R. *Acc. Chem. Res.* **2000**, *33*, 704-714.

(178) Herrmann, W. A.; Denk, M.; Behm, J.; Scherer, W.; Klingan, F. R.; Bock, H.; Solouki, B.; Wagner, M. *Angew. Chem. Int. Ed. Engl.* **1992**, *31*, 1485-1488.

(179) Gans-Eichler, T.; Gudat, D.; Nieger, M. *Angew. Chem. Int. Ed.* **2002**, *41*, 1888-1891.

(180) Morris, T. L.; Taylor, R. C. *Dalton Trans.* **1973**, 175-179.

(181) Levason, W.; Sheikh, B. *J. Organomet. Chem.* **1981**, *209*, 161-168.

(182) Majoral, J.-P.; Caminade, A.-M.; Maraval, V. *Chem. Commun.* **2002**, 2929-2942.

(183) Mulvey, R. E. *Chem. Commun.* **2001**, 1049-1056.

(184) Shriver, D. F.; Drezdzon, M. A. *The Manipulation of Air-Sensitive Compounds*; John Wiley and Sons: Toronto, 1986.

(185) Burford, N.; Muller, J.; Parks, T. M. *J. Chem. Educ.* **1994**, *71*, 807-809.

(186) Sheldrick, G. M. *SHELXL-97, Program for crystal structure determination, University of Goettingen, Germany* **1997**.

(187) Sluis, P. v. d.; Spek, A. L. *Acta Crystallogr.* **1990**, *A46*, 194-201.

(188) Spek, A. L. *J. Appl. Crystallogr.* **2003**, *36*, 7-13.